Title
A role for mechanosensitive channels during myegenesis and in muscular dystrophy

Author
Franco-Obregon, Alfredo,

Publication Date
1993

Peer reviewed|Thesis/dissertation

A role for mechanosensitive channels during myogenesis
and in muscular dystrophy.

by

ALFREDO FRANCO-OBREGON

DISSERTATION

Submitted in partial satisfaction of the requirements for the degree of

DOCTOR OF PHILOSOPHY

in

NEUROSCIENCE

in the

GRADUATE DIVISION

of the

UNIVERSITY OF CALIFORNIA

San Francisco

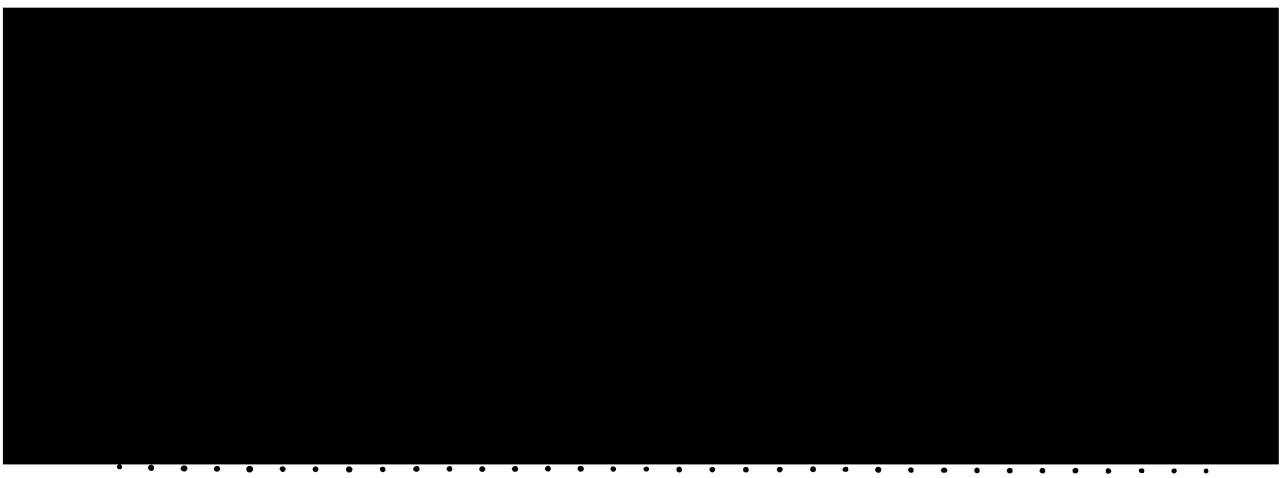

Date University Librarian

Degree Conferred: 6-13-93

I dedicate this thesis to the people who not only gave me love and support but a sense of purpose. To Mary, my soulmate and dear love, who believes in my abilities and our future endeavors, to Yannie and the Little man who are always a source of laughter and happiness, to my family for their loyalty and love, and to the Chicano and Latino community for replenishing my spirit.

Acknowledgements

I'd like to acknowledge my advisor and friend, Jeff Lansman, for his guidance and interest in me, but most importantly for his giving me the independence I needed to pursue my work. To Zach Hall, my mentor. Zach was someone I could always talk to and whose advise was invaluable. To the Hall lab who provided a home away from home. To Juan Korenbrot, whom I admire and respect and whose advise was always constructive and fair. Juan was the Soloman of my graduate student career.

I'd like to thank Richard Krauzlis, Cristina Weaver and Paul Slesinger for their friendship and support . To my homeboys in the School of Dentistry, Frank, Ceasar, Malcolm, Manny, and Rudy for keeping me in touch with whom I am. To the members of the Wednesday night (moved to Friday night) drinking club, Mike, Rhein, Janice, David and Ray. Cheers! To the students in the Summer Research Training Program who allowed me to give back the opportunities given to me and unknowingly gave me strength to achieve my goals.

I would also like to acknowledge and thank the Office of the President for giving me fellowship monies which carried me through Graduate school. I would especially like to thank Eugene Cota-Robles for pushing the University of California to make available graduate fellowships for minority students and to have the persistence to make affirmative action a viable and important issue.

The Society for the Advancement of Chicanos and Native American Indians in Science reinforced my commitment to provide opportunities for young minority students to pursue an academic life.

Finally, thanks to the Yellow Submarine.

A role for mechanosensitive channels during myogenesis and in muscular dystrophy.

Alfredo Franco-Obrégon

Abstract

In this thesis I use single-channel recordings to follow the expression of mechanosensitive channels throughout muscle development and in the skeletal muscle from the *mdx* mouse, an animal model of X-linked muscular dystrophy. Mechanosensitive channels transduce the work done in deforming the muscle membrane into energy to open channels. The integrity of the membrane-associated cytoskeleton is important for the normal functioning of mechanosensitive channels. X-linked muscular dystrophy recapitulates early stages of myogenesis in that a specific component of the membrane-associated cytoskeleton, known as dystrophin, is absent. The absence of dystrophin may have profound consequences on the gating of mechanosensitive channels in muscle cells from animals with X-linked muscular dystrophy and in myoblasts, the progenitor cells of adult skeletal muscle. Another important feature of mechanosensitive channels in skeletal muscle is that they are more selective for Ca^{2+} than for Na^{+} or K^{+}. The muscle degeneration observed in X-linked muscular dystrophy is thought to be due to elevated myoplasmic Ca^{2+} levels. Similarly, early myogenesis requires the influx of extracellular Ca^{2+} into myoblasts. In this thesis I test the hypothesis that mechanosensitive ion channels provide a pathway for Ca^{2+} entry into muscle cells, and that developmental or genetically-based alterations in the membrane-associated cytoskeleton influence their activity.

Table of Contents

Table of Contents

List of Figures

Figure page

Chapter 1

Chapter 2

List of Figures

List of Figures

Figure page

Chapter 3

List of Figures

Figure page

Chapter 3

Chapter 4

List of Tables

Chapter 1

Chapter 3

Introduction

The proper development and function of skeletal muscle is dependent upon Ca^{2+} influx from the extracellular space into skeletal muscle (see below). However, the ion channels that provide a pathway for resting Ca^{2+} entry into skeletal muscle are poorly understood. Adult skeletal muscle posses two distinct classes of voltage-gated Ca^{2+}-channels (Cognard et al., 1986; Beam and Knudson, 1988a; Kano et al., 1989). These channels produce macroscopic Ca^{2+} currents which are distinguished electrophysiologically as having high and low thresholds of voltage-activation. The low threshold component activates at relatively negative membrane potentials (~-40 mV) and quickly inactivates (50-100 msecs). The high threshold component activates at relatively depolarized membrane potentials (0 mV) and decays more slowly (>200 msec). Although both channel types are highly selective for Ca^{2+} (Tsien and Tsien, 1990), they require prior depolarization from the resting potential to open and inactivate thereafter. The magnitude of the high threshold Ca^{2+}-current increases with age in myotubes in culture and neonatal skeletal muscle (Beam and Knudson, 1988b; Kano et al., 1989) and there is some dispute as to whether it plays some role in excitation-contraction coupling (Sandow, 1952; Sanchez and Stefani, 1978; Luttgau and Spiecker, 1979; Gonzalez-Serratos et al., 1982; Eisenberg et al., 1983; Brum et al., 1987). The function of the low threshold channel is unknown but it decreases with age.

In addition to voltage-gated Ca^{2+} channels, skeletal muscle posses other classes of cation-selective channels that can also support Ca^{2+} entry such as the nicotinic acetylcholine-receptor (nAChR) channel (Bregestovsky et al.,1979; Adams et al., 1980; Decker and Danni, 1990). Ca^{2+} entry through the nAChR may participate in triggering myogenesis (Entwistle et al., 1988a, b) and may also contribute to the expression of several forms of skeletal muscle disorders in humans (Hart et al., 1979; Engel et al., 1981;

Mongini et al., 1988; Mancinelli et al., 1989) and animals (Leonard and Salpeter, 1979, 1982; Howlett and Hoekman, 1988; Meshul, 1989). In addition to nAChR channels, skeletal muscle also posses mechanosensitive channels which open in response to membrane deformation (Guharay and Sachs, 1984). Mechanosensitive channels are found throughout myogenesis and are permeable to monovalent and divalent cations, but are especially selective for Ca^{2+} (Franco and Lansman, 1990a, b; Franco-Obrégon and Lansman, 1993b). The resting activity of mechanosensitive channels is the predominant form of channel activity observed in muscle cells at negative membrane potentials and may therefore be responsible for the majority of resting Ca^{2+} leakage into skeletal muscle. Ca^{2+} leak channels which resemble mechanosensitive channels have been previously described in bilayers (Benham and Tsien, 1986; Rosenberg et al., 1988) and more recently in skeletal muscle (Fong et al., 1990). The observation of Ca^{2+} leak channels may in some cases represent the resting activity of mechanosensitive ions channels in the absence of tension applied to the membrane.

Although resting Ca^{2+} entry through mechanosensitive ion channels into skeletal muscle may be significant, the physiological impetus for mechanically-gated ion channels is not understood. Stretch, however, applied to skeletal muscle can induce subsequent muscle contraction (Ford et al., 1977; Pringle, 1978). Skeletal muscle which is unable to develop tension (deficits of excitation-contraction coupling), due to specific deficits of either voltage-gated Ca^{2+} channels (Beam et al.,1986) or the sarcoplasmic reticulum Ca^{2+} release channel (Hymel et al., 1988; Lai et al., 1988) show abnormal muscle development (Kieny et al., 1988; Ashby et al., 1993). There is also evidence indicating that physically stretching the cell substrate can stimulate proliferation (DeWitt et al., 1984; Sumpio et al., 1987). These results imply that stretch may provide a physiologically relevant stimulus that influences muscle development.

Ca^{2+} entry during myogenesis.

Adult skeletal muscle is a multinucleated synchitial tissue arising from the joining of membranes of hundreds of progenitor cells. In the animal these progenitor cells, or myoblasts, fuse their membranes in response to environmental cues present during development (Wakelam, 1985) or factors that are released during muscle injury (John and Jones, 1988). One of the best described events preceding myoblast fusion is the influx of extracellular Ca^{2+} (David et al., 1981; David and Higginbotham, 1981; Entwistle et al., 1983, 1988a; David et al., 1990). In addition, extracellular Ca^{2+} is necessary for myoblasts aggregation, alignment and fusion to form myotubes (Shainberg et al., 1969; Knudsen and Horwitz, 1977; Konieczny et al., 1982). The alignment and fusion of myoblasts is associated with the induction of muscle-specific genes which is also dependent upon extracellular Ca^{2+} (Konieczny et al., 1982; Endo and Nadal-Ginard, 1987). Although the a role for Ca^{2+} influx in early myogenesis is well established, the mechanism for Ca^{2+} entry is not known.

I have examined the activity of ion channels in muscle cells grown in culture at morphologically distinct stages of myogenesis: proliferative myoblasts (at low density), myoblasts that had aligned in preparation for fusion, and newly formed myotubes. My major goal was to distinguish Ca^{2+}-permeable ion channels whose expression was correlated well with the time course of Ca^{2+} entry in myoblasts prior to fusion.

The expression of voltage-gated Ca^{2+}-channels are only detected after myotube formation (Caffrey et al., 1987; Kano et al., 1989). Conventional voltage-gated Ca^{2+} channels are therefore not likely to contribute to Ca^{2+} entry in early myogenesis as they appear relatively late in development and require depolarization of the resting membrane potential to open. nAChR channels are expressed in myoblasts prior to fusion (Siegelbaum et al., 1984; Franco and Lansman, 1990b; Franco-Obrégon and Lansman, 1993a, b) and Ca^{2+}-entry through the nAChR channel may be a prerequisite for myoblasts fusion (Entwistle et al., 1988a, b). However, the amount of Ca^{2+} entry through the nAChR

channel is limited by low channel density in myoblasts (Chapter 1; Siegelbaum et al., 1984; Franco and Lansman, 1990b) and the relatively small permeability of nAChR channels to Ca^{2+} (Bregestovsky et al.,1979; Adams et al., 1980; Decker and Danni, 1990). Mechanosensitive channels, on the other hand, are detected in all stages of myogenesis (Guharay and Sachs, 1984; Franco-Obrégon and Lansman, 1993b), especially in myoblasts where their density is highest (Franco and Lansman, 1990b) and are more permeable to Ca^{2+} than nAChR channels. In our examination of Ca^{2+}-permeable ion channels in myoblasts we only detect the activity of nAChR channels and mechanosensitive channels at negative membrane potentials near the resting potential of the cell (Franco and Lansman, 1990a, b; Franco-Obrégon and Lansman, 1993a, b). The behavior of mechanosensitive channels in myoblasts had not been examined previously and is considered in Chapter 1 of this thesis.

Ca^{2+} entry in muscular dystrophy.

Muscular dystrophy is described as a progressive, degenerative condition of skeletal muscle (Carpenter and Karpati, 1984; Kakulas and Adams, 1985; Walton and Gardner-Medwin, 1988). In humans the most common form of muscular dystrophy is inherited with the X chromosome and is manifested in its most severe form as Duchenne muscular dystrophy. Afflicted boys with this disease appear normal up until ~2 years of age, by ~10 years of age are no longer ambulatory and typically die of cardiac or respiratory failure by their early twenties.

There is now considerable evidence indicating that intracellular free Ca^{2+} is elevated in skeletal muscle from individuals with X-linked muscular dystrophy (Bodensteiner and Engel,1978; Emery and Burt, 1980; Mongini et al., 1988). Furthermore, studies on animal models of X-linked muscular dystrophy suggests that uncontrolled Ca^{2+} leakage from the extracellular space into skeletal muscle can account for proteolysis (Turner et al., 1988;

Martonosi, 1989) by the activation of myoplasmic, Ca^{2+}-dependent proteases which produces muscle fiber necrosis (Neerunjun and Dubowitz, 1979).

A major advance in understanding the pathogenesis of Duchenne muscular dystrophy was made with the identification of the gene responsible for X-linked muscular dystrophies (Monaco et al., 1986; Koenig et al., 1987, 1988). The gene codes for the protein, dystrophin, which belongs to the family of cytoskeletal proteins including α-actinin and spectrin (Dubreuil, 1991). Dystrophin is localized to the cytoplasmic surface of the muscle membrane (Arahata et al., 1988; Bonilla et al., 1988; Zubrzycka-Gaarn et al., 1988; Salviati et al., 1989) where it complexes with a unique set of glycoproteins via its carboxyl terminal end (Campbell and Kahl, 1989; Ervasti et al., 1990; Ervasti and Campbell, 1991; Ohlendieck et al., 1991c) and is thought to interact with the actin-based cytoskeleton via its amino terminal end (Isobe and Shimada, 1986; Bennett, 1990; Koenig et al., 1988). Individuals with Duchenne muscular dystrophy also lack the dystrophin-associated glycoproteins (Ervasti et al., 1990; Ohlendieck and Campbell, 1991) suggesting that an absence of dystrophin alone may not fully account for the pathogenesis of Duchenne muscular dystrophy (Matsumura et al., 1992).

The mdx mouse, an animal model for human X-linked muscular dystrophies.

An animal model for human X-linked muscular dystrophy has been described in the *mdx* mouse (Bulfield et al., 1984). As in humans, the *mdx* mouse exhibits an inability to regulate myoplasmic calcium concentrations (Turner et al., 1988). The mutation that gives rise to muscular dystrophy in the *mdx* mouse involves the mouse homologue of the dystrophin gene (Ryder-Cook et al., 1988; Sicinski et al., 1989) resulting in the absence of dystrophin at the skeletal muscle surface (Hoffman et al., 1987a; Arahata et al., 1988; Chamberlain et al., 1988; Watkins et al., 1988) and the concomitant down regulation of the dystrophin-associated glycoproteins (Ervasti et al., 1990; Ervasti and Campbell, 1991; Ohlendieck and Campbell, 1991a).

Membrane fragility hypothesis of muscular dystrophy.

Stretch applied to skeletal muscle at rest (Ashmore, et al., 1988) or while actively contracting (McCully and Faulkner, 1985, 1986; Weller et al., 1990; Stauber et al., 1991), results in conditions of skeletal muscle which resemble naturally occurring forms of muscular dystrophy. One obvious possibility is that muscle membranes are mechanically more fragile when dystrophin is absent, tearing under the stress of normal muscular activity and creating a pathway for the non-specific influx of Ca^{2+} into the muscle's interior. In support of this hypothesis Menke and Jockusch (1991) have demonstrated that muscle fibers isolated form mice expressing X-linked muscular dystrophy are less likely to survive hyposmotic swelling when compared to wild type fibers. However, I and others have found that the pressure needed to rupture membrane patches, does not differ significantly between wild type and dystrophic muscle membranes suggesting that dystrophic muscle membranes are not more mechanically fragile (Cooper and Hamill, 1989; Franco and Lansman, 1990a; Hutter et al., 1991). Studies using fluorescent, ion-sensitive, dyes indicate that the resting ionic influx into dystrophic muscle fibers is more selective for Ca^{2+} than for Na^{+}, which is inconsistent with lesions of the membrane giving rise to the leakage pathway (Turner et al., 1991).

Ion channel hypothesis of muscular dystrophy.

An alternative hypothesis to the membrane fragility hypothesis is that extracellular Ca^{2+} enters skeletal muscle through Ca^{2+}-permeable ion channels. Implicit to this second hypothesis is the notion that channels whose activity are normally tightly regulated become hyperactive under dystrophic conditions establishing an inappropriate influx of Ca^{2+} into the cell's interior at rest. In support of the ion channel hypothesis of muscular dystrophy, Leonard and Salpeter (1979) have shown that the small influx of Ca^{2+} that occurs through the acetylcholine receptor channel (Bregestovsky et al.,1979; Adams et al., 1980; Decker

and Dani, 1990), under conditions which prohibited the degradation of acetylcholine, is sufficient to result in a myopathic condition that closely resembles the necrosis observed in human and mouse models of muscular dystrophy (Pearce and Walton, 1963; Mokri and Engel, 1975; Bulfield et al.,1984).

The examination of mechanosensitive ion channels in muscle cells from the mdx mouse.

In 1984 Guharay and Sachs described the existence of ion channels which open in response to tension applied to the muscle membrane. The activity of mechanosensitive channels greatly increased with agents that depolymerize cytosolic actin filaments (Guharay and Sachs, 1985) suggesting that membrane tension is conveyed to mechanosensitive channels through an association with the cell cytoskeleton. Sachs (1989) proposed that, spectrin, a cytoskeletal cousin of dystrophin (Dubreuil, 1991), could function as a protein intermediate, coupling the actin-based cytoskeleton with mechanosensitive channels.

As an extension of this earlier work I proposed that the activity of mechanosensitive channels may be altered due to the disruption of the cytoskeleton in dystrophic muscle allowing extracellular Ca^{2+} to enter skeletal muscle (Franco and Lansman, 1990b). We detected elevated activity of mechanosensitive channels in *mdx* myotubes (Chapter 2; Franco and Lansman, 1990a) and in intact fibers acutely removed from the *mdx* mouse (Chapter 3; Franco-Obrégon and Lansman, 1993b) when compared to normal muscle cells. Like those previously described in myoblasts (Chapter 1; Franco and Lansman, 1990b), the mechanosensitive channels from *mdx* muscle show a selectivity for Ca^{2+} over monovalent cations (Franco and Lansman, 1990a, b; Franco-Obrégon and Lansman, 1993b). Although mechanosensitive channels exhibit a slight voltage-dependency (Guharay and Sachs, 1985; Franco and Lansman, 1990b; Franco-Obrégon and Lansman, 1993b) they do not require depolarization of the resting membrane potential to open. Mechanosensitive channels may then be open at the resting membrane potential of the cell as long as there exist the appropriate tension on the membrane. Finally, the involvement of

mechanosensitive channels in the manifestation of muscular dystrophy raised the possibility of pharmacologically targeting these channels with specific channel blockers (Chapter 4; Franco and Lansman, 1990b; Franco et al., 1991). Ramifications of this work may lead to possible therapeutic approaches of slowing the progression X-linked muscular dystrophies

Chapter 1

Mechanosensitive channels in developing muscle cells from a mouse cell line: a putative role for mechanosensitive channels in myogenesis.

Introduction

The differentiation of myoblasts into adult skeletal muscle myotubes *in vitro* has been a useful model for studying the mechanisms which control the various stages of myogenesis. Myoblasts dissociated from the animal and maintained in tissue culture are proliferative until stimulated to withdraw from the cell cycle by the removal of growth factors from the culture media. Upon withdrawal from the cell cycle myoblasts subsequently aggregate and align with their long axes oriented in parallel. Fusion of aligned myoblasts produces multi-nucleated myotubes which shortly thereafter acquire the ability to contract. During the period these cellular events are taking place, there is a coordinated induction of an array of muscle-specific gene products representing commitment to terminal biochemical differentiation (reviewed in Wakelam, 1985).

The mechanisms controlling the onset of myogenesis from the time myoblasts withdraw from the cell cycle to terminal biochemical differentiation are poorly understood. Evidence suggests that one of the earliest events preceding myoblast fusion is an influx of extracellular Ca^{2+} (David et al., 1981; David and Higginbotham, 1981; Konieczny et al., 1982; David et al., 1990). However, myoblast fusion appears to be influenced by a rather diverse set of stimuli, including membrane depolarization in response to elevating extracellular K^+, activation of acetylcholine-receptor channels, and the synthesis of prostaglandins (Entwistle et al., 1983; Entwistle et al., 1988a; Entwistle et al., 1988b).

Each of these could act by stimulating a voltage-dependent increase in membrane permeability to Ca^{2+} (Entwistle et al, 1988a).

Electrophysiological recordings from myoblasts can provide direct evidence for the existence of voltage-dependent changes in membrane permeability to Ca^{2+}. Whole-cell recordings from myoblasts, however, fail to show voltage-gated Ca^{2+} currents similar to those found in adult muscle (Caffrey et al., 1987; Kano et al., 1989) suggesting that the pathway responsible for Ca^{2+} influx may be different from conventional Ca^{2+} channels (Cognard et al., 1986; Beam and Knudson, 1988a; Tsien and Tsien, 1990). In this paper, I describe recordings of single-channel activity from cell-attached patches on the surface of C2 muscle cells developing in culture with the purpose of identifying ion channels which might provide such a pathway. Taking advantage of methods for following myogenesis *in vitro*, I have identified cation channels that open in response to applying suction to the patch electrode. In many recordings, the activity of these channels can be observed at negative membrane potentials in the absence of applied suction. Both types of channel activity increased with patch depolarization. I suggest that Ca^{2+}-permeable, mechanosensitive ion channels may account for Ca^{2+} entry into developing muscle cells.

Methods

Culture of C2 muscle cells

C2 cells were originally isolated from adult mouse skeletal muscle by Yaffe and Saxel (1977) and are cultured according to the methods described by Inestrosa et al., (1983). Cells were grown in plastic tissue culture dishes in Dulbecco's modified Eagle's medium containing 20% fetal calf serum and 0.5% chick embryo extract (growth medium) at 37° C in an incubator containing 95% air/5% CO_2. Cells were passaged at about 75% confluency every 2-3 days to maintain stocks of growing cells. The generation time was roughly 14 hours.

To study the differentiation of myoblasts *in vitro*, undifferentiated myoblasts were plated at low density (~5,000 cells per cm^2) in growth medium. This produced cultures of individual cells from which recordings could be made ~24 hours after plating. Within 2-3 days myoblasts had proliferated and began to align prior to fusion. Replacing the media with Dulbecco's modified Eagle's medium containing 2% calf serum supplemented with 0.4 % insulin (fusion medium) was a sufficient stimulus to cause myoblasts to begin to fuse and form multi-nucleated myotubes (Linkhart et al., 1981; Olson et al., 1986). The culture media was replaced with fresh media every three days or the night before single-channel recording. Cells were routinely maintained in culture for about three weeks.

Electrophysiological methods

Single channel activity was recorded from cell-attached patches on the surface of C2 cells with the technique described by Hamill et al. (1981). Patch pipettes were pulled in two steps from Boralex hematocrit pipettes (Rochester Scientific), coated with Sylgard (Dow Corning), and fire-polished with a microforge. Pipettes had resistances of 2-4 megaohms with 110 mM $BaCl_2$ in the pipette and isotonic potassium-aspartate in the bath.

Membrane current was recorded with a List EPC-7 patch clamp amplifier at constant holding potentials and were stored on video tape. All experiments were done at room temperature (~21-25°C).

Solutions

Standard saline contained 150 mM NaCl, 5 mM KCl, 1 mM $MgCl_2$, 2.5 mM $CaCl_2$, 10 mM N-2-hydroxyethylpiperazine-N'-2-ethanesulfonic acid (HEPES), and 17 mM glucose. Recordings of single-channel activity in the presence of divalent cations were made with patch pipettes filled with either 110 mM $BaCl_2$ or 110 $CaCl_2$, 10 mM HEPES, and 10 mM glucose. Electrode filling solutions for recording single-channel activity in the presence of monovalent cations contained 155 mM of the chloride salt, 5 mM $MgCl_2$, 10 mM HEPES and 10 mM glucose. Gadolinium (>99.9% purity, Aldrich Chemical Co., Milwaukee, WI) was added to the standard saline electrode filling solution directly as the chloride salt. Hydrolysis of gadolinium occurs at pH 7.5 (Smith and Martell, 1976), but because of the uncertainties in the determination of lanthanide affinity constants, the concentration of free trivalent was not calculated (see Lansman, 1990 for discussion). The pH of all solutions was adjusted to 7.5 by adding tetraethylammonium hydroxide (TEA-OH) or NaOH for gadolinium containing standard saline. The osmolarity was adjusted to 320-330 mosM by adding glucose.

The bathing solution was an isotonic potassium solution (K-aspartate) containing 150 mM KOH, 150 mM aspartic acid, 5 mM $MgCl_2$, 10 mM K-EGTA and 10 mM HEPES. The K-aspartate bathing solution was used to zero the cell's resting potential so that the patch potential was identical to the applied voltage command. This was verified by the fact that the single-channel current-voltage relationship measured after patch excision was not measurably different from that obtained prior to excising the patch. The K-aspartate bathing solution produced no detectable signs of cell deterioration.

Data analysis

Current records stored on video tape were replayed onto the hard disk of a PDP 11/73 laboratory computer (Indec Systems, Sunnyvale) for analysis after filtering with an eight-pole Bessel filter. For kinetic analysis, current records were filtered at 1 kHz and digitized at 5 kHz. For plotting current records, the data were filtered at either 0.5, 1, or 2 kHz and digitized at 2.5, 5 or 10 kHz, respectively.

Mean channel open probability was calculated by taking the integral of the current trace and dividing by the unitary current after setting the closed channel level. Channel open and closed times were determined by setting a threshold at half the amplitude of the open channel current (see Colquhoun and Sigworth, 1983). The open channel level was manually set with cursors on the computer display. From the idealized reconstruction of open and closed intervals, histograms of closed times and burst durations were constructed. At least 2-10 minutes of channel activity was obtained at each holding potential for analysis of channel kinetics.

A maximum likelihood fitting routine was used to fit histograms of closed times and burst durations as a sum of exponentials of the form

$$f(t) = \sum a_i \, (1/\tau_i) \exp -t/\tau_i$$

where a_i represents the area of the ith component ($\sum a_i = 1$) and τ_i its time constant (Colquhoun and Sigworth, 1983). Events that were twice the sampling interval were exclude from the histogram and a correction for missed events made during the fitting procedure.

Burst duration histograms were generated from channel open and closed time measurements by setting a cutoff at twice the fastest component of the closed time histogram (figure 4B). Excluding the short closings by assigning this cutoff generated

idealized records of bursts which began and ended at transitions to one of the two longer closed time intervals. Fewer than 1% of the shortest closings which separate individual bursts would be misassigned and so no correction was made for this error. Increasing the cutoff by a factor of two did not alter the distribution of burst durations.

Results

Inward current channels in myoblasts

The possibility that ion channels participate in the early stages of myogenesis by controlling ion fluxes and/or membrane potential at critical stages of development prompted us to investigate the types of channels that are expressed at the earliest stages of muscle development. Two distinct types of channels that carry inward current at negative membrane potentials could be detected in myoblasts plated at low density.

Figure 1 (top record) shows activity corresponding to the immature form of the nicotinic acetylcholine-receptor channel recorded with standard saline containing 500 nM acetylcholine in the patch electrode. The single-channel *i*-V relation gave a slope conductance of ~46 pS and current reversed at ~+12 mV. The nicotinic acetylcholine-receptor channel in C2 myoblasts had a mean open time at -60 mV of ~2.5 ms, somewhat shorter than that reported in rat myotubes (cf Siegelbaum et al., 1984).

In addition to the activity of the nicotinic acetylcholine-receptor channel, I also observed the activity of a novel class of channel that carried inward current at negative membrane potentials in recordings from cell-attached patches (figure 1, bottom). Channel gating was distinctly different from that of the acetylcholine-receptor channel and could be observed in experiments in which the patch electrode did not contain cholinergic agonist.

Ionic selectivity

To compare the activity of this novel channel with other ion channels which carry inward current at negative membrane potentials, I investigated its selectivity to a variety of monovalent and divalent cations. Records of channel activity with monovalent cations in the patch electrode are shown in figure 2a. The single-channel *i*-V relations were linear over a wide voltage range and currents reversed between +10 and +20 mV.

Figure 2a shows that the channel does not show strong selectivity among the various alkali metal ions as judged by either single channel conductance or reversal potential. The conduction properties are similar in both myoblasts and myotubes (figure 2b). Replacing chloride in the electrode filling solution with aspartate or methanesulfonate had no effect on either the channel conductance or the reversal potential, strongly suggesting the channel is not permeable to anions. In some experiments, I observed channel activity with roughly twice the conductance seen in most patches (figure 2a, record with KCl). The large conductance form of this channel was observed in less than 5% of our recordings.

The possibility that the channel provides a pathway for Ca^{2+} entry was tested by recording unitary inward currents through the channel with divalent cations as the only inward charge carrier. Records of channel activity with Ca^{2+} or Ba^{2+} as the inward charge carrier are shown in figure 3a. With 110 mM $CaCl_2$ in the electrode, the slope conductance was 13 ± 1 pS (S.D., n= 8) and current reversed at +22 ± 6 mV; with $BaCl_2$ as the charge carrier, the slope conductance was somewhat larger, 24 ± 4 pS (S.D., n= 7), and current reversed at +17 ± 8 mV (figure 3b). The single-channel current-voltage relation was similar for recordings of channel activity from myoblasts (open symbols) and from multi-nucleated myotubes (solid symbols), suggesting channel selectivity does not change during development.

To evaluate how much Ca^{2+} enters through the cation channel I calculated the relative selectivity of divalent over monovalent cations from reversal potential measurements utilizing the Goldman-Hodgkin-Katz equation modified for divalent cations (see Lee and Tsien, 1984). With 110 mM $CaCl_2$ in the electrode and assuming K^+ to be the predominant intracellular cation, the channel is slightly more permeable to Ca^{2+} than to K^+ with $P_{Ca^{2+}}/P_{K^+} = \sim 2$ (range 1 to 4).

Kinetic analysis of spontaneous channel activity

Figure 4Aa shows the pattern of channel opening on a compressed time scale representing ~1 minute of channel activity recorded while the patch potential was held continuously at -60 mV. Channel activity appeared as bursts of short openings and closings. Individual bursts often occurred in clusters made up of several bursts separated by very long closings. This is shown in figure 4Ab where three bursts (indicated by the bar in figure 4Aa) are replotted on an expanded time scale. Clustering of channel bursts produced periods of intense activity followed by long periods of relative quiescence. This behavior was typical of the activity of this channel in all recordings from cell-attached patches on either myoblasts or myotubes. Figure 4Ac shows the rapid openings and closings within individual bursts on an even more expanded time scale (see legend, figure 4).

To analyze channel gating, I constructed histograms of channel closed times and burst duration from records of channel activity recorded at different holding potentials. Open times were not analyzed because they were poorly resolved. I found that at least three exponential components were necessary to fit the histogram of closed times (figure 4B, left). A fit with two exponentials was insufficient to describe the closed time histogram, while fits with greater than three exponentials did not produce a better fit to the data as judged by the estimate of maximum likelihood. Histograms of burst duration were fit by the sum of two exponential components (figure 4B, right), reflecting the short and long bursts which can be seen in the single channel records (figure 4A). The frequency at which bursts occurred varied considerably from experiment to experiment but did not appear to depend upon the developmental stage at which recordings were made.

Stretch-sensitive gating

Channel activity was often observed to be high shortly after forming a seal, but then decreased with time. This suggested that channels were being activated by mechanical

deformation of the cell membrane during seal formation. To examine the possibility that channel activity occurred in response to a mechanical disturbance of the cell membrane, I applied suction to the patch electrode while recording from both cell-attached and excised membrane patches at a constant holding potential.

Figure 5a shows the effect of applying suction to the patch electrode while recording from a patch of membrane after excising it from the surface of a myoblast. Before applying suction (0 mm Hg, top), there was no detectable single channel activity. Suction was applied to the patch electrode in the sequence shown in the figure. Channel activity first appeared with ~10 mm of Hg of suction and was observed as openings to a discrete current level. Channel activity occurred as bursts of rapid openings and closings separated by well-resolved excursions to the zero current level. The overall pattern of opening and closing resembled that of the activity recorded at steady negative potentials in the absence of applied suction (see *Kinetic analysis of spontaneous channel activity*).

Increasing the suction applied to the electrode increased channel activity. In this experiment, the suction was released following each period during which suction was applied and channel activity returned to zero (not shown). Figure 5b shows the effects on mean channel open probability of the amount of suction applied to the electrode. The natural logarithm of the mean open probability is plotted as a function of the square of the applied pressure (cm^2 of Hg). The relation is more or less linear (cf Guharay and Sachs, 1985; Cooper et al., 1986). Recordings from other patches showed that channel open probability increased with the square of the applied pressure; however the absolute value of the pressure require to open channels varied considerably. Inspecting the current records in figure 5a suggests the increase in open probability with pressure may result from a decrease in the longer closed periods (cf Guharay and Sachs, 1984).

I compared the ion selectivity of the channel activity induced by suction with the channel activity recorded at steady negative membrane potentials in the absence of suction. The results are shown in Table 1 for currents recorded in standard saline or in the presence

of 110 mM $BaCl_2$ or $CaCl_2$. The ion selectivity of the spontaneous channel activity and that produced in response to suction were indistinguishable within the experimental error of the recording method. I tentatively assume that channel activity arises from the same channel type. This issue is taken up further in the Discussion.

I next asked whether the response to suction depends on voltage. Stretch-activated channel activity that increases with depolarization has been described in chick skeletal muscle (Guharay and Sachs, 1985), *E. coli* (Martinac et al., 1987), and yeast (Gustin et al., 1988). Figure 6 shows a recording from a cell-attached patch on a myoblast before and after applying -20 mm of Hg of suction at +40 mV (top traces) and -60 mV (bottom traces). The channel activity induced with suction was greater at the more positive membrane potential (~62% at +40 mV versus ~2% at -60 mV). I noticed that channel activity elicited in response to suction in recordings from cell-attached patches was substantially less than in recordings from excised patches (compare the response to 20 mm of Hg in figures 5 & 6). Because patches were unstable when suction was applied to the patch electrode and frequently ruptured, it was difficult to maintain recordings for sufficiently long times to analyze the response to suction over a wide range of voltages during a single recording. None the less, I consistently found higher levels of channel activity at positive membrane potentials at a given level of applied suction in recordings from both cell-attached and excised membrane patches.

Voltage-sensitive gating

If mechanosensitive channel activity is greater at positive potentials, I wondered whether the spontaneous channel activity recorded from cell-attached patches at negative membrane potentials and in the absence of suction also increases in response to depolarization. Figure 7 shows an example of how channel activity varied with the holding potential in a recording from a cell-attached patch on a myoblast. In this experiment, the patch electrode contained 140 mM CsCl. At negative holding potentials (-90 mV), channel

activity occurred as short bursts of channel openings. At more depolarized potentials (-60 to -10 mV), the amount of time the channel spent open increased. When the patch potential was held at potentials more positive than 0 mV (+20 to +40 mV), the channel was open during most of the recording and closed only occasionally. This recording represents the activity of a single channel because multiple channel openings were not observed, even though channel open probability approached unity at very positive patch potentials.

I believe the same channel carries both the inward and outward currents because the presence of outward current always coincided with the presence of inward current, the current-voltage relationships observed with potassium (also the predominant intracellular cation) in the electrode was linear over the voltage range where the single-channel current reversed direction, and the duration of the rapid closings within bursts of channel activity were identical for both inward and outward currents (below, figure 9, inset).

Mean channel open probability was measured at different holding potentials in four separate cells and is plotted as a function of membrane potential in figure 8. Channel open probability increased as the patch holding potential was made more positive. With holding potentials more positive than 0 mV, the single-channel current became large and outward and the channel was open most of the time. The relation between open probability and membrane potential was fit to a Boltzmann relation with a half-activation voltage $V_{1/2}$ = -9 mV and steepness k = 26 mV. On average, channel activity recorded from cell-attached patches in the absence of suction applied to the electrode increased ~*e*-fold per 38 mV depolarization.

The scatter in the absolute value of mean open probability at any given membrane potential illustrates the considerable cell to cell variability in channel activity which ranged from a low value of ~1% to a maximum of ~25% at -60 mV. The voltage-dependence of channel opening was similar in recordings from myoblasts (open symbols) or myotubes (filled symbols). The species of charge carrier in the electrode filling solution had no obvious influence on channel gating.

Figure 9 shows the individual time constant from the exponential fits to the closed time distribution plotted against the patch holding potential. The briefest component of the distribution of closed times (τ_{Cf}) did not vary over the voltage range of -90 mV to +60 mV. The time constant of the intermediate component of the closed-time distribution (τ_{Ci}) varied from cell to cell; within an experiment, the voltage-dependence was not marked (data not shown). The slowest component of the closed time histogram (τ_{Cs}), on the other hand, depended much more strongly on membrane potential (figure 9).

Inhibition by inorganic cations

The lanthanide cation Gd has been shown to block stretch-activated channels in *Xenopus* oocytes (Yang and Sachs, 1989). I examined the effect of Gd on the spontaneous activity as shown in figure 10. Figure 10a shows recordings of channel activity from cell attached patches in which the electrode contained either 0, 2.5, 5.0, or 7.5 μM Gd. As the concentration of Gd in the electrode was increased, the amplitude of the unitary current was reduced. Gd reduced both the inward and outward current as shown in the *i*-V relationship (figure 10b). However, the reduction of the unitary current appeared to be greater at negative potentials. Figure 10c shows the dose-response relation for the reduction of the unitary current (measured at -60 mV). The concentration of Gd which produced half-inhibition was ~6 μM.

Developmental regulation of channel activity

Because mechanosensitive channels appear to be the only detectable pathway which might carry significant Ca^{2+} current in developing muscle cells, I looked for changes in channel expression during identifiable stages of myogenesis. I recorded single-channel activity from cell-attached patches with physiological saline in the patch electrode at the three distinct stages of myogenesis *in vitro* as indicated in plate 1: solitary myoblasts ~24 hours after plating at low density (plate 1A), myoblasts that had proliferated in culture and

had aligned prior to fusion (plate 1B), and multi-nucleated myotubes (plate 1C). The patch electrode also contained 500 nM acetylcholine so that I could follow the expression of the acetylcholine-receptor channel as a guide to the process of differentiation.

To quantify channel expression, I determined the fraction of the total number of recordings from cell-attached patches which showed spontaneous channel activity in the absence of suction (Spont.), channel activity induced by suction (stretch-activated or SAC), and activity of the acetylcholine-receptor channel at each of the developmental stages shown in plate 1. Approximately twenty to thirty recordings from cell-attached patches were made from cells maintained in parallel cultures at each of the three stages of development. Four replicate sets of cultures were studied. The results of this experiment are shown in figure 11.

Activity of the acetylcholine-receptor channel could be detected in myoblasts as previously reported (Siegelbaum et al, 1984), but the fraction of patches showing channel activity was low, ~8% in recordings from C2 myoblasts plated at low density, but increased significantly to ~83% in recordings from myotubes. Recordings from myotubes, furthermore, showed activity of the larger conductance acetylcholine-receptor channel (Hamill and Sakmann, 1981; Mishina et al., 1986). On the other hand, the frequency of observing either spontaneous channel activity or suction-activated channel activity depended differently on the state of development: suction-activated channel activity was detected far more frequently in solitary myoblasts plated at low density than in myotubes (~80% versus ~30%), while the spontaneous channel activity was detected in roughly the same fraction of patches at each developmental stage.

Discussion

The main finding of this study is that muscle cells at the earliest stages of myogenesis possess a distinct class of ion channel that are more permeable to Ca^{2+} than to either Na^{+} or K^{+}. These channels can be detected in recordings from cell-attached patches by applying suction to the electrode or as spontaneous activity in the absence of suction. That these two forms of activity arise from similar types of channel is supported by measurements of single-channel conductance and reversal potential with either monovalent and divalent cations in the electrode showing that the conductance properties are indistinguishable. The observation that both types of channel activity increase with depolarization further supports this hypothesis.

The origin of the spontaneous channel activity is uncertain. With the present experimental method, I cannot exclude the possibility that it is produced by mechanical deformation of cell membrane during the sealing of the electrode to the cell membrane. In certain instances spontaneous channel activity could be increased with suction applied to the electrode. However, in other cases spontaneous channel activity was unaffected by suction, suggesting that it did not arise as a result of residual tension on the membrane. The insensitivity of some patches showing spontaneous activity to suction may indicate they represent a different class of channel with very similar conductance properties (table 1) and voltage-sensitive gating mechanisms (figure 6 and 7). This, however, is unlikely. Alternatively, channels which were unresponsive to suction may represent mechanosensitive channels which have been newly inserted into the membrane and are not yet linked into the tension-sensing apparatus of the cell or may indicate channels which are unable to perceive changes in tension due to the configuration of the membrane bleb within the patch electrode.

The channels in C2 myoblasts and myotubes are similar to the stretch-activated channels described in embryonic skeletal muscle (Brehm et al., 1984; Guharay and Sachs, 1984,1985). They are cation-selective and have a conductance in physiological saline of 30-35 pS. Like the stretch-activated channels in chick muscle, channel open probability depended linearly on the square of the applied pressure suggesting a model in which mechanical work on a linear elastic element provides the energy for channel gating (Sachs, 1989).

The mechanosensitive channels previously described in chick skeletal muscle (Guharay and Sachs, 1985) and the channels reported here show similar voltage-sensitivities, increasing *e*-fold for ~45 and ~38 mV depolarization, respectively. The mechanism of the voltage-sensitive gating appears to involve a shortening of the longest closings (figure 9) which is also consistent with the results of Guharay and Sachs (1985). On the other hand, the gating of the mechanosensitive channel in *E. coli*, which is anion selective, depends more steeply on membrane potential, changing *e*-fold for ~15 mV in membrane potential (Martinac et al., 1987). The voltage-sensitive gating mechanism of the mechanosensitive channels in C2 cells does not involve voltage-dependent block by Mg^{2+} as it was observed when Mg^{2+} was omitted from the electrode recording solution. I conclude that the voltage dependence involves an inherent gating mechanism.

Current through the mechanosensitive channels described in C2 muscle cells would be difficult to detect while recordings whole-cell currents. Because current through these channels reverses near 0 mV and responds relatively slowly to depolarization, it would resemble the leakage current which flows through both the cell membrane and the seal resistance. At the single channel level, however, channel activity was a consistent finding in recordings from cell-attached patches.

Physiological significance:

Myogenesis

The channels described in this paper are likely to provide a significant pathway for Ca^{2+} influx into developing muscle cells. My results indicate that mechanosensitive channels are expressed at their highest density in unaligned myoblasts (~80% of the patches examined; figure 11). At negative membrane potentials where the driving force for Ca^{2+} entry is high, these channels could support significant Ca^{2+} influx into myoblasts. It is also known that myoblasts fusion (Shainberg et al., 1969; Knudsen and Horwitz, 1977; Konieczny et al., 1982) and subsequent biochemical differentiation (Konieczny et al., 1982; Endo and Nadal-Ginard, 1987) are dependent upon extracellular Ca^{2+}. It is interesting to speculate that myoblast- and myotube-specific gene expression are differentially dependent on Ca^{2+}. In other words, when mechanosensitive channel density is high and Ca^{2+} influx possibly at its greatest, myoblast-specific gene expression would be favored. On the other hand, a reduction of Ca^{2+} influx may be the trigger that induces the expression of myotube-specific genes, but would be first contingent upon myoblast-specific gene expression.

The differentiation of myoblasts into multi-nucleated myotubes is associated with large changes in the density of mechanosensitive channels (figure 11). Although my experiments provide no direct information on the mechanism responsible for the changes in channel density, the results are consistent with muscle differentiation being associated with a large reduction in the number of mechanosensitive channels just prior to myotube formation. Growth factors or other autocrine agents may serve to modulate the transcription of those genes coding for proteins that makeup, or regulate the activity of, mechanosensitive channels and in this way modulate Ca^{2+} influx and subsequent morphological and biochemical differentiation. In accordance with this idea, removing growth factors (embryo extract) from the culture media results in cardiac myocytes which do not express mechanosensitive channels nor mechanically-mediated Ca^{2+} fluxes

(Martinac, 1993). Generally, the presence of growth factors is correlated with changes in gene transcription and an influx of Ca^{2+} (Endo and Nadal-Ginard, 1987; Kojima et al., 1988; Roe et al., 1989).

Changes in the way mechanosensitive channels perceive tension either through changes in how they respond to tension or, alternatively, in how tension is distributed across the membrane of myoblasts may alter Ca^{2+} entry through mechanosensitive channels. The energy in deforming the membrane is thought to be conveyed to mechanosensitive channels through an association with the cell cytoskeleton (Guharay and Sachs, 1984; Sachs, 1989). One component of the skeletal muscle cytoskeleton, dystrophin (Monaco et al., 1986; Koenig et al., 1987, 1988), has been shown to be developmentally regulated. Dystrophin transcripts are undetectable in myoblasts but become first apparent following the formation of myotubes (Lev et al., 1987; Nudel et al., 1988; Oronzi-Scott et al., 1988). I will later show evidence that muscle cells which genetically lack dystrophin (Bulfield et al., 1984) show elevated activity of mechanosensitive channels at later stages of development (Chapters 2 and 3; see also below) and fuse less readily when compared to wild type muscle cells (Delaporte, 1984; Tautmann et al., 1986). In addition, fibroblasts lacking dystrophin maintain a higher proliferative capacity than wild type cells (Fingerman et al., 1984). Therefore, in a developmentally-specific fashion myoblasts not yet expressing dystrophin may express elevated levels of mechanosensitive channel activity which may in turn regulate the rate at which they withdraw from the cell cycle to fuse and differentiate (Chapter 3).

Substrate-associated changes in membrane tension may also influence the activity of mechanosensitive channels. Focal contacts (adhesion plaques), made by the cell with the substrate, exert tension on the cell membrane through cytoskeletal stress fibers which radiate from the site of substrate contact. Increased expression of focal contacts with the substrate is correlated with increased rates of cell division (O'Nell et al., 1990) and are present at their highest density in myoblasts prior to alignment (Lakonishok et al., 1992).

These results suggests that increased membrane tension, as indicated from the number of focal contacts made with the substrate, can increase the rate of cell-division. There is also evidence that physically stretching the cell substrate can stimulate proliferation (DeWitt et al., 1984; Sumpio et al., 1987).

Although the expression of cellular organelles, such as focal contacts, may modulate how cells respond to tension, changes in the makeup of the substrate may also influence the activity of mechanosensitive channels. The extracellular matrix protein, laminin, is a major component of the basement membrane of skeletal muscle (Sanes and Cheney, 1982). The basement membrane is essential not only for the formation of adult skeletal muscle but also for regeneration (Anglister et al., 1985). Interestingly, laminin is also known to induce the proliferation and subsequent differentiation of myoblasts in culture (Ocalan et al., 1988). I have also shown that the activity of mechanosensitive channels is higher in muscle cell cultures grown in the presence of laminin (Chapter 3, figure 8). I, therefore, propose that the mitogenic effects of laminin are mediated through increases in the amount of contact made with the substrate, increasing membrane tension and the activity of mechanosensitive channels.

Differences in substrate (extracellular matrix) "stickiness" may also exist between different cell types and the interstitial space. It is intriguing to speculate that increasing contact between myoblasts, as would occur during proliferation, may relieve membrane tension thereby reducing Ca^{2+} entry through mechanosensitive channels and possibly reducing the transcription of those genes coding for mechanosensitive related proteins. In this manner myoblasts proliferating *in vitro* (Wakelam, 1985) or *in vivo* in response to muscle injury (John and Jones, 1988) may autoregulate the rate at which they grow and subsequently fuse to form myotubes. However, how membrane tension, Ca^{2+} influx and growth factors interplay to regulate the cell cycle in myoblasts is at this point merely speculation. Finally, although acetylcholine receptors are permeable to Ca^{2+}, they are present in myoblasts at much lower densities (figure 11) and their permeability to divalent

cations is relatively small (Bregestovsky et al.,1979; Adams et al., 1980; Decker and Danni, 1990).

Table 1-1

Ion selectivity of stretch-activated and spontaneously active channel activity.

	Stretch-activated channel			Spontaneously active channel		
	γ (pS)	E_{rev} (mV)	n	γ (pS)	E_{rev} (mV)	n
Isotonic Calcium	16.0 ± 2.0	21.0 ± 11.0	4	13.0 ± 1.0	22.0 ± 6.0	8
Isotonic Barium	20.0 ± 3.0	20.0 ± 3.0	4	24.0 ± 4.0	17.0 ± 8.0	7
Saline	37.0 ± 3.0	10.0 ± 5.0	4	34.0 ± 1.0	14.0 ± 3.0	3

γ, single-channel conductance; E_{rev}, reversal potential; n, number of experiments; ± S.D.
Isotonic divalent recordings where made with 110 mM solutions of the chloride salt (see Methods).

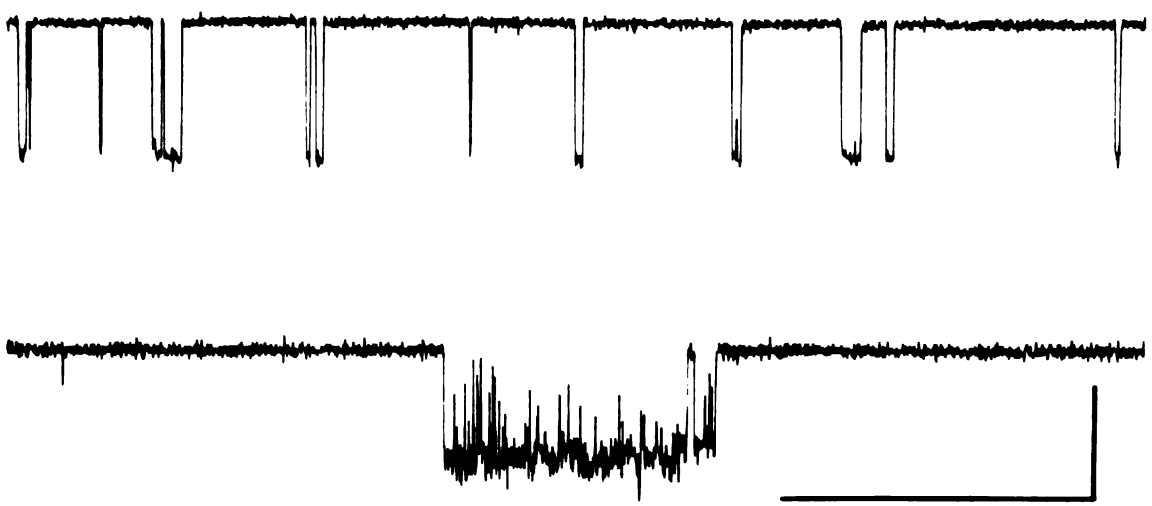

Figure 1-1. A novel cation channel is observed in cell-attached recordings from C2 myoblasts. Single-channel activity recorded from cell-attached patches from the surface of C2 myoblasts with standard saline containing 0.5 mM acetylcholine in the patch electrode. Top record, immature form of the acetylcholine-receptor channel; bottom record, novel, inward current channel. The holding potential = -50 mV. Horizontal scale bar = 200 msec; vertical bar = 2 pA.

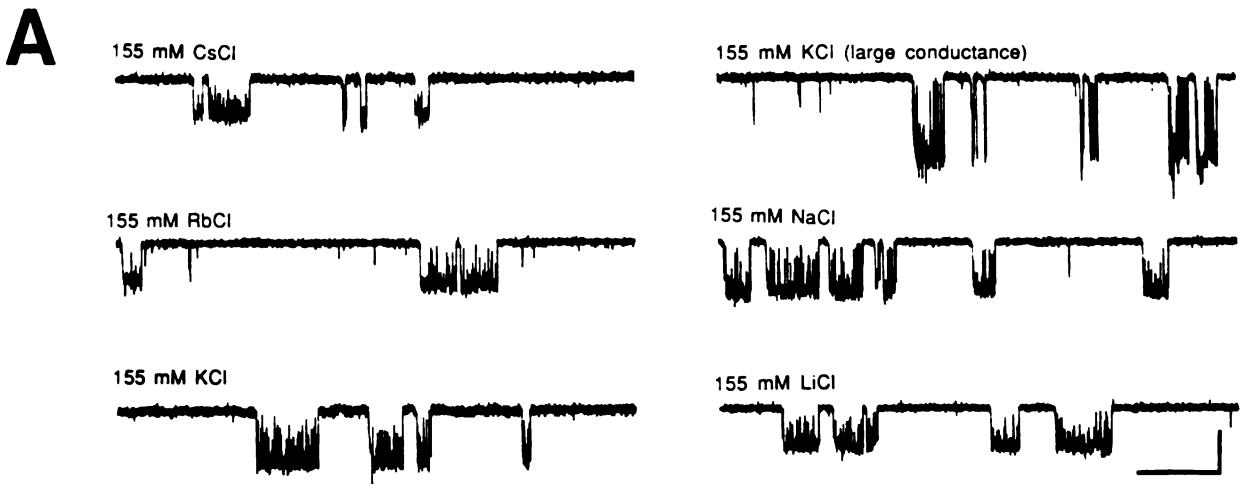
A
155 mM CsCl
155 mM KCl (large conductance)
155 mM RbCl
155 mM NaCl
155 mM KCl
155 mM LiCl

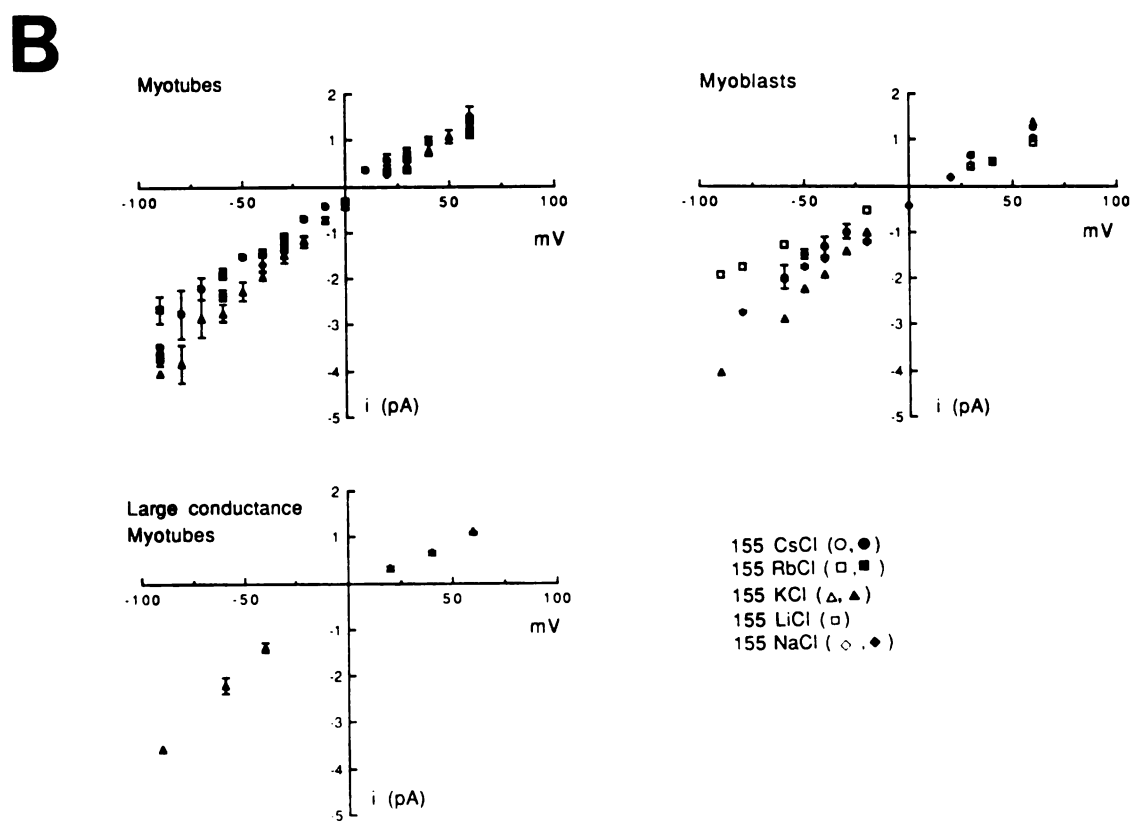
B
Myotubes
Myoblasts
Large conductance
Myotubes
-100
-50
50
100
mV
i (pA)
2
1
-1
-2
-3
-4
-5
155 CsCl (○,●)
155 RbCl (□,■)
155 KCl (△,▲)
155 LiCl (▫)
155 NaCl (◇,◆)

Figure 1-2. The myoblast channel is permeable to monovalent cations. Unitary current carried by monovalent cations. **A**). Records of single-channel activity from cell-attached patches with either 155 mM-LiCl, NaCl, KCl, RbCl or CsCl as indicated. Holding potential was -50 mV. Horizontal scale bar = 200 msec; vertical bar = 2 pA. **B**) Current-voltage relationships with monovalent cations in the electrode. Open symbols (left), recordings from myoblasts; filled symbols (right), recordings from myotubes. Bottom, *i*-V for large-conductance channel in the presence of KCl.

Conductance and reversal potentials for myotubes were: LiCl, 27 ± 5 pS and 14 ± 4 mV (n=5); NaCl, 32 ± 6 pS and 14 ± 8 mV (n=5); KCl (small conductance), 35 ± 8 pS and 16 ± 4 mV (n=5); KCl (large conductance), 57 ± 4 pS and 5 ± 4 mV (n=4); RbCl, 38.5 ± 6 pS and 7.5 ± 8 mV (n=4); CsCl, 29 ± 5 pS and 6 ± 4 mV (n=5). Conductance and reversal potentials for myoblasts were: NaCl, 24 ± 5 pS and 19 ± 10 mV (n=5); KCl, 40 ± 6 pS and 10 ± 2 mV (n=4); RbCl, 18 pS and 9 mV (n=1); CsCl, 26 ± 2 pS and 5 ± 3 mV (n=3).

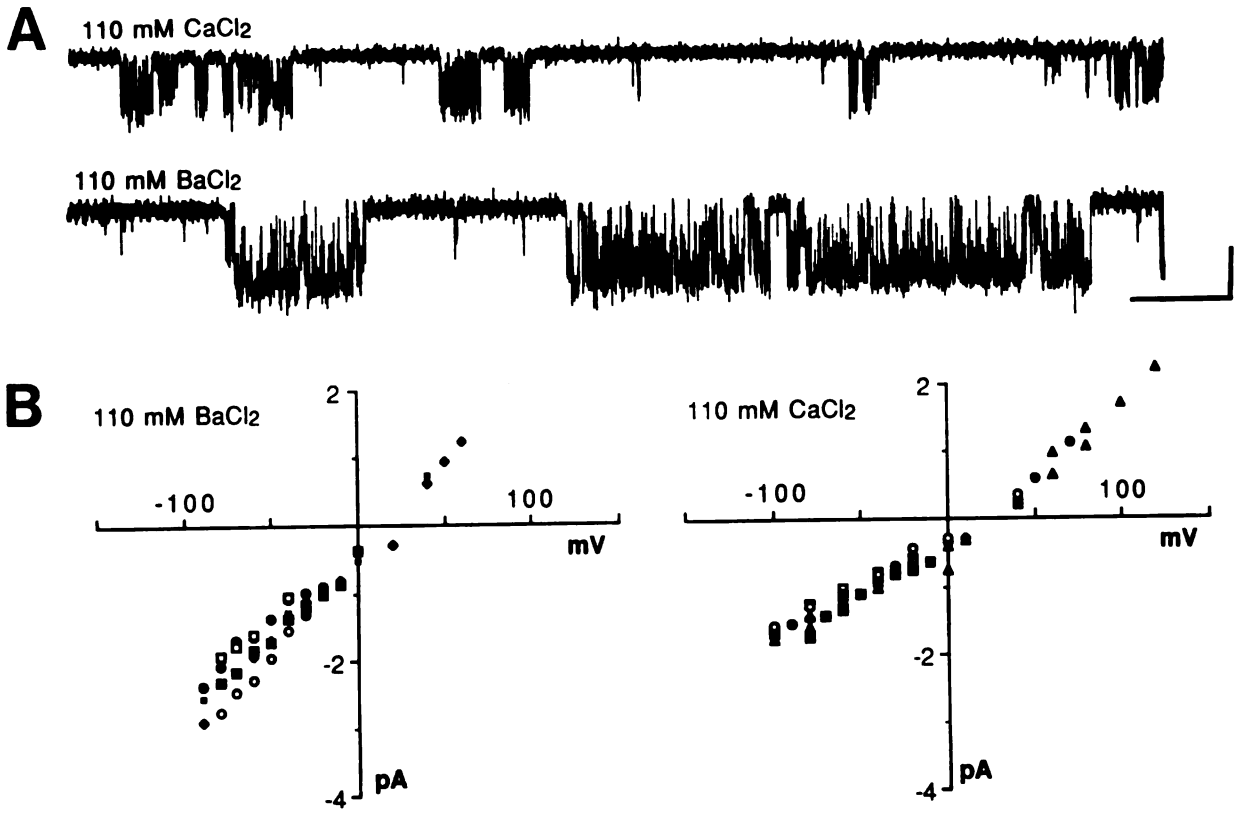

Figure 1-3. The myoblast channel is also permeable to divalent cations. Unitary currents carried by divalent cations. A) Recordings from cell-attached patches on a myoblast with 110 mM $CaCl_2$ (top record) and a myotube with 110 mM $BaCl_2$ (bottom record) in the electrode. Holding potential = -60 mV. Horizontal scale bar = 200 msec; vertical bar = 1 pA. B) Current-voltage relationships for recordings of channel activity with either 110 mM $BaCl_2$ or 110 mM $CaCl_2$ in the electrode. Filled symbols represent recordings obtained from myotubes; open symbols represent recordings obtained from myoblasts. Different symbols represent recordings from different patches.

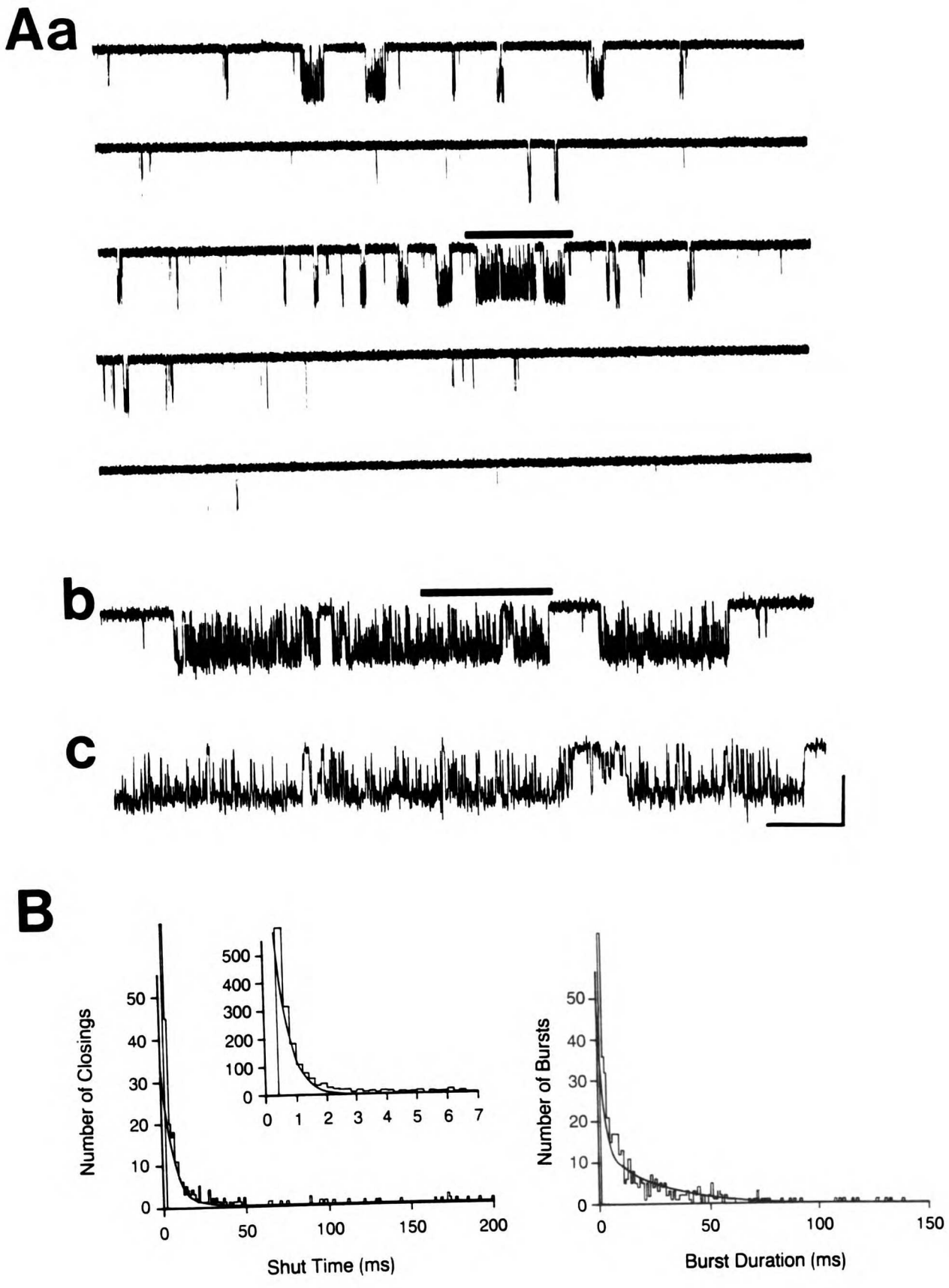
Aa
b
c
B
Number of Closings
Shut Time (ms)
Number of Bursts
Burst Duration (ms)

Figure 1-4. The myoblast channel shows a characteristic pattern of gating. Examples of spontaneous channel activity at negative holding potentials recorded at three different time resolutions. The recording was from the surface of an aligned myoblast with the patch potential held at -60 mV. The patch electrode contained 110 mM $BaCl_2$. **Aa)**, five sequential current traces corresponding to ~1 minute of channel activity filtered at 500 Hz and digitized at 2.5 kHz; **Ab)**, an expansion of the record marked with a bar in (**Aa**) filtered at 1 kHz and digitized at 5 kHz; **Ac)**, an expansion of the record marked by a bar in (**Ab**) filtered at 2 kHz and digitized at 10 kHz. Horizontal calibration bar = 1.2 sec in (**Aa**), 200 msec in (**Ab**), and 40 msec in (**Ac**). Vertical scale bar = 2 pA. **B)** Analysis of the kinetics of channel activity at a constant holding potential. Left, histogram of closed times were fitted with the sum of three exponentials, designated as fast (τ_{Cf} = 0.63 ms), intermediate (τ_{Ci} = 3.3 ms) and slow (τ_{Cs} = 1313.0 ms) components. The continuous curve shows the maximum likelihood fit with three exponential components. **Inset,** expansion showing the fit to the fastest closings. Right, histogram of burst duration fitted as the sum of two exponential compoents, designated as short (τ_{bs} = 0.85 ms) and long (τ_{bl} = 23.2 ms). Continuous lines represent the two exponential maximum likelihood fit to the entire histogram of burst durations.

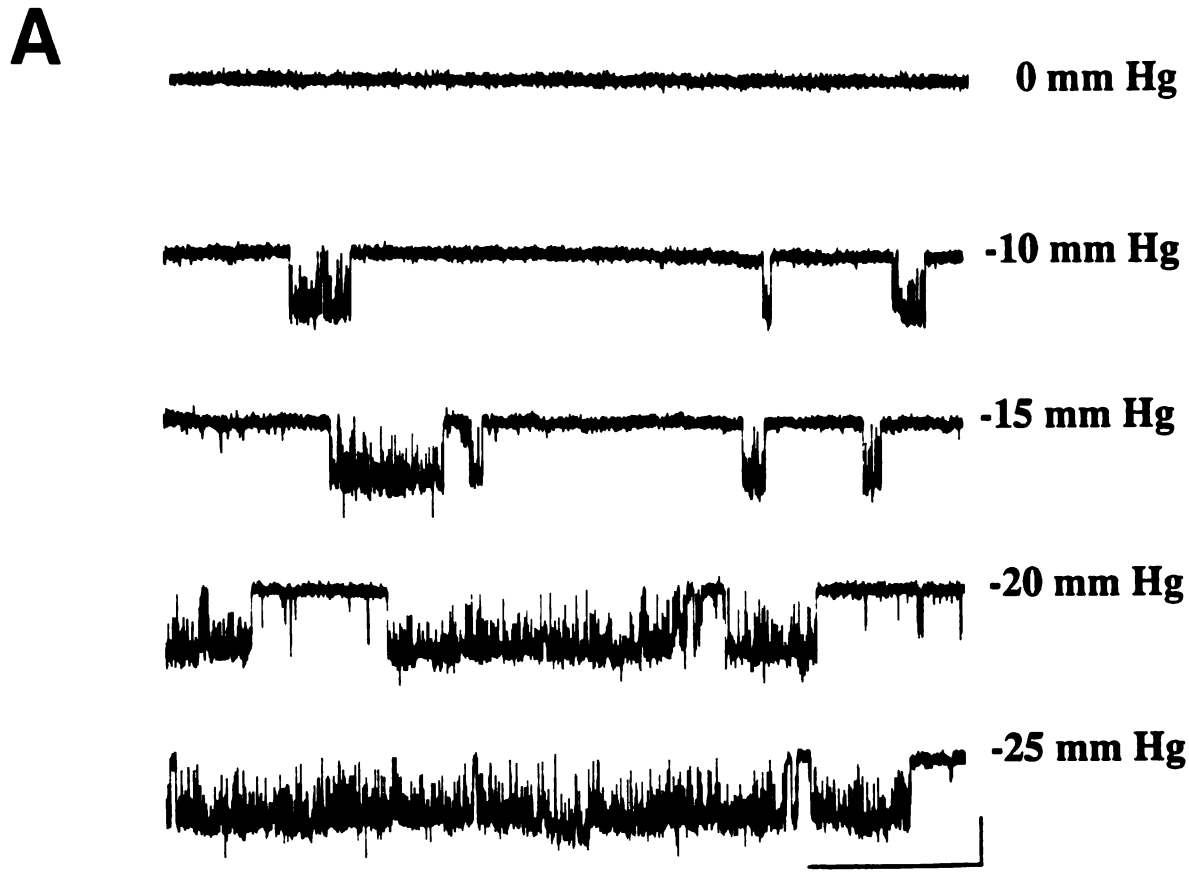
A
0 mm Hg
-10 mm Hg
-15 mm Hg
-20 mm Hg
-25 mm Hg
B
2.0
1.5
1.0
0.5
0.0
ln open probability
0
2
4
6
8
P2 (cm2 Hg)

Figure 1-5. The myoblast channel is a mechanosensitive channel. A) recording from an excised patch of membrane (inside-out) from a myoblast in which there was no channel activity in the absence of applied suction. Suction was applied to the patch electrode (pressure indicated next to record in mm of Hg) and channel activity recorded. After each recording, the suction was released and channel activity returned to zero (not shown). Horizontal scale bar = 200 msec; vertical bar = 1 pA. **B)** The natural logarithm of the mean channel open probability plotted as a function of the square of the applied pressure (cm of Hg^2).

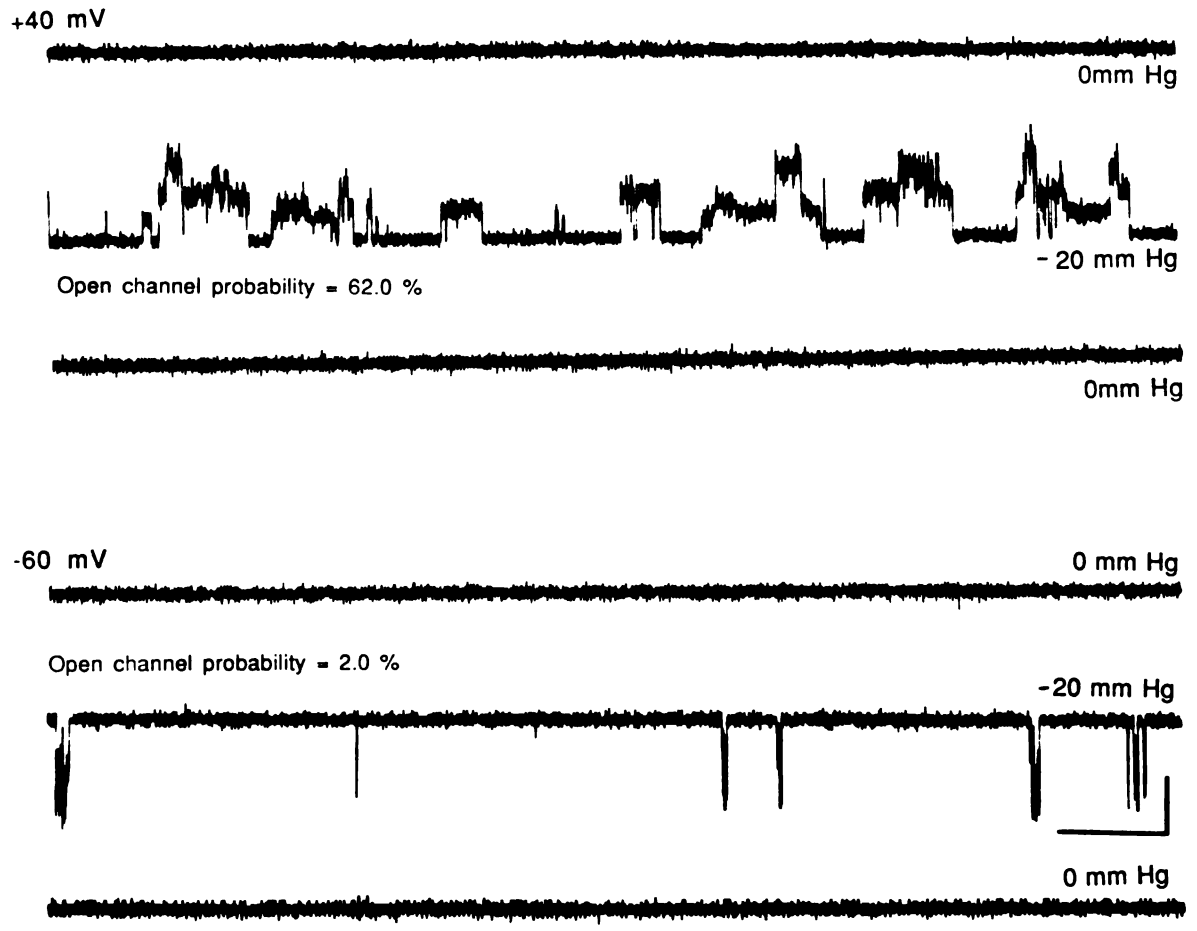

Figure 1-6. Depolarization of the patch membrane potential increases the probability that mechanosensitive channels will open when suction is applied to the electrode. Recording of channel activity from a cell-attached patch on a myoblast. The records show channel activity before and after applying 20 mm of Hg of suction to the electrode. The patch was held at +40 mV (top record) and -60 mV (bottom record). Horizontal scale bar = 200 msec; vertical bar = 2 pA. The patch electrode contained normal saline.

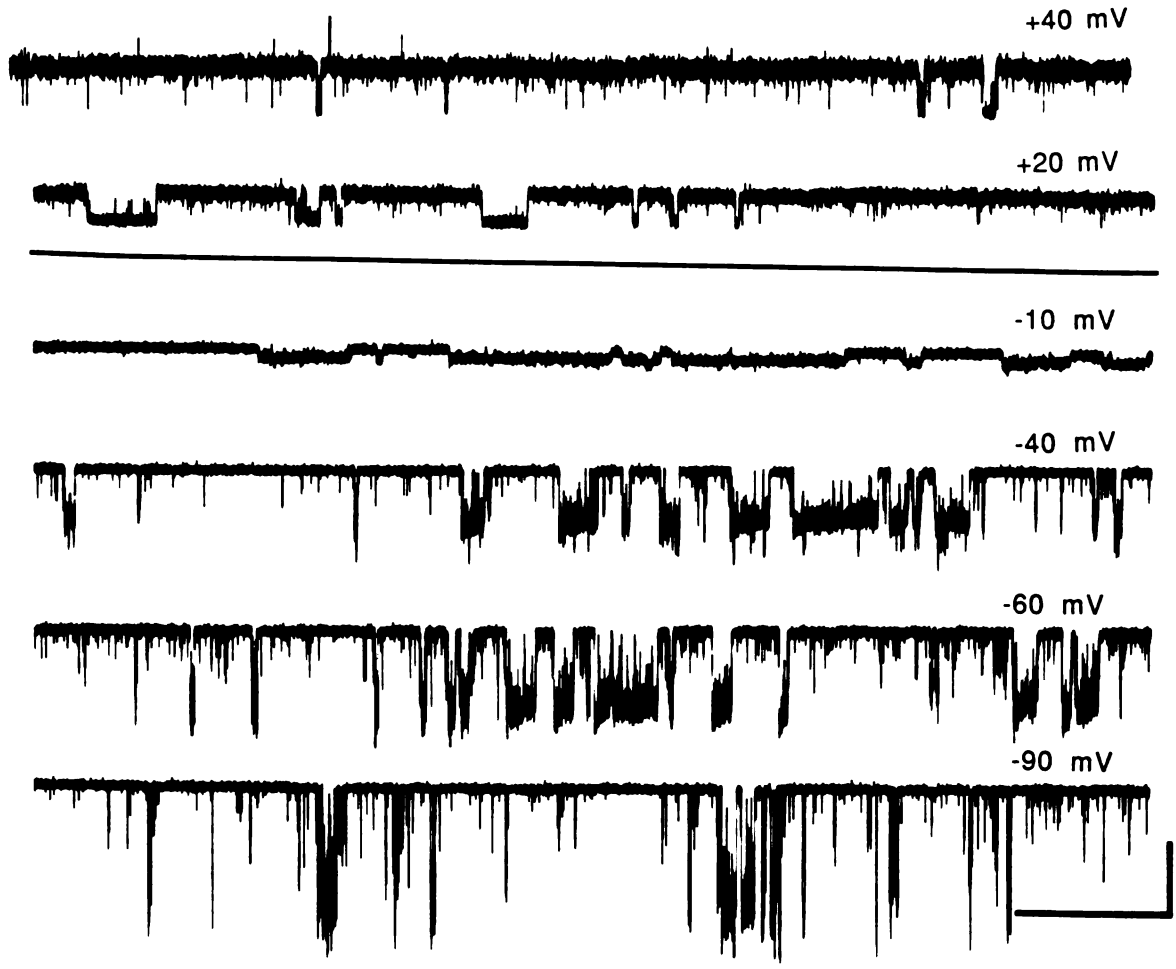

Figure 1-7. Increase in channel activity in response to depolarization for a spontaneously active channel. Recording from the surface of an aligned myoblast with 140 mM CsCl in the electrode. Mean channel open probabilities were: ~9% at -90 mV; 25% at -60 mV; 20% at -40 mV; 89% at 20 mV; 98% at 40 mV. Currents traces were filtered at 500 Hz and digitized at 2.5 kHz; for kinetic analysis, currents were filtered at 1 kHz and digitized at 5 kHz. Horizontal scale bar = 2 sec; vertical bar = 2 pA.

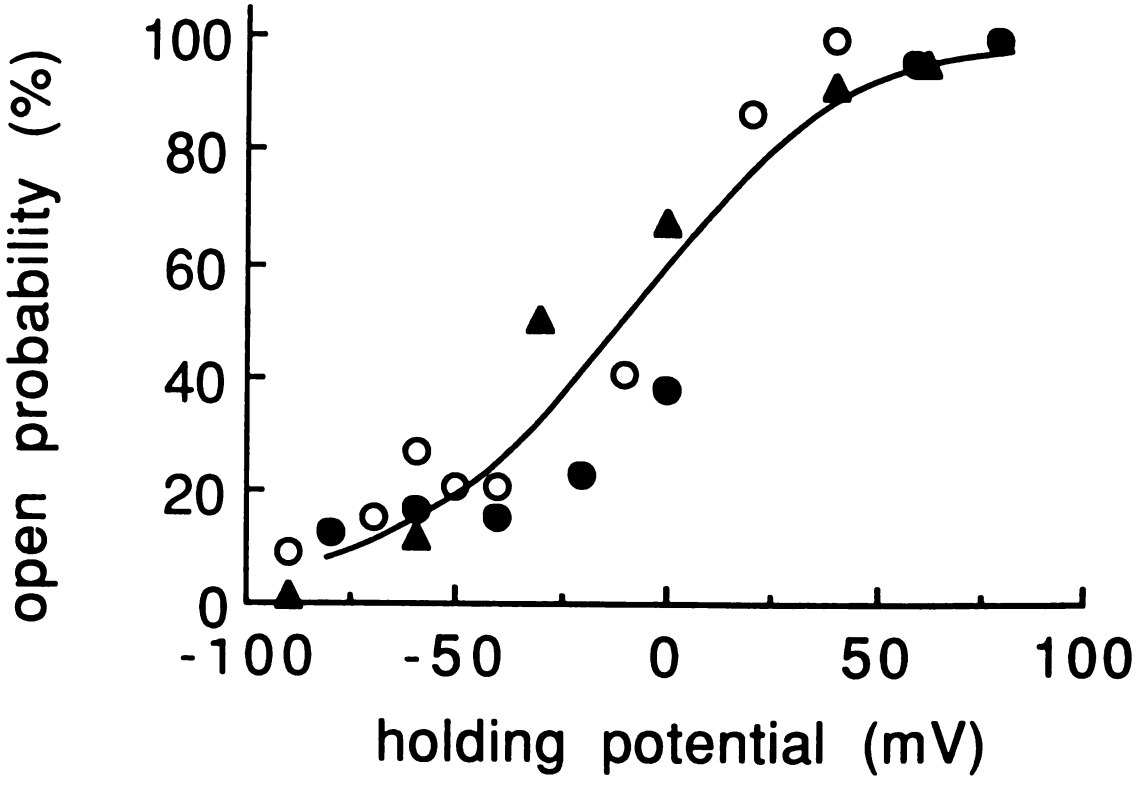

Figure 1-8. Channel open probability as a function of membrane potential in recordings of spontaneous channel activity. Smooth curve drawn through the experimental points represents the fit to a Boltzmann equation of the form $1/1+\exp-(V-V_{1/2})/k$, where $V_{1/2}$ = -9.3 mV and k = 26 mV). Different symbols represent recordings from different cells. Recordings from cell-attached patches on myoblasts (open circles, 140 mM CsCl; filled circles, 110 mM $CaCl_2$) and a myotube (filled triangles, 110 mM $BaCl_2$).

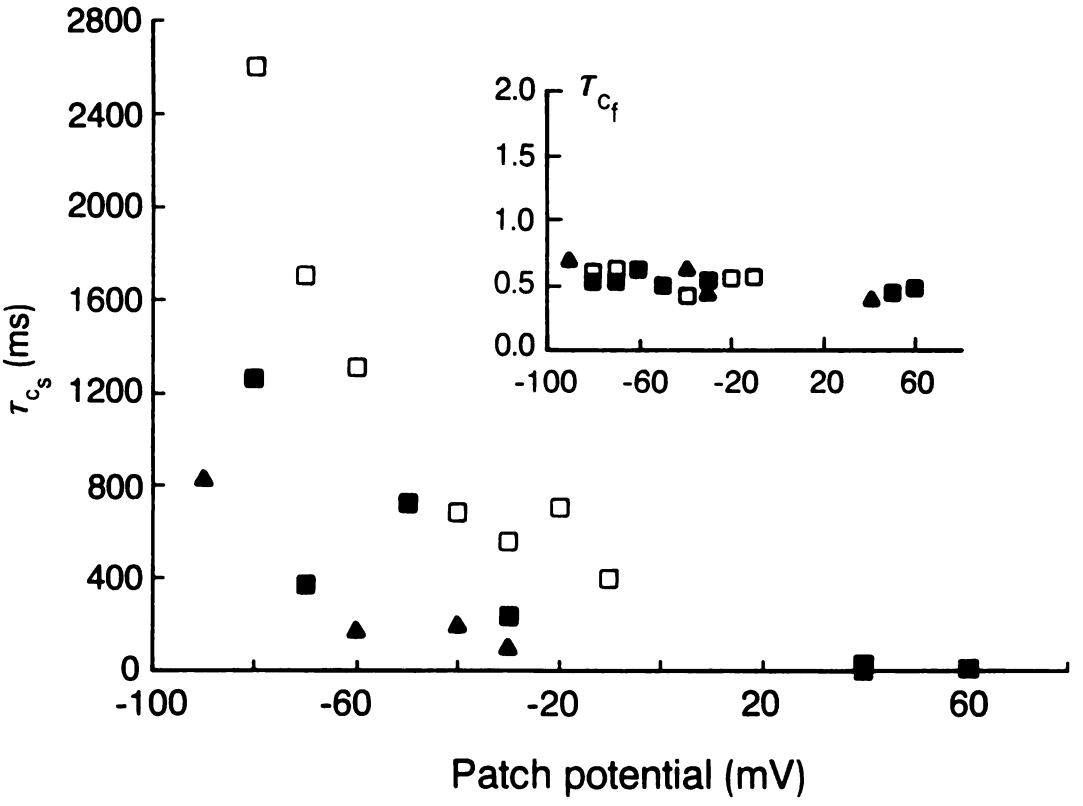

Figure 1-9. Depolarization of the patch membrane potential decreases the duration of the longest closed time. Individual time constants were obtained from the three exponential fit to the entire closed time distribution and plotted as a function of patch holding potential. A) Slow component of the closed time histogram (τ_{cs}) plotted as a function of the patch potential. Filled triangles and open squares represent recordings from an early myotube and an aligned myoblast with 110 mM $BaCl_2$ in the electrode, respectively; (filled squares), recording from an early myotube with 155 mM KCl in the electrode. **Inset**, fast (τ_{cf}) component of the closed time histogram plotted as a function of the patch potential.

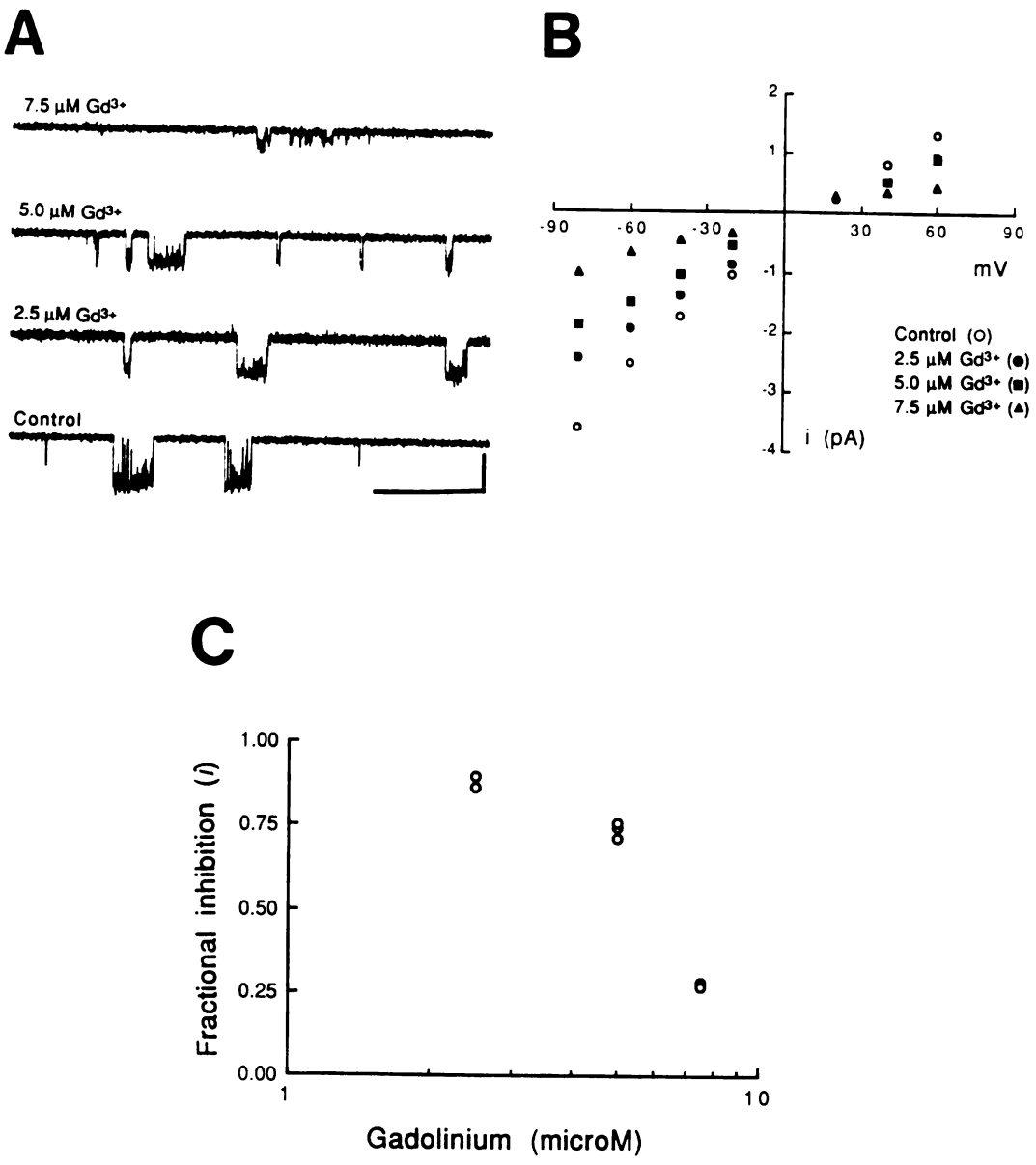

Figure 1-10. Gadolinium blocks single-channel current through mechanosensitive channels. A) Records of channel activity from different patches in which the electrode contained either 0, 2.5, 5.0, or 7.5 μM Gd as indicated. Horizontal scale bar = 200 msec; vertical bar = 2 pA. B) Single channel *i*-V relation for the experiment shown in (A). C). The single-channel current in the presence of Gd normalized to the current in its absence plotted as a function of the concentration of Gd.

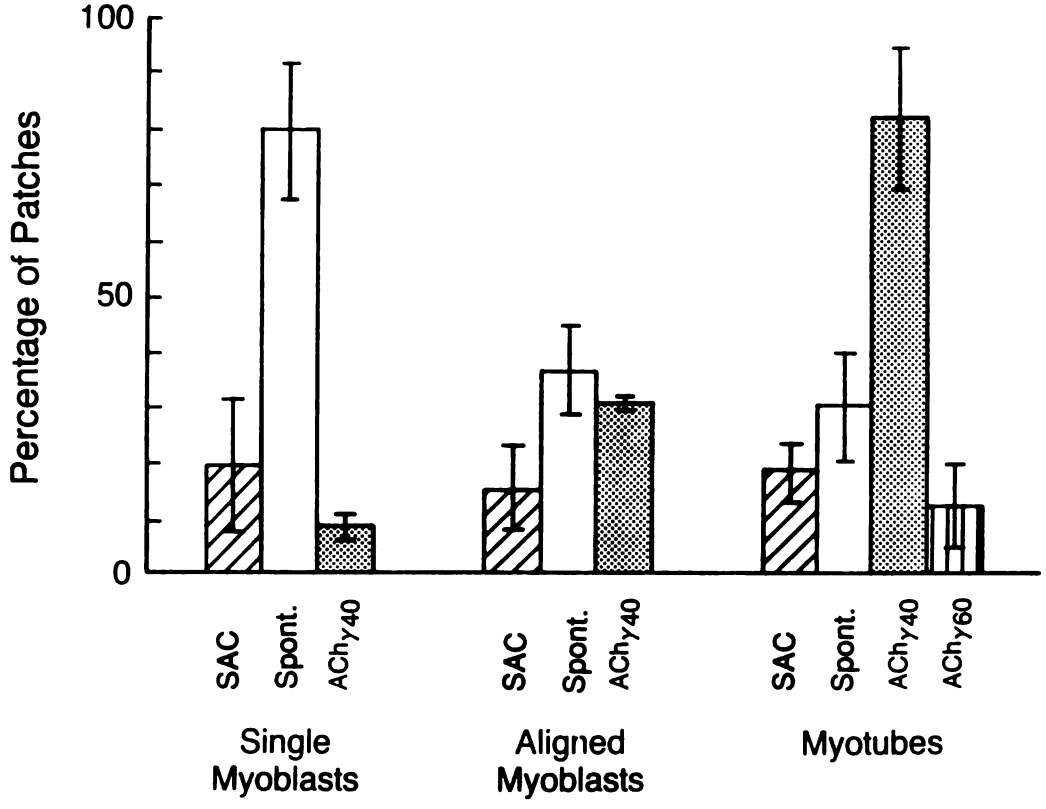

Figure 1-11. The expression of mechanosensitive channels appears to be developmentally regulated. Fraction of patches containing the acetylcholine-receptor channel, stretch-activated channel, and spontaneous channel activity at each developmental stage. $ACh_{\gamma 40}$ and $ACh_{\gamma 60}$ refer to the small (embryonic) and large (adult) conductance acetylcholine-receptor channels (Hamill and Sakmann, 1981; Mishina et al., 1986). "Stretch-activated" (SAC) corresponds to channel activity induced by applying suction to the electrode; "Spontaneous" (Spont.) indicates spontaneous channel activity that was detected in the absence of suction. Three separate cultures of C2 cells were sampled at each developmental stage (twenty to thirty patches).

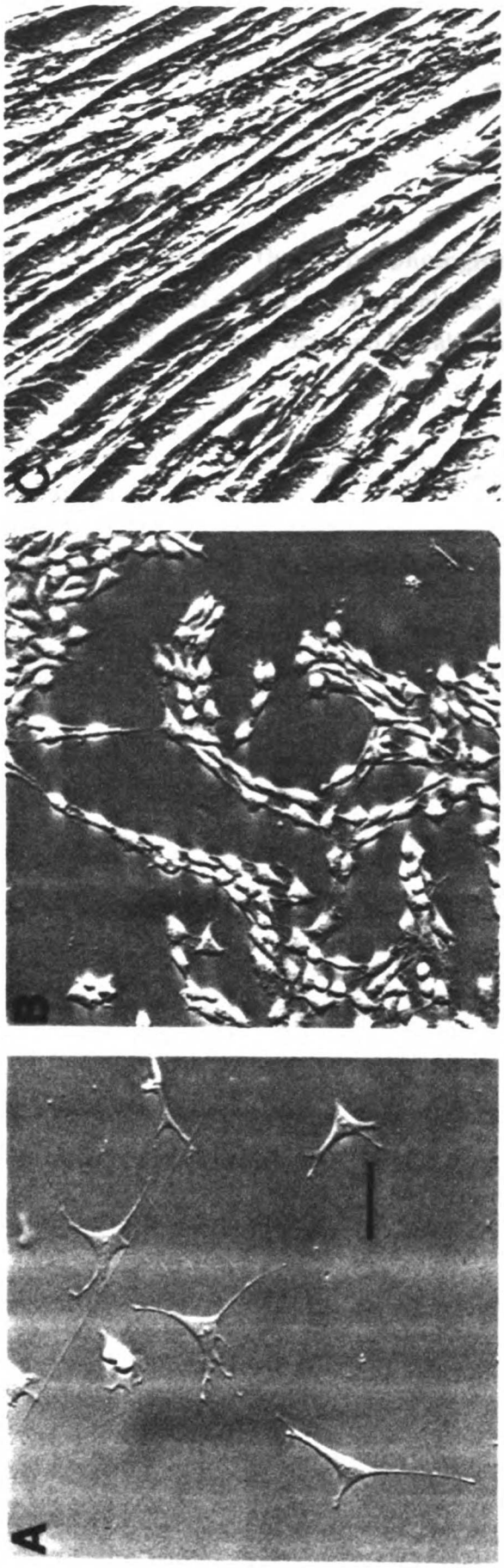
C
B
A

Plate 1-1. Photomicrographs of the three morphologically-distinguishable stages during which recordings were made: (A) myoblasts plated at low density, (B) myoblasts that had proliferated for several days and had aligned prior to fusion, (C) multi-nucleated myotubes. Scale bar = 10 μm.

Chapter 2

Calcium entry through stretch-inactivated ion channels in *mdx* myotubes: a pathophysiological mechanism for muscular dystrophy

Introduction

Recent advances in understanding the molecular basis of human X-linked muscular dystrophies (reviewed in Hoffman and Kunkel, 1989) has come from the identification of dystrophin, a cytoskeletal protein associated with the surface membrane (Knudson et al., 1988; Watkins et al., 1988; Campbell and Kahl, 1989). Although dystrophin is reduced or virtually absent in affected individuals (Webster et al., 1988; Bonilla et al., 1988), it is not known how this causes muscle degeneration. One possibility is that the membrane of dystrophic muscle is weakened and becomes leaky to Ca^{2+} (Bodensteiner and Engel, 1978; Fingerman et al., 1984; Mongini et al., 1988). In muscle from *mdx* mice, an animal model of the human disease (Bulfield et al., 1984), intracellular Ca^{2+} is elevated and associated with a high rate of protein degradation (Turner et al., 1988). The possibility that a lack of dystrophin alters the resting permeability of skeletal muscle to Ca^{2+} prompted us to compare Ca^{2+}-permeable ionic channels in muscle cells from normal and *mdx* mice. Recordings of single channel activity from *mdx* myotubes are dominated by the presence of Ca^{2+}-permeable mechanotransducing ion channels. Like similar channels in normal skeletal muscle, they are rarely open at rest, but open in response to stretching the membrane by applying suction to the electrode (Brehm et al., 1984; Guharay and Sachs, 1984; Franco and Lansman, 1990). Other channels in *mdx* myotubes, however, are frequently found to be open for extended periods of time at rest and close in response to

applying suction to the electrode. The results show a novel type of mechanotransducing ion channel in *mdx* myotubes that may provide a pathway for Ca^{2+} to leak into the cell.

Methods

Muscle cell preparation

Myotubes were prepared by dissecting hind limb or cutaneous pectoris muscles from seven day old normal C57B controls or *mdx* mice (Jackson Laboratory) after sacrificing by cervical dislocation. The muscle was minced and incubated for ~15 minutes at 37° C in Ca^{2+}- and Mg^{2+}-free Hank's buffer containing 0.125% trypsin. Cells were dissociated by passing through a small bore pipette and filtered through 100 μm gauze. The suspension was preplated for ~1 hour to remove fibroblasts, after which the remaining cells in suspension were plated on gelatin coated tissue culture dishes at a density of ~5,000 cells per cm^2 in DMEM supplemented with 20% fetal calf serum and chick embryo extract. Myoblasts began to fuse and form myotubes after ~4-5 days in culture. Recordings were made from myotubes 1-5 days after the first myotubes formed.

Solutions

Isotonic barium and calcium solutions contained 110 mM of the chloride salts with 10 mM N-2-hydroxyethylpiperazine-N'-2-ethanesulfonic acid (HEPES). The bathing solution was an isotonic potassium aspartate solution (K-aspartate) containing 150 mM KOH, 150 mM aspartic acid, 5 mM $MgCl_2$, 10 mM K-EGTA and 10 mM HEPES. The pH of all solutions was adjusted to 7.5 by adding NaOH. The osmolarity of all solutions was adjusted to 320-330 mosM by adding glucose.

The K-aspartate bathing solution was used to zero the cell's resting potential so that the patch potential would be equal to the applied voltage command. Measuring the single-channel current-voltage relationship before and after patch excision indicated a maximum voltage error of ~5 mV, but often produced no voltage offset. The K-aspartate bathing solution produced no detectable signs of cell deterioration.

Electrophysiological methods

Single channel activity was recorded from cell-attached patches with the technique described by Hamill et al. (1981). Patch electrodes were pulled in two steps from Boralex hematocrit pipettes (Rochester Scientific), coated with Sylgard (Dow Corning), and the tips heat polished with a microforge. Membrane currents were recorded with a List EPC-7 patch clamp amplifier. Current records were stored on video tape and replayed onto the hard disk of a laboratory computer (LSI 11/73) for analysis. Current records were filtered with an eight-pole Bessel filter (-3 dB at 1kHz) and digitized at 5-10 kHz. Unless otherwise noted, all cell-attached recordings were made at a constant holding potential of -60 mV and at room temperature (~21-25°C). A holding potential of -60 mV was chosen because it is near the physiological resting potential of myotubes in culture (data not shown).

Data analysis

Channel open probability was measured by integrating idealized reconstructions of channel openings and closings which were determined by setting a threshold at half the amplitude of the open channel current (Colquhoun and Sigworth, 1983). My best results in measuring mechanosensitive channel activity was obtained by using electrodes of intermediate size (2.5-4.5 MΩs when filled with 110 mM $BaCl_2$ and immersed in the bath), however, membrane patches of this diameter (1-2 microns) often contained several channels. Since the number of channels per patch varied, the resting activity represents the product of the number of channels per patch of membrane (N) and the open probability of each individual channel (P_o) , or NP_o, and was calculated from an approximately 1-2 minute segment of continuous channel activity.

Results

I recorded single channel activity from cell-attached patches on myotubes from normal and *mdx* mice with 110 mM $BaCl_2$ in the patch electrode. Figure 1A shows a continuous record of single channel activity recorded approximately one minute after the patch electrode formed a seal on the surface of a myotube from normal mouse muscle. At a holding potential of -60 mV, the single channel currents carried by Ba^{2+} appeared as discrete steps of ~1.5 pA. A plot of the amplitude of the unitary Ba^{2+} current as a function of the patch potential is shown in figure 2Aa (open circles). The relation is linear with a slope conductance of 17.5 pS. Channel events could also be detected with 110 mM $CaCl_2$ in the electrode, although they were somewhat smaller ~1.0 pA at -60 mV and had a slope conductance of ~8 pS (open squares). The current-voltage relations measured in the presence of both Ba^{2+} and Ca^{2+} reverse more positive than 0 mV, but below the equilibrium potential for Ca^{2+} suggesting the channel is more permeable to divalent than to monovalent cations. The relative permeability of Ca^{2+} to K^+, the main intracellular cation, is $P_{Ca^{2+}}/P_{K^+} = \sim 5$.

Figures 1B&C show two different recordings from cell-attached patches on the surface of *mdx* myotubes. In many recordings from *mdx* myotubes, single channel activity was low and appeared similar to that recorded from normal myotubes (figure 1B). The single-channel i-V relations in the presence of 110 mM Ba^{2+} was similar to that recorded from normal myotubes (compare figures 2A a&b). Roughly 30% of the recordings from cell-attached patches on *mdx* myotubes, however, showed very high levels of channel activity (figure 1C). The single channel current-voltage relations for high level activity recorded from *mdx* myotubes like that shown in figure 1C are plotted in figure 2Ac. The single channel conductance and reversal potentials measured in the presence of 110 mM $BaCl_2$ and $CaCl_2$ were 18 pS and +18.0 mV and 8.5 pS and +32.0 mV, respectively. This

can be compared with that measured for the low level activity in normal myotubes which was 17.5 pS and +23 mV and 8 pS and +38 mV in the presence of Ba^{2+} and Ca^{2+}, respectively. The results suggest that the low activity channels in normal myotubes and the high activity channels in *mdx* myotubes have very similar permeabilities to divalent cations.

I analyzed channel closed times and burst durations to compare channel gating for the channel activity recorded from *mdx* myotubes with that recorded from normal myotubes. Figures 2B and 2C show the results of the kinetic analysis for activity recorded at a holding potential of -60 mV. The distribution of closed times was best fit as the sum of three exponential components with roughly similar time constants (details in figure legend). The distribution of channel burst durations for the low level activity in both normal and *mdx* myotubes (figure 2Ca&b) were best fit with a single rapidly decaying exponential component, while that for the high level activity from *mdx* myotubes (figure 2Cc) was better fit as the sum of two more slowly decaying exponential components, reflecting the longer openings in the single channel records. The results suggest that the low level channel activity in normal and *mdx* muscle have similar gating properties.

In recordings from both normal and *mdx* myotubes in which resting activity was low (figures 1a, b), applying suction to the electrode frequently increased channel opening, as expected for the behavior of stretch-activated channels (Brehm et al., 1984; Guharay and Sachs, 1984; Franco and Lansman, 1990). To test the possibility that the unusually high channel activity recorded from *mdx* myotubes shown in figure 1C might arise from mechanotransducing ion channels, I applied suction to the patch electrode while recording at a constant holding potential. Surprisingly, applying suction to the electrode decreased, rather than increased, channel activity. A reduction in the activity of mechanotransducing channels with increased suction has previously been reported in invertebrate neurones (Morris and Sigurdson, 1989), but not in vertebrate skeletal muscle in which only channels that are opened by suction have been observed (Brehm et al., 1984; Guharay and Sachs, 1984; Franco and Lansman, 1990).

The records in figure 3a show the response to suction applied to the electrode in a recording from an *mdx* myotube in which resting channel open probability was high. There were at least three channels in the patch as indicated by the maximum number of superimposed unitary current steps (opening levels shown at the right of the top record). The top record is the control activity in the absence of applied pressure. Applying -20 mm Hg of suction to the electrode reduced channel opening by more than half. After releasing the pressure, channel activity once again returned to high levels. Applying -40 mm Hg of suction to the electrode virtually suppressed channel activity, although very brief openings could still be observed which had the same unitary amplitude as the openings observed in the absence of applied pressure (figure 3b, expansion of records marked by asterisks in 3A). Releasing the suction applied to the electrode once again restored activity, although it was somewhat less than that recorded at the beginning of the experiment, suggesting a slow loss of channel activity which occurs over minutes. The results suggest that the activity of all the channels in the patch were reduced by applying suction to the electrode.

Apparently, *mdx* myotubes possess a class of mechanotransducing channels that are open for extended periods of time and close when the membrane is stretched by applying suction to the electrode. To determine whether stretch-inactivation of open mechanotransducing channels is a unique characteristic of *mdx* muscle, I compared the frequency of observing stretch-activated and stretch-inactivated channels in myotubes from both *mdx* and normal mice. Figure 4a shows a histogram of the fraction of the total number of patches which contained zero or a given number (N=number of channels per patch) of stretch-activated or stretch-inactivated channels. *Mdx* myotubes had roughly half the number of stretch-activated channels. On the other hand, 21% of the patches on *mdx* myotubes had stretch-inactivated channel activity, compared with ~2% of the patches (one patch) on normal myotubes. The results show that stretch-inactivated channels are found far more frequently in *mdx* myotubes.

Can the appearance of channels that are open at rest account for Ca^{2+} leakage into *mdx* myotubes? I addressed this question by comparing the average time a channel spends open in patches from normal and *mdx* myotubes without regard to the channel's response to pressure. Figure 4b shows a frequency histogram of channel open probability obtained from recordings from different cell-attached patches. In 90% of the recordings from normal myotubes, channel open probability in the absence of applied pressure was less than 10%. On the other hand, openings in myotubes from *mdx* mice fell into two classes: low activity (<10% open probability) which was observed in ~70% of the patches and showed a roughly similar distribution as the activity from control myotubes (inset, figure 4b) and patches showing very high levels of activity (~30% of all patches). The recordings from *mdx* myotubes showing high levels of channel activity (eg figures 1c & 3) arose from stretch-inactivated channels in those cases where the response to pressure was tested (7 out of 9 patches).

Discussion

My recordings of single channel activity from newly formed myotubes from normal and *mdx* mice suggest both possess Ca^{2+}-permeable mechanotransducing ion channels. These channels are likely to account for much of the resting Ca^{2+} entry as they produce the only detectable unitary currents in recordings with divalent cations as the only inward charge carrier in the electrode. The prolonged channel openings in *mdx* myotubes, which often lasted tens of seconds, could allow sufficient Ca^{2+} influx to elevate intracellular Ca^{2+}, since activation of acetylcholine receptors, which are less permeable to Ca^{2+} (Adams et al., 1980), produces a Ca^{2+}-dependent myopathy (Leonard and Salpeter, 1979).

My results show that myotubes lacking dystrophin possess a novel type of mechanotransducing channel that is open for extended periods of time and closes when suction is applied to the electrode. The present results provide no information on the origin of that stretch-inactivated channels in *mdx* myotubes. It is interesting to speculate that dystrophin binds to channels (cf Campbell and Kahl, 1989) providing a counterforce to the resting membrane tension. In muscle lacking dystrophin, the resting tension in the cell membrane may be sufficient to keep some channels in the open state. On the other hand, stretch-inactivated channels may represent a new population of channels that becomes unmasked by some other mechanism during the development of differentiated myotubes. Further experiments are required to understand the mechanism linking an absence of dystrophin to the appearance of stretch-inactivated channels. The results, nevertheless, are the first to point to mechanotransducing ion channels as a possible pathophysiological mechanism underlying elevated intracellular Ca^{2+} in dystrophic muscle.

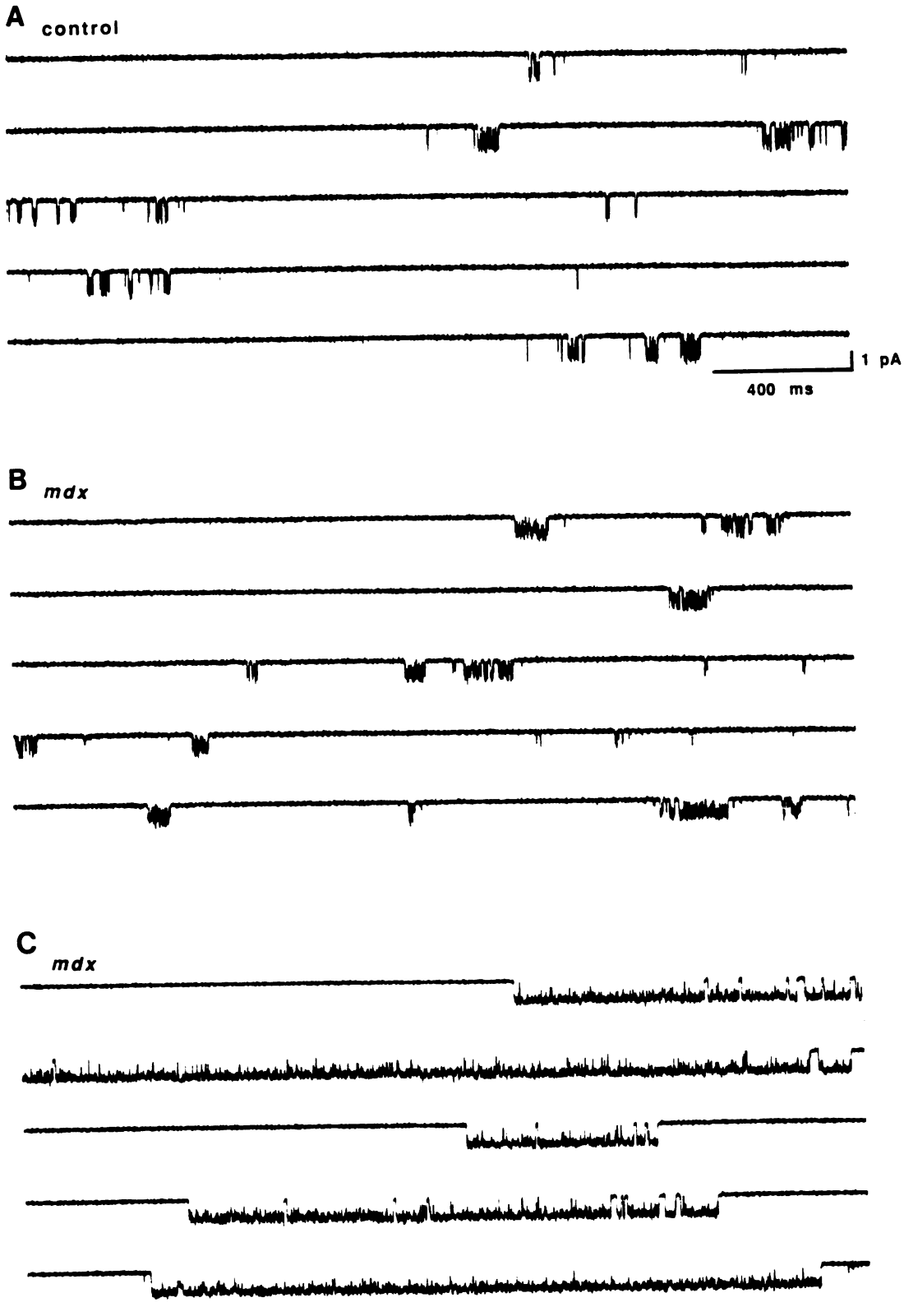
A control
1 pA
400 ms
B mdx
C mdx

Figure 2-1. Two forms of mechanosensitive channel activity can be detected in *mdx* myotubes. Channel activity recorded from the surface of myotubes from normal and *mdx* mice with 110 mM $BaCl_2$ in the patch electrode showing unitary Ba^{2+} currents at a constant holding potential of -60 mV. The traces are sequential and represent a segment of a continuous recording (~10 seconds of channel activity). Currents were filtered at 1 kHz with an 8-pole Bessel filter and sampled at 5 kHz. **A)** Recording from a cell-attached patch on a normal myotube; **B)** Recording from a cell-attached patch on *mdx* myotube showing low level channel activity; **C)** Recording from a different *mdx* myotube in which channel activity was high.

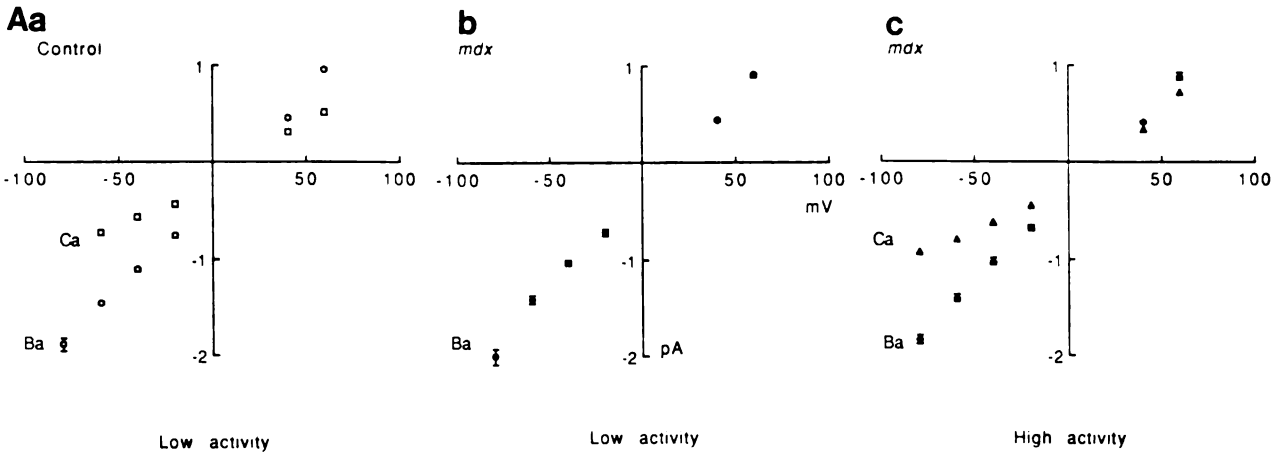
Aa
Control
b
mdx
c
mdx
Ca
Ba
mV
pA
Low activity
Low activity
High activity

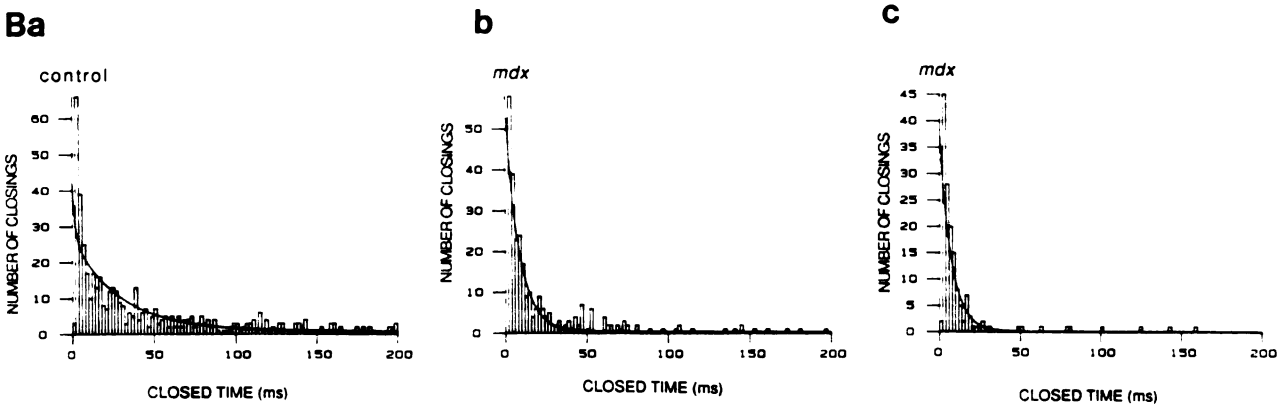
Ba
control
b
mdx
c
mdx
NUMBER OF CLOSINGS
CLOSED TIME (ms)

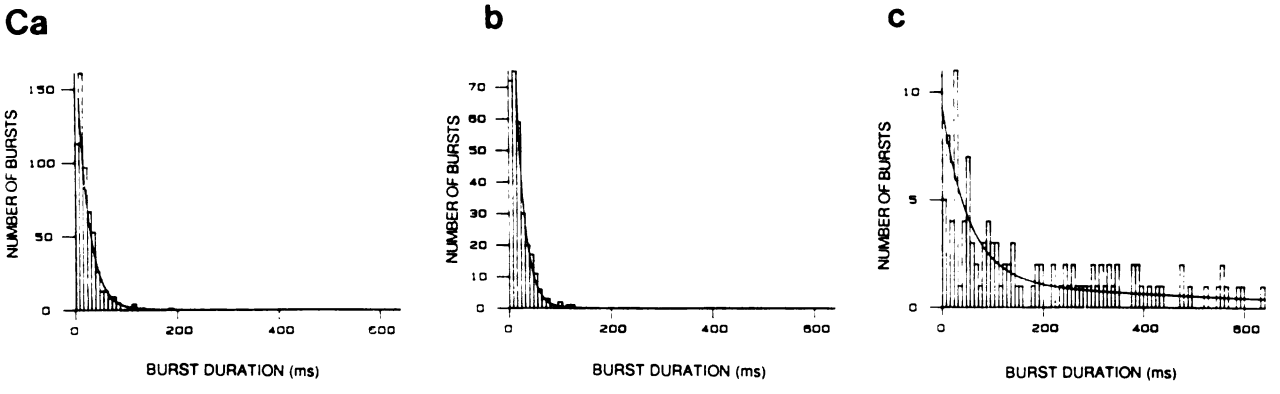
Ca
b
c
NUMBER OF BURSTS
BURST DURATION (ms)

Figure 2-2. Comparison of channel activity recorded from wild type and *mdx* myotubes. A) The effect of the patch holding potential on the amplitude of unitary Ba^{2+} currents recorded from normal (**Aa**) and from *mdx* myotubes (**Ab**, low activity; **Ac**, high activity). The single channel current-voltage relation obtained with electrodes filled with 110 mM Ca^{2+} is also shown. The single channel current-voltage relation give slope conductances and reversal potentials of 17.5 pS and +23 mV (n=5) and 8 pS and +38 mV (n=2) for low level channel activity in normal myotubes in the presence of 110 mM Ba^{2+} and Ca^{2+}, respectively. In *mdx* myotubes, the i-V relation for the low level activity (**Ab**) gave a conductance and reversal potential in the presence of 110 mM Ba^{2+} of 17.0 pS and +23.0 mV (n=5); the i-V relations in the presence of Ba^{2+} and Ca^{2+} for the high level channel activity (Ac) gave conductances and reversal potentials of 18.0 pS and +18.0 mV (n=9) and 8.5 pS and +32.0 mV (n=2), respectively. **B** and **C**). Comparison of channel kinetics for the three forms of channel activity recorded at a constant holding potential of -60 mV. Histograms of closed times (**B**) and burst durations (**C**) for activity recorded from normal (**Ba** and **Ca**) and *mdx* myotubes (low activity, **Bb** and **Cb**; high activity, **Bc** and **Cc**). The smooth curves drawn through the histograms represent the maximum likelihood fit to three exponentials for closed times for normal (**Ba**, tau_1 = 1.7 ms, tau_2 = 29 ms and tau_3 = 491 ms), *mdx* low activity (**Bb**, tau_1 = 1.3 ms, tau_2 = 9 ms, and tau_3 = 692 ms), and *mdx* high activity (**Bc**, tau_1 = 1.3 ms, tau_2 = 7.3 ms, and tau_3 = 1168 ms). **C**) Histograms of burst durations for normal (**Ca**, tau_1 = 22 ms), low *mdx* activity (**Cc=**, tau =17 ms); and high *mdx* activity (**Cc**, tau_1= 53 ms and tau_2 = 587 ms). For the analysis, currents were filtered at 100 Hz to observe the better resolved slower gating transitions.

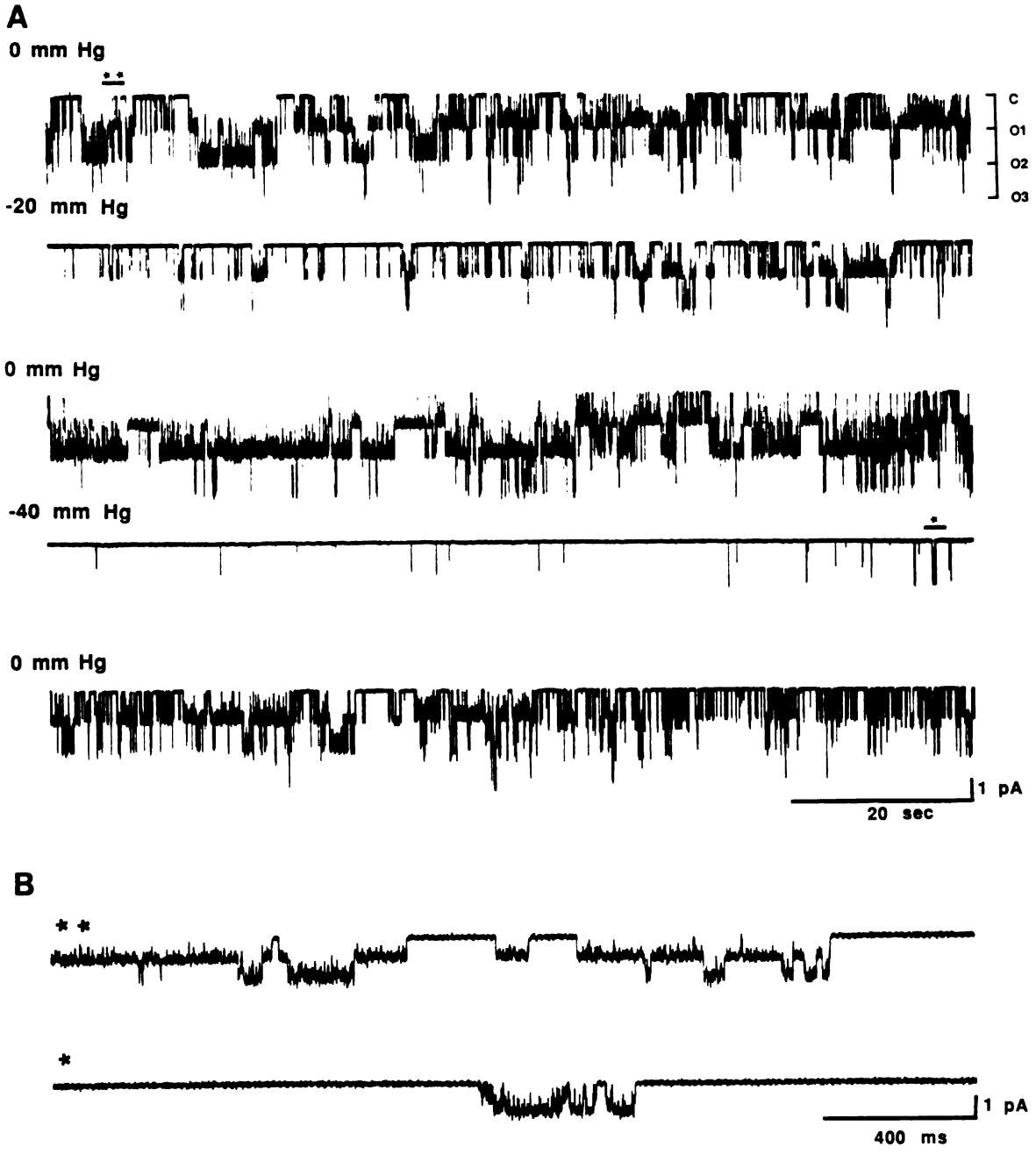
A
0 mm Hg
C
O1
O2
O3
-20 mm Hg
0 mm Hg
-40 mm Hg
0 mm Hg
1 pA
20 sec
B
1 pA
400 ms

Figure 2-3. Suction applied to the electrode reduces the activity of some channels in *mdx* myotubes. A) Records of single channel activity recorded from the surface of an *mdx* myotube. The records were taken in sequence. Each trace represents a continuous record of channel activity lasting ~100 seconds. Currents were filtered at 100 Hz and sampled at 1 kHz. The pressure applied to the patch electrode is indicated in mm Hg above each record. Channel open probability was 30% (0 mm, top record), 10% (-20 mm, second record), 43% (0 mm, third record), 0.4% (-40 mm, fourth record), and 16% (0 mm, bottom record). B) Records marked with double (control) and single (-40 mm Hg) asterisks plotted on an expanded time scale. Note, the records in (A) are filtered at 100 Hz, while the expanded records in (B) are filtered at 1 KHz. The unitary amplitude varied in some cases by ~0.3 pA. Although we cannot rule out this variation represents the contribution of channels with slightly different unitary conductances in the multichannel patch, this variability is within the range expected for the current fluctuations in the open channel noise as well as artifacts arising from sight variations in patch potential.

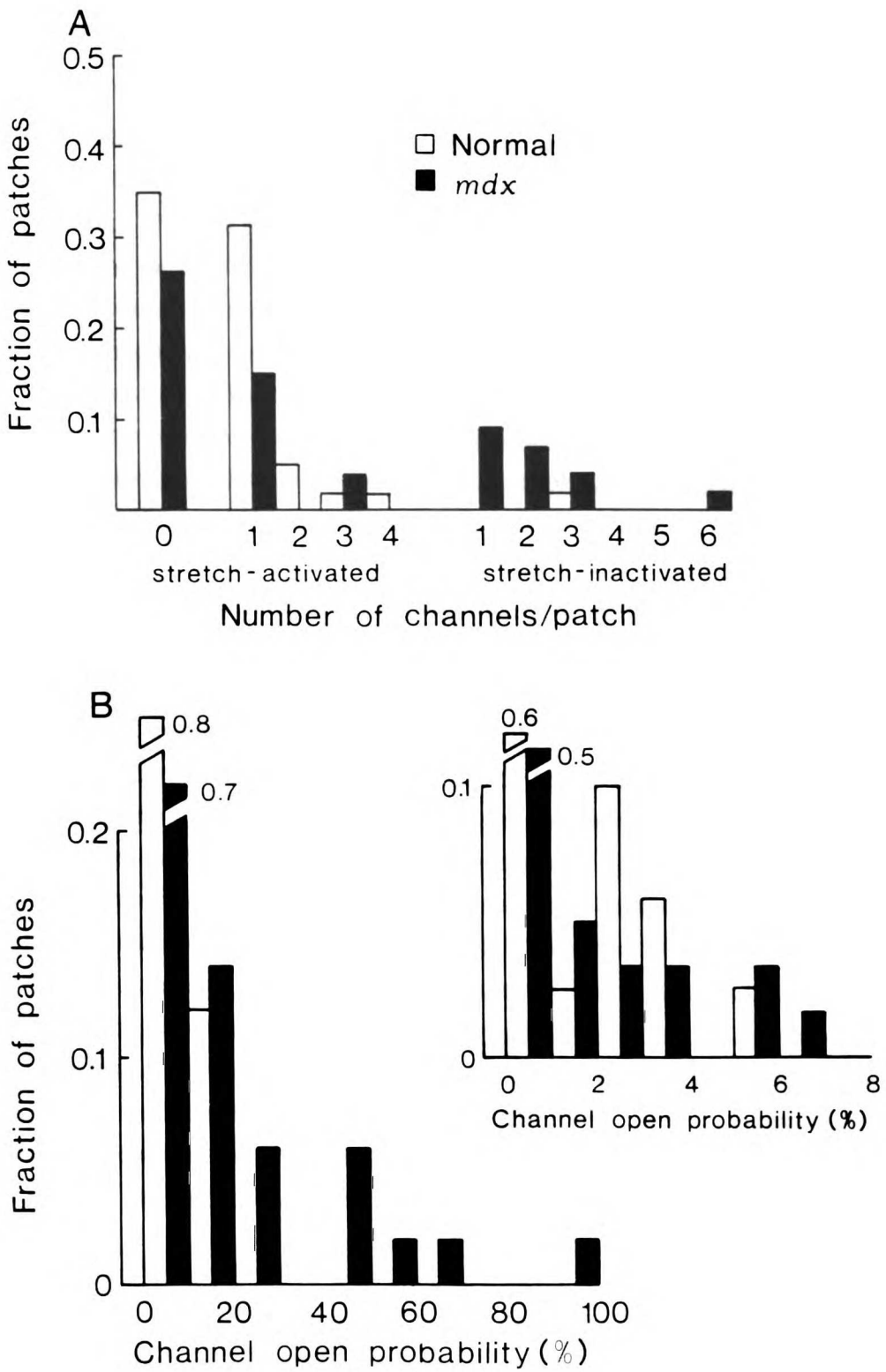
A
0.5
0.4
0.3
0.2
0.1
Fraction of patches
Normal
mdx
0 1 2 3 4
1 2 3 4 5 6
stretch-activated
stretch-inactivated
Number of channels/patch
B
0.8
0.7
0.2
0.1
0
Fraction of patches
0 20 40 60 80 100
Channel open probability (%)
0.6
0.5
0.1
0
0 2 4 6 8
Channel open probability (%)

Figure 2-4. The channels which showed the highest activity were exclusively those which expressed stretch-inactivated gating. Comparison of recordings of channel activity from cell-attached on normal (open bars) and *mdx* (filled bars) myotubes. The data represent samplings from two separate sets of cultures prepared from normal and *mdx* muscle as described above. **A)** Histogram showing the fraction of all patches without channel activity (0 channels) and with a number (N) of stretch-activated (N = 1-4) or stretch-inactivated (N = 1-6) channels. Total number of patches was 43 for normal myotubes and 57 for *mdx* myotubes. The number of channels in a patch was taken as the maximum number of simultaneous openings observed in the single channel record. Spontaneous activity that was insensitive to suction applied to the electrode (cf Franco and Lansman, 1990b; Chapter 1) is not shown but accounted for 21% of the patches on normal myotubes and 33% of the patches on *mdx* myotubes. Stretch-activated channels were observed in 42% of the patches on normal myotubes and 19% of the patches on *mdx* myotubes; stretch-inactivated channels were observed in 2% of the patches on normal myotubes and 21% of the patches on *mdx* myotubes. The number of stretch-inactivated channels observed may be an underestimate if the suction applied to the patch membrane during seal formation deformed the patch sufficiently so that channels were inactivated during the experiment. **B)** Histogram comparing mean channel open probability recorded from cell-attached patches on normal (30 patches) and *mdx* (51 patches) myotubes. Channel open probability was measured from ~1 minute of channel activity shortly after obtaining a cell-attached recording (~1-2 minutes). Mean open probability was calculated by integrating the current record and dividing by the number of channels in the patch times the unitary current. For very low levels of activity where simultaneous openings were not observed, we assumed only one channel was in the patch. The abscissa then represents open probability multiplied by the number of channels (NP_o). If N>1, P_o would be overestimated, however, any error would be minimal because $P_o << 1\%$. Inset, expansion of the first bin of the probability histogram.

Chapter 3

Ion channels in skeletal muscle from wild type and dystrophic mice: alterations in mechanosensitive-gating. in dystrophin-deficient muscle cells.

Introduction

Studies of single ion channels in vertebrate skeletal muscle have demonstrated the presence of a class of mechanosensitive ion channels (Guharay and Sachs, 1984, Franco and Lansman, 1990b; Chapter 1). These channels are permeable to both monovalent and divalent cations and have been suggested to provide a pathway for resting Ca^{2+} entry into muscle cells (Franco and Lansman, 1990b; Chapter 1). The pathways responsible for resting Ca^{2+} influx are of considerable interest since Ca^{2+} participates in controlling myogenesis during normal development (Shainberg et al., 1969), and there is now strong evidence indicating that intracellular free Ca^{2+} is elevated in dystrophic skeletal muscle (reviewed in Martonosi, 1989).

The absence of the cytoskeletal protein, dystrophin (Koenig et al., 1988), from skeletal muscle membrane is the primary defect in Duchenne muscular dystrophy (Hoffman et al., 1987; Bonilla et al., 1988). Yet how the absence of dystrophin is related to alterations in myoplasmic Ca^{2+} homeostasis remains a central question concerning the pathophysiology of Duchenne muscular dystrophy. Two general hypothesis have been put forth. The first proposes that dystrophin acts as a structural protein supporting the integrity of the membrane. In this view, the membrane of dystrophin-deficient muscle is considered to be more mechanically fragile than the membrane of wild type muscle, tearing under the stress of normal contractile activity, and creating a pathway for the nonspecific leakage of

Ca^{2+} into the muscle's interior. Measurements of the pressure needed to rupture the membrane, however, have demonstrated no appreciable difference between wild type and dystrophic muscle cells (Franco and Lansman, 1990a, Hutter et al., 1991; see results, *Measurements of mechanical strength of dystrophin-deficient and dystrophin-containing membranes.*). The second hypothesis proposes that Ca^{2+} enters through Ca^{2+}-permeable ion channels (Franco and Lansman, 1990a; Fong et al., 1990; Chapter 2). Implicit to this second hypothesis is the notion that channels whose activity are normally tightly regulated become hyperactive when dystrophin is absent. The second hypothesis is supported by the fact that the activity of mechanosensitive channels is elevated in the *mdx* mouse (Franco and Lansman 1990a; Chapter 2), an animal model for human Duchenne muscular dystrophy (Bulfield et al., 1984).

In this study, I examine the activity of mechanosensitive ion channels at different stages of muscle development. Undifferentiated myoblasts do not express dystrophin (Lev et al., 1987; Nudel et al., 1988; Oronzi-Scott et al., 1988) and it is expected that the behavior of mechanosensitive channels should be similar regardless of myoblast genotype. In the adult *mdx* mouse, small caliber muscle fibers are spared from muscle damage (Karpati et al., 1988; Matsumura et al., 1992), despite the absence of dystrophin (Arahata et al., 1988; Watkins et al., 1988). I examined small caliber muscle fibers acutely dissociated from *mdx* mice to determine if alterations in mechanosensitive-gating are evident in dystrophic-deficient muscle fibers that do not undergo myonecrosis. To determine whether changes in channel behavior are strictly associated with dystrophin-deficiency or may be a general consequence of the dystrophic process I studied the expression of mechanosensitive channels in the dystrophic *dy* mouse (Meier and Southard, 1970), which expresses normal levels of dystrophin (Ohlendieck et al., 1991), but in which myoplasmic Ca^{2+} is elevated and is associated with extensive muscle degeneration (Dangain and Vrbova, 1990; Williams et al., 1990).

Methods

Muscle cell preparation

Wild type (C57BL/6J), *mdx* (C57BL/10ScSn-*mdx*) and *dy* (C57BL/6J-*dy*/*dy*) mice were obtained from Jackson Laboratories (Bar Harbor, Maine). Mice were sacrificed by cervical dislocation under a protocol approved by the UCSF Committee for Animal Research. Myotubes were grown in tissue culture from enriched populations of myoblasts as previously described (Franco and Lansman, 1990a; Chapter 2). In brief, the hind limbs of 3-7 week old mice were removed and placed in cold (4° C) Ca^{2+}-and Mg^{2+}-free Hank's Buffered Saline. After cleaning away bone and connective tissue, the pieces of muscle were then incubated for 30 minutes at 37°C in 1% Collagenase B (Boehringer-Mannheim) and 0.125% Trypsin (UCSF Tissue Culture Facility) under constant agitation. Satellite cells were dissociated by repeatedly trituating the muscle digest through the tip of a pipette and the debris removed by filtering the suspension through a fine mesh nylon cloth (100 μm). Fibroblasts were selectively removed by preplating the suspension on glass for 1 hour. The remaining cells were plated at a density of ~3000-5000 cells/cm^2 on plastic tissue culture dishes (Falcon). In some experiments, myoblasts were plated on tissue culture dishes that had been coated with 1 μg/cm^2 laminin (Sigma).

Myoblasts were grown in DMEM H-16 supplemented with 20.0 % fetal calf serum and 0.5% chick embryo extract (GIBCO). After reaching 30-40% confluency (~5-6 days in culture), myoblasts were induced to fuse and form myotubes by changing the content of the media to 5.0% fetal calf serum, 5.0% horse serum and excluding chick embryo extract. Wild type myoblasts divided and grew more quickly than either *mdx* or *dy*/*dy* myoblasts grown under identical tissue culture conditions. In addition, myoblasts grown on laminin fused more quickly and formed more extensive myotube networks than nontreated cultures of similar genotype (Ocalan et al., 1988).

Single-channel recordings were made from myoblast cultures after their reaching 10-20% confluency (~2-4 days). Recordings were made from myotubes 2-5 days after the first myotubes appeared in culture (~7-8 days after first plating myoblasts). Cultures were not used after 6 days post fusion. The age of the mouse from which myoblasts were isolated did not noticeably influence any of the results. All cultures were maintained at 37°C, 95.0 % air/ 5.0% CO_2.

Intact skeletal muscle fibers were dissociated from the flexor digitorum brevis muscle (FDB) following the procedure described by Bekoff and Betz (1977). The FDB muscle is composed of small caliber fibers and was dissected from the planar surface of the hind limb of mice and then suspended under constant agitation in 0.25% collagenase B (Boehringer-Mannheim) in DMEM-H16 media for approximately 30 minutes. The muscle was then rinsed in DMEM-H16 media supplemented with 0.5% horse serum and mechanically dissociated by trituration using a fire-polished pasteur pipette. Dissociated fibers are then plated onto plastic tissue culture dishes (Falcon) that had been coated with Matrigel® (Collaborative Research Incorporated) and allowed to adhere to the bottom of the dish for 15 minutes at room temperature (~21-25°C).

In the *mdx* mouse muscle fiber degeneration first becomes apparent after 3 weeks of age (Bulfield et al., 1984; DiMario et al., 1991). Electrophysiological recordings were made from FDB fibers before the onset of muscle fiber degeneration had begun in other muscle groups of the *mdx* mouse (2-3 weeks of age). I did not use *dy* FDB fibers in these experiments because homozygous mutants are indistinguishable from heterozygous mutants prior to 4-6 weeks of age. Surprisingly, when 4-6 week old *dy/dy* FDB fibers were examined, resting channel activity was rarely observed (~15% or 6 of 41 cell-attached patches) and, when apparent, was not significantly different than that observed in either wild type or *mdx* fibers (see results). Suction applied to the membranes of *dy* fibers show channel responses similar in sensitivity to that observed in wild type fibers (figure 5).

Histology of FDB fibers

Between 4 and 10 weeks of age muscle fiber degeneration and regeneration is highest in other muscle groups examined in the *mdx* mouse (Bulfield et al., 1984; DiMario et al., 1991). Histology was performed on FDB fibers removed from 6 week old mice in the same manner as those prepared for electrophysiology. Dissociated fibers were fixed overnight in 4.0% paraformaldehyde in 0.1 M Cacodylate Buffer at 4°C. Next the fibers were rinsed (0.1 M Cacodylate Buffer) and dehydrated through a graded series of ethanol washes to 100%. After dehydration the fibers were infiltrated and embedded in GMA (Polysciences) and sectioned on a Sorvall (JB4) microtome at a thickness of 2.5 μm. The resulting sections were stained with Toluidine Blue and photographed on a Nikon Optiphot inverted microscope.

Solutions

Physiological saline contained 150 mM NaCl, 5 mM KCl, 1 mM $MgCl_2$, 2.5 mM $CaCl_2$ and 10 mM N-2-hydroxyethylpiperazine-N'-2-ethanesulfonic acid (HEPES). Isotonic barium and calcium solutions contained 110 mM of the chloride salts with 10 mM HEPES. The bathing solution was an isotonic potassium aspartate solution (K-aspartate) containing 150 mM KOH, 150 mM aspartic acid, 5 mM $MgCl_2$, 10 mM K-EGTA and 10 mM HEPES. The pH of all solutions was adjusted to 7.5 by adding NaOH. The osmolarity of all solutions was adjusted to 320-330 mosM by adding glucose.

The K-aspartate bathing solution was used to zero the cell's resting potential so that the patch potential would be equal to the applied voltage command. Measuring the single-channel current-voltage relationship before and after patch excision indicated a maximum voltage error of ~5 mV, but often produced no voltage offset. The K-aspartate bathing solution produced no detectable signs of cell deterioration.

Electrophysiological methods

Single channel activity was recorded from cell-attached patches with the technique described by Hamill et al. (1981). Patch electrodes were pulled in two steps from Boralex hematocrit pipettes (Rochester Scientific), coated with Sylgard (Dow Corning), and the tips heat polished with a microforge. Membrane currents were recorded with a List EPC-7 patch clamp amplifier. Current records were stored on video tape and replayed onto the hard disk of a laboratory computer (LSI 11/73) for analysis. Current records were filtered with an eight-pole Bessel filter (-3 dB at 1kHz) and digitized at 5-10 kHz. Unless otherwise noted, all cell-attached recordings were made at a constant holding potential of -60 mV and at room temperature (~21-25°C). A holding potential of -60 mV was chosen because it is near the physiological resting potential of myotubes in culture (Siegelbaum et al., 1984; Guharay and Sachs, 1985).

Data analysis

Channel open probability was measured by integrating idealized reconstructions of channel openings and closings which were determined by setting a threshold at half the amplitude of the open channel current as previously described (Franco and Lansman, 1990b; Chapter 1). Channel activity was measured using electrodes of intermediate size (~4 MΩs with normal saline in the electrode and K-aspartate in the bath) which often contained more than one channel. Since the number of channels varied from patch to patch, the measured open probability is the open probability of each individual channel (P_o) multiplied by the number of channels (N), or NP_o. By making patch electrodes with uniform tip shapes and resistances, we tried to minimize variations channel number per membrane patch or in membrane tension due to differences in the amount of membrane taken up into the patch electrode. There were no obvious characteristics of the patch electrode which appeared to influence channel activity.

Resting activity was measured at a holding potential of -60 mV without suction applied to the electrode, except that associated with forming a seal with the membrane. The first minute of single-channel recording was used to measure resting activity. Resting activity varied significantly from patch to patch and did not follow a normal distribution. I chose to represent the distribution of NP_os measured from different experiments in the form of box plots (Chatfield, 1983). The median value of the distribution is represented as the center line through the box and the values at which one quarter of the observations lie above and below define its outer margins. The outlying points represent the three highest values and the single lowest value of each data set.

In calculating stretch-activation, baseline activity before the application of pressure was subtracted from the channel activity elicited in response to pressure and was normalized to the number of channels in the patch. The number of channels was indicated by the maximum number of superimposed openings when the channels were maximally activated with pressure. Stretch-inactivation was calculated as the channel activity measured in the presence of pressure divided by the baseline activity measured immediately before. In this manner, both stretch-activation and stretch-inactivation where normalized to the number of channels per patch. Channel density did not differ within muscle cell classes (see results, *Channel density*).

The activity of stretch-activated channels often declined within a few seconds after the initiation of a pressure pulse (Gustin et al., 1988; Hamill and McBride, 1992). Therefore, only the first 10-15 seconds of channel activity after the initiation of pressure where used in calculating stretch-activation . Channel adaptation of this sort did not significantly differ between wild type and *mdx* muscle cells (cf McBride and Hamill, 1992). In contrast, stretch-inactivated channel activity did not adapt following the application of pressure. Because the response of mechanosensitive channels to suction often changed with successive applications of suction, only the responses of the first few

applications of suction were used in measuring the relationship between open probability and pressure.

Measurements of channel open probability are shown as a function of pressure applied to the patch electrode. The relationship between the amount of pressure applied to the patch electrode and channel open probability was fit with a Boltzmann relation of the form

$$p_o = p_{max}/[1+\exp(P-P_{1/2})/\pi]$$

where p_o is the mean channel open probability, p_{max} is the maximum channel open probability, P is the pressure applied to the electrode (mm Hg), $P_{1/2}$ the amount of pressure to give p_o=0.5, and π is the steepness of the relation. The data points were fit using a non-linear, least-squares algorithm.

To determine if mechanosensitive channels opened independently of one another I fit channel openings according to the predictions of the binomial distribution. If there are *N* independent channels within a patch, then the probability that *r* channels are simultaneously open should follow a binomial distribution where

$$P(r) = N!/r!\ (N-r)!\ \times p^r(1-p)^{N-r} \qquad r=0,1,\ldots..,\ N$$

and *r* is the number of channels open at one time and *p* is the probability that any one channel is open.

Results

Section 1

Activity of Ca^{2+}-permeable ion channels near the resting potential of the cell.

The first set of experiments investigated the types of ion channels that could support Ca^{2+} influx into muscle cells at various stages of myogenesis near the resting potential of the cell (see Methods). With physiological saline in the patch electrode, recordings of single-channel activity showed two distinct classes of ion channel at a holding potential of -60 mV (figure 1). In muscle cells from wild type and *mdx* mice, the predominant form of channel activity arose from mechanosensitive ion channels (Guharay and Sachs, 1984; Franco and Lansman, 1990a, b; Chapters 1, 2). I was, however, surprised to find that *dy/dy* myoblasts and myotubes consistently showed activity of the nicotinic acetylcholine-receptor (nAChR) channel in the absence of acetylcholine in the patch electrode (>95% of cell-attached patches; cf Jackson, 1984). Spontaneous openings of nAChR channels were rarely observed in wild type or *mdx* muscle cells. Although the nAChR channel is permeable to Ca^{2+} (Decker and Dani, 1990), it will not be dealt with here.

Mechanosensitive channels show a pattern of channel gating that is distinct from other types of channels in skeletal muscle. Channel activity occurred as bursts of openings created by rapid excursions to the closed channel level. Bursts of channel activity were interrupted by a series of longer closed periods (Franco and Lansman, 1990b, Chapter 1). Channel activity could also be observed at negative membrane potentials where most other forms of channel activity is inactivated. Perfusing the cytoplasmic surface of excised patches with 1-10 mM Ca^{2+} did not influence channel activity (data not shown). Similarly, increasing myoplasmic cAMP or prostaglandin levels had no apparent effect on channel activity. Finally, the activity of mechanosensitive channels can be maintained for extended periods in excised patches (Guharay and Sachs, 1984, Sachs, 1988; Franco and Lansman,

1990b), suggesting that intracellular second messengers may not necessary for channel function.

Previous work has demonstrated the presence of mechanosensitive ion channels in vertebrate skeletal muscle myoblasts (Franco and Lansman, 1990b; Chapter 1) and myotubes (Guharay and Sachs, 1984, Franco and Lansman, 1990a; Chapter 2) raised in culture. Here I show that mechanosensitive channels are also found in intact skeletal muscle fibers acutely removed from the animal. In the majority of cell-attached recordings the openings of mechanosensitive ion channels appeared to be similar at all stages of development in both wild type, and dystrophic muscle cells (figure 1). *Mdx* myotubes, however, frequently showed a form of channel activity with greatly prolonged openings (figure 1b, third trace). These long duration openings were rarely observed in myoblasts or FDB fibers in the absence of suction applied to the electrode. Experiments aimed at determining whether these long duration openings represent different types of mechanosensitive channel or different gating patterns of the same channel are described in Section 2.

Table 1 compares the single-channel conductance and cation selectivity of mechanosensitive channels from myotubes and FDB fibers. Channel activity from either myotubes or intact fibers had indistinguishable single-channel conductances with either physiological saline or isotonic Ca^{2+} in the patch electrode. The reversal potential for current through mechanosensitive channels with isotonic Ca^{2+} in the electrode is positive, indicating that the channels are more permeable to Ca^{2+} than to K^+, the predominant intracellular cation ($P_{Ca^{2+}}/P_{K^+}$ = ~5; Franco and Lansman, 1990a; Chapter 2). At negative membrane potentials where the driving force on Ca^{2+} is high, these channels would allow a significant influx of Ca^{2+} (eg Decker and Dani, 1990). Replacing chloride in the electrode filling solution with aspartate or methanesulfonate had no effect on either the channel conductance or the reversal potential, indicating that these channels are not permeable to anions.

Resting activity of mechanosensitive channels

Ca^{2+} leakage through mechanosensitive channels would be greatest at negative membrane potentials. I therefore examined the single-channel activity of mechanosensitive channels in muscle cells from wild type and *mdx* mice under "resting conditions", which I define as that activity observed in the absence of suction applied to the electrode and at holding potential of -60 mV. Figure 2 shows that the fraction of cell-attached patches containing discernable resting channel activity was similar in all classes of myoblasts and in *mdx* myotubes, but was lower in wild type myotubes. By comparison, both wild type and *mdx* FDB fibers showed a larger fraction of cell-attached patches with resting channel activity. For myoblasts and myotubes, the overall level of resting channel activity increased in accordance with the fraction of cell-attached patches containing channel activity. That is, the overall level of resting activity was similar in myoblasts, but was greater for *mdx* myotubes when compared to wild type myotubes (figure 3). On the other hand, FDB fibers showed low levels of resting activity that did not differ significantly in wild type and *mdx* FDB fibers. Therefore, resting channel activity is higher than normal in myotubes, but not FDB fibers, from the *mdx* mouse.

I also examined muscle cells from *dy/dy* mice (Meier and Southard, 1970), which have elevated levels of myoplasmic Ca^{2+} (Dangain and Vrbova, 1990; Williams et al., 1990), but which express normal levels of dystrophin (Ohlendieck et al., 1991). Resting activity in *dy/dy* myoblasts did not differ significantly from that measured in wild type or *mdx* myoblasts. Although the fraction of patches showing channel activity was high in *dy/dy* myotubes (figure 2), the overall level of resting activity was low and similar to that in wild type fibers (figure 3). Resting activity was not measured from FDB fibers from *dy/dy* mice because it was not possible to obtain age-matched animals (see Methods). Therefore, at least in muscle cells grown in culture, elevated channel activity does not appear to be a nonspecific consequence of Ca^{2+}-dependent proteolysis (Martonosi, 1989).

Channel density

Cell-attached patches often contained channels that were closed under resting conditions. Therefore, the fraction of cell-attached patches showing resting channel activity (figure 2), does not necessarily reflect channel density. While measuring the pressure responses of channels (see below), which should reveal quiescent channels, I found no significant difference in the mean number of channels per patch between wild type myotubes (1.5 ± 0.15, S.E.M., n=46) and *mdx* myotubes (1.5 ± 0.14, S.E.M., n=52), suggesting that elevated resting activity is an inherent property of the channels in *mdx* myotubes cells, rather than a consequence of channel density. I found little difference in channel density in wild type FDB fibers (3.0 ± 0.18, S.E.M., n= 32) and *mdx* FDB fibers (2.5 ± 0.17, S.E.M., n= 34). It is striking that, although channel density is approximately two-fold higher in FDB fibers, the mean resting channel activity is ~6-12 times lower in FDB fibers than in myotubes. The tip size of the patch electrode did not vary between conditions (see methods).

Section 2

Mechanosensitive-gating in wild type and mdx FDB fibers

Small caliber fibers in the *mdx* mouse do not suffer the degeneration that is typical of the larger muscle groups (Karpati et al., 1988). In agreement with this earlier finding, histological examination of *mdx* FDB fibers, which are also small caliber fibers, revealed no signs of degeneration or of regenerating fibers as indicated by fibers having centrally located nuclei (plate 1; also see legend). Therefore, electrophysiological recordings were made from *mdx* fibers that were phenotypically normal, which also may explain why wild type and *mdx* FDB fibers showed similar levels of resting channel activity.

To elucidate any further differences we compared the gating of mechanosensitive channels in wild type and *mdx* FDB fibers. Figure 4 shows a recording from a *mdx* FDB

fiber where channel activity increased with either positive (A) or negative pressures (B). This is consistent with what has been shown previously for stretch-activated channels, and indicates that membrane tension (not pressure) opens mechanosensitive channels (McBride and Hamill, 1992; Sachs, 1989). The mechanosensitive channels in *mdx* FDB fibers thus behave in the manner previously described for stretch-activated channels in wild type muscle cells (Guharay and Sachs, 1984; Franco and Lansman, 1990b). Figure 5 shows the response of mechanosensitive channels from both wild type (A) and *mdx* fibers (B) to negative pressure (suction). In all cases, channel activity was low at the onset of recording and increased when suction was applied to the electrode. Figure 5c shows channel open probability as a function of the amount of suction applied to the patch electrode in recordings from wild type and *mdx* fibers. Although channel activity recorded from both wild type (open circles) and *mdx* (filled circles) fibers increased with suction, mechanosensitive channel activity in *mdx* fibers was consistently less at each applied pressure.

That relationship between pressure and channel activity shown in figure 4c reached a minimum between ~2-3 mm Hg positive pressure, as if, when using suction to form a seal with the membrane, a small amount of residual tension persisted on the membrane. To determine whether residual tension on the membrane influences the level of resting activity measured in the absence of applied pressure, I applied suction to the membrane, and after releasing the applied pressure, measured the level of channel activity recovered (see legend for details). Figure 6a shows recordings of single-channel activity from wild type and *mdx* fibers before, during and after applying suction to the membrane. In all cases channel activity increased while suction was being applied to the electrode. However, in recordings from *mdx* fibers, channel activity did not return to previous levels, but was reduced after releasing suction. In wild type fibers, on the other hand, channel activity often increased following suction, but generally the response was more reversible than in *mdx* fibers.

Figure 6b shows the average responses in a number of experiments on wild type and *mdx* fibers before and after suction. An explanation for this behavior is given in the discussion.

Voltage-sensitive gating of mechanosensitive channels in wild type and mdx fibers

Mechanosensitive channels possess an intrinsic voltage-sensitive gating mechanism (Guharay and Sachs, 1985; Franco and Lansman, 1990b; Morris, 1990; Chapter 1). To determine if there is an alteration in voltage-sensitive gating in *mdx* FDB fibers, I examined channel activity from wild type and *mdx* fibers at different holding potentials. Figure 7a shows representative records of single-channel activity recorded from a *mdx* fiber at the indicated patch potentials. From the current records it is apparent that channel activity increases as the patch potential is made more positive. Figure 7b shows the responses of several recordings of channel activity to depolarization. Mechanosensitive channel activity increased *e*-fold for ~56 mV (open symbols, wild type fibers) and ~53 mV (solid symbols, *mdx* fibers) depolarization. As judged by the voltage-dependence of gating, I find no difference between wild type and *mdx* fibers and conclude that the intrinsic voltage-sensitive gating mechanism is not altered in dystrophin-deficient FDB fibers.

Mechanosensitive-gating in mdx myotubes

In some recordings from *mdx* myotubes, a dramatic increase in channel activity was observed shortly after commencing single-channel recording. Figure 8a shows an experiment in which channel activity recorded at -60 mV increased with time after the electrode sealed to the myotube surface. At the beginning of the recording only a single channel was active, however, within 90 seconds the simultaneous activity of three channels could be observed. This behavior may be explained if assumed that the open state of the channel becomes energetically favored under resting conditions. By contrast, figure 8b shows that channel activity in wild type myotubes was initially high and fell within seconds of beginning single-channel recording.

I tested whether the long duration openings represented a complete loss of channel gating or an alteration of the existing mechanosensitive-gating mechanism. In contrast to the behavior of stretch-activated channels (figure 5), suction applied to the electrode caused channel activity to decrease, rather than increase. Figure 9 shows that the reduction in channel activity with suction was stable and reversible over many minutes. Applying suction consistently inactivated channel activity during the entire time it was applied, and there was no evidence of a gradual adaptation to the inactivating pressure. This contrasts with the activity of stretch-activated channels in wild type muscle cells where channel activity decreases following a rapid step of suction to the electrode (see methods, *Data analysis*; Gustin et al., 1988; Hamill and McBride, 1992).

A decreased responsiveness of stretch-inactivated channels following successive applications of suction could often be counteracted with slight positive pressure applied to the electrode. This suggested that resting tension across the membrane patch was increasing with time in response to suction. On the other hand, larger positive pressures (>+10 mm Hg) reduced stretch-inactivated channel activity (data not shown). Therefore, both positive and negative pressures close stretch-inactivated channels. Similarly, both positive and negative pressures open stretch-activated channels (figure 4). These results are consistent with the interpretation that membrane tension, and not pressure, per se, is the stimulus that gates mechanically-gated channels (McBride and Hamill, 1992; Sachs, 1989).

To investigate whether suction reduced channel activity through the mechanosensitive gating mechanism, I applied different amounts of suction to cell-attached patches showing high channel activity. Figure 10a shows suction reduced channel activity in a graded manner. Because there were three channels in this patch, I was able to test whether channel openings occurred independently of one another as expected for the random behavior of individual ion channels. Comparing the predictions of the binomial distribution (hatched bars) for channels in the 1, 2 or 3 open levels with the measured

channel openings (solid bars) showed good agreement. I conclude that the ability of suction to inactivate channel activity involves an effect on the channel gating mechanism.

Figure 11 shows mean channel open probability of stretch-activated (top) and stretch-inactivated (bottom) channels from wild type (open circles) and *mdx* (solid circles) myotubes as a function of pressure. Although the two relationships in *mdx* myotubes are similar in steepness, the curve for stretch-inactivated gating is shifted to lower pressures. In the one observation of stretch-inactivated gating in wild type myotubes, the sensitivity of the channel to suction was similar to that observed for stretch-inactivated channels in *mdx* myotubes, suggesting that similar processes are occurring in both wild type and *mdx* myotubes to produce stretch-inactivated channels (open circles, figure 11b). On the other hand, stretch-activated channels recorded from wild type myotubes required greater amounts of pressure to open (open circles, figure 11a). The higher threshold for mechanosensitive-gating in wild type myotubes is consistent with previous results showing that disrupting the actin-based cytoskeleton increases the sensitivity of stretch-activated channels to pressure (Guharay and Sachs, 1984).

Voltage-sensitive gating in mdx myotubes

The channels showing the highest levels of resting activity elaborated stretch-inactivated gating (see figure legend 11 for details). Conversely, the channels with the lowest levels of resting activity were stretch-activated. To determine if alterations in voltage-sensitive gating are also exhibited by stretch-inactivated channels, I compared the responses of channels showing either high or low levels of resting activity to depolarization. Figure 12a shows current records from a recording of a channel that showed low levels of resting activity at the indicated holding potentials. The increase in channel activity in response to depolarization resembles that in FDB fibers (figure 7). Figure 12b shows the responses of many channels showing either high or low levels of resting activity to depolarization. Although all recordings were made from the surface of

mdx myotubes in the absence of pressure, the open symbols corresponded to recordings where channel activity could be increased with suction, and the solid symbols to those recordings where channel activity could be decreased with suction. Therefore, in the absence of pressure both stretch-activated and stretch-inactivated channels showed identical voltage-sensitivities, increasing ~*e*-fold per 36 and 38 mV, respectively.

Figure 12b also shows that there is an apparent shift in voltage-sensitivity to lower potentials for stretch-inactivated channels relative to stretch-activated channels. Whether this is a true shift in voltage-sensitivity or simply an increase in channel openings at every potential is not clear. However, figure 12c shows that the voltage-sensitivity of stretch-inactivated gating becomes identical to that of stretch-activated gating (~*e*-fold change per 37 mV; -10 mm Hg; open squares) when channel activity is reduced by applying suction to the electrode (~*e*-fold change per 38 mV; -20 mm Hg; solid squares). Moreover, the voltage-dependent component of channel gating remains constant over a hundred-fold change in channel open probability (compare solid circles with solid squares). It is therefore my belief that the apparent shift in voltage sensitivity is a secondary consequence of elevated channel activity.

Irreversible changes in mechanosensitive-gating in mdx myotubes

The gradual buildup in channel activity shown in figure 8, suggested that expression of stretch-inactivated gating is dependent on time dependent changes within the membrane. In support of this, I occasionally observed an irreversible change in channel gating in response to suction. Figure 13 shows that in such cases channel activity was initially low shortly after forming a seal with the membrane. Suction applied to the electrode then increased channel activity which, after releasing suction, failed to return to previously low levels. Channel activity induced in this manner, could then be reversibly suppressed by applying suction to the electrode as previously shown for stretch-inactivated channels. The solid squares in figure 11b are from channels that underwent such a change

in channel gating and shows that their response to suction is indistinguishable from channels that were stretch-inactivated from the onset of recording.

Is mechanical deformation of the membrane patch a prerequisite for the induction of stretch-inactivated channel activity? Figure 14a shows that depolarizing the patch membrane potential could also induce a change in channel gating mechanisms. The top record shows the channel opening in response to depolarization. The second depolarizing pulse, however, produced a channel which failed to reclose upon repolarization and which could be subsequently inactivated with suction applied to the electrode (data not shown). Figure 14b shows channel activity after tonic activation on an expanded time scale. Irreversible changes in channel gating were not observed in FDB fibers whether wild type or *mdx*, and only rarely in wild type myotubes (see legends figure 4 and 11). Stretch-inactivated channels, on the other hand, were never observed to acquire stretch-activated channel characteristics. We interpret these results to indicate that there are independent pressure and voltage-dependent processes which (when dystrophin is absent) can alter the normal energetic constraints on the channel so that the open, rather than closed, state is favored at rest.

Mechanosensitive-gating in wild type and mdx myoblasts

To determine if changes in channel-gating are specific for myotubes grown in tissue culture, I examined the characteristics of mechanosensitive-gating in myoblasts. I detected no difference in mechanosensitive-gating between wild type and *mdx* myoblasts. Figure 15a shows a recording from a *mdx* myoblast where applying suction to the electrode increased the amount of time the channel spent open. The sensitivity of mechanosensitive channels to applied pressure was similar to that observed for stretch-activated channels in dystrophin-deficient myotubes (see legend for details). I also detected stretch-inactivated channels in both wild type and *mdx* myoblasts (data not shown). There were proportionately fewer stretch-inactivated channels in myoblasts than in dystrophin-deficient

myotubes (compare figure legends 11 and 15). On the other hand, there were more stretch-activated channels in myoblasts than in dystrophin-deficient myotubes. Figure 15 b shows that although channel activity increased during the application of suction, it was suppressed relative to resting levels after releasing suction. This effect was more pronounced in myoblasts than in *mdx* FDB fibers (Figure 15c; compare with figure 6b).

Effects of laminin on the resting activity of mechanosensitive channels in wild type and mdx myotubes

Dystrophin associates with a unique complex of glycoproteins at the muscle surface (Campbell and Kahl, 1989; Ervasti and Campbell, 1991), one of which has been proposed to be a laminin-binding protein (Ibraghimov-Beskrovnaya et al., 1992). To test the possibility that substrate interactions might influence channel activity, myotubes were grown on tissue culture dishes that had been treated with laminin. Laminin did not change the relative difference in resting activity measured between wild type and *mdx* myotubes or increase the percentage of stretch-inactivated channels. However, myotubes grown on laminin-treated dishes had higher levels of resting activity regardless of whether they expressed or lacked dystrophin (figure 16). My result suggests that elevated channel activity does not result from a reduction in laminin-binding, since channel activity is highest in the presence of laminin.

Measurements of mechanical strength of dystrophin-deficient and dystrophin-containing membranes.

An alternative to the idea that dystrophin is involved in regulating Ca^{2+}-permeable ion channels is that dystrophin supports the mechanical integrity of the sarcolemma. According to this second hypothesis, muscle membranes deficient of dystrophin would be mechanically more fragile than wild type muscle membranes (cf Cooper and Hamill, 1989; Hutter et al., 1991; Menke and Jockusch, 1991). As an indication of membrane strength, I

measured the pressure that had to be applied to a patch electrode to rupture the membrane of muscle cells from wild type and dystrophic mice. Figure 17 shows the results of this experiment. Pressure was gradually applied to the patch electrode until the membrane ruptured and electrical continuity with the inside of the cell was established. I detected no significant difference in the mechanical strength of dystrophin-deficient or dystrophin-containing membranes. I also detected no difference in membrane lytic pressures between wild type and *dy/dy* muscle cells, suggesting that membrane weakness does not result from Ca^{2+}-dependent proteolysis. The results suggests that the membranes of dystrophin-deficient muscle cells are not mechanically more fragile, and that Ca^{2+} entry into dystrophin-deficient muscle cells may not be due to a general leakiness of the membrane.

Discussion

A major finding of this study is that the activity of mechanosensitive ion channels can be detected at all stages of myogenesis in tissue culture, and in intact fibers removed from wild type and dystrophic mice. While other channel properties are virtually identical throughout muscle development, channel activity is elevated in myotubes from the *mdx* mouse. Consistent with the idea that dystrophin contributes to the mechanisms that gate mechanosensitive channels, the level of resting activity was similar in myoblasts regardless of genotype. Elevated resting activity is not a secondary consequence of Ca^{2+}-dependent proteolysis (Martonosi, 1989), as it was not characteristic of dystrophic muscle cells from the *dy* mouse (Dangain and Vrbova, 1990; Williams et al., 1990). On the other hand, resting channel activity in FDB fibers is lower in comparison to resting activity in muscle cells grown in tissue culture. Since, we detect no histological differences between wild type and *mdx* FDB fibers, it may not be surprising that the differences in resting activity is small.

My results may be compared with those of Fong et al., (1990) who described a unique class of Ca^{2+} leak channel whose activity was higher in *mdx* myotubes than in wild type myotubes. The channels described by Fong et al., (1990) were not sensitive to membrane voltage and had a smaller single-channel conductance than the channels described here. Other than spontaneous openings of the nAChR channel in *dy/dy* muscle cells (figure 1), I only detected the activity of mechanosensitive channels in muscle cells from wild type and dystrophic mice (*mdx* and *dy/dy*). I find no evidence of Ca^{2+} leak channels at any stage of myogenesis *in vitro* nor in intact fibers. The source of the discrepancy between the results presented here and those of Fong et al. may reflect differences in tissue culture, such as substrate (see results). Nonetheless, our results strongly support the interpretation that there is an alteration in the gating of pre-existing

mechanosensitive channels in dystrophin-deficient muscle rather than the induction of a new class of channel.

Mechanosensitive and voltage-sensitive gating in muscle cells grown in culture

Mdx myotubes show a novel form of mechanosensitive-gating which is distinguished by channels that are open almost continuously at rest, and are closed when suction is applied to the electrode (figure 9). This type of channel activity can be induced in *mdx*, but not wild type myotubes, with either pressure applied to the electrode or by strong depolarization of the patch holding potential (figures 13 and 14). These results, in conjunction with the facts that stretch-activated and stretch-inactivated channels displayed identical single-channel conductances and voltage-sensitivities, suggests that both channel types arise from the same channel protein.

The expression of mechanosensitive channels is similar in wild type and *mdx* myoblasts. The pressure-sensitivity of channels in myoblasts is similar to that for analogous channels in dystrophin-deficient myotubes (see figure legends 11 and 15). On the other hand, the relative proportion of either channel type more closely resembles that in wild type myotubes. These results also imply that the expression of mechanosensitive channels is not developmentally-regulated.

The appearance of stretch-inactivated channels in dystrophin-deficient myotubes coincides well with the time that myotubes become electrically excitable and begin to twitch in culture. Myoblasts, on the other hand, are noncontractile, and do not express voltage-gated ion channels (Caffrey et al., 1987; Kano et al., 1989). Accordingly, myoblasts exhibit fewer stretch-inactivated channels. Irreversible changes in mechanosensitive channel gating may arise in dystrophin-deficient myotubes while twitching or undergoing electrical activity. The expression of stretch-inactivated channels can be induced in dystrophin-deficient myotubes with either mechanical deformation (figure 13), or depolarization of the membrane (figure 14), supporting this conclusion. The relatively late

acquisition of dystrophin (following fusion) may therefore be required to support the integrity of the cytoskeleton as myotubes becomes electrically excitable.

Implications of the role of dystrophin in mechanosensitive-gating

Previous studies have suggested a role for cytoskeletal proteins in the gating of mechanosensitive ion channels (Guharay and Sachs, 1984; Sokabe et al., 1991). However, the mechanisms which operate in dystrophin-deficient muscle cells to produce stretch-inactivated channels are not understood and attempts to explain their existence must be considered speculative. Since stretch-activated channels are frequently detected in both myoblasts and dystrophin-deficient myotubes (see legends figures 11 and 15), the presence of dystrophin is not exclusively required for the tension-sensing apparatus of mechanosensitive channels to function and the absence of dystrophin is in itself not sufficient to induce the expression of stretch-inactivated channels.

Dystrophin is a very large rod-like protein of ~150 nm in length, which connects areas of membrane this distance apart (Koenig et al., 1988). On the other hand, the nAChR channel, one of the largest channels, occupies an area of only ~25 nm^2 (Guharay and Sachs, 1984). One would expect that alterations in the membrane cytoskeleton when dystrophin is absent must encompass areas of membrane larger than that associated with a single mechanosensitive ion channel. In support of this, I never observe both stretch-activated and stretch-inactivated channels within the same patch of membrane, suggesting that the membrane alteration must involve an area of membrane larger than that encompassed by the patch electrode (1-2 μm^2). This point is illustrated in Figure 18 which shows a cell-attached patch from a *mdx* myotube containing -6-7 channels that were simultaneously open at rest, but which were all inactivated with suction applied to the electrode. Within a single patch, multiple channels were also observed to undergo simultaneous switches in channel gating following suction or depolarization. The existence of local changes in the membrane is also suggested by the observation of a predominance

of either stretch-activated or stretch-inactivated gating within a localized region of the muscle surface (5-20 μm^2; data not shown).

Is stretch-inactivated gating a form of channel adaptation?

In response to maintained applications of pressure, mechanosensitive channels first open and then close as they adapt to the mechanical stimulus (Gustin et al., 1988; Hamill and McBride, 1992). In dystrophin-deficient myotubes, merely opening channels is sometimes sufficient to result in irreversible channel activation, that can be subsequently inactivated with pressure applied through the electrode. I propose that stretch-inactivated gating as in dystrophin-deficient myotubes is synonymous with the adaptation process that normally closes channels after a delay.

Howard and Hudspeth (1984) proposed a model for mechanotransduction in saccular hair cells. Figure 19 is a schematic of the hair cell model. Deflection of the hair cell bundle produces an inward current that rapidly adapts with time. The time course of current adaptation correlates well with a relaxation in the stiffness of the hair cell bundle. The mechanical relaxation of the hair cell bundle is modelled as a damping element (dashpot) in series with a cytoskeletal gating spring coupled to mechanosensitive channels. The transduction event is initiated by the deflection of the hair cell bundle and is mediated by channels which open when the gating spring is stressed. After a short delay, the dashpot concomitantly releases tension on the gating spring (closing channels) and reduces the stiffness of the hair cell bundle.

The membrane-associated cytoskeleton functions as a scaffolding that supports the structure of the membrane. In response to stretch, expansion of the muscle membrane would be opposed by the cortical cytoskeleton. Adapting (no pun intended) from the Howard and Hudspeth model, channel adaptation in skeletal muscle may involve reversible relaxations of the membrane-associated cytoskeleton while under stretch. The concomitant loss of dystrophin, and the dystrophin-associated proteins in the *mdx* mouse (Ervasti et al.,

1990; Ohlendieck and Campbell, 1991), would be expected to have profound consequences on the resilience of the muscle membrane, and accordingly, the gating of mechanosensitive channels.

Although mechanically-gated ion channels are proposed to underlie mechanically-gated ion fluxes in hair cells, the relationship between the gating mechanisms of the channels in hair cells and those reported here in skeletal muscle cells is not known. Figure 20 depicts a model I propose to explain mechanosensitive-gating in wild type skeletal muscle cells. The channel is modeled to be composed of four barrels (channel subunits) that separate (channel opening) and come together (channel closing) in response to stretching the membrane. Under resting conditions, several forces may act to keep the channel closed (figure 20Aa; rest). These forces may include, compressional forces arising within the membrane phospholipid, hydrophobic attraction between neighboring channel subunits, and tension imposed by the membrane-associated cytoskeleton onto the channel.

Initially, tension applied to the electrode stretches the membrane equally in all directions. If the symmetrical stretch on the membrane is sufficient to overcome the forces that keep the channel closed, the channel will open (figure 20Ab; open). This would be equivalent to channel activation. Asymmetrical relaxation of the membrane cytoskeleton along one axis would increase the amount of area expansion in that direction. This process would reclose the channel by drawing the channel subunits in the orthogonal direction together (figure 20Ac; adapted). This would be equivalent to channel adaptation following pressure. This model may explain why adaptation is both lost (Hamill and McBride, 1992) and overcome (Gustin et al., 1988; Hamill and McBride, 1992) with large pressures applied to the electrode. Under these conditions, the relaxation of the membrane can not accommodate for the pull on the channel in the orthogonal direction.

The induction of prolonged openings following pressure has been previously interpreted as a loss of adaptation in dystrophin-deficient myotubes (McBride and Hamill, 1992). I, however, prefer the interpretation that the mechanisms which close

mechanosensitive channels are defective in dystrophin-deficient myotubes. In dystrophin-deficient myotubes, once mechanosensitive channels open, they may remain open and releasing suction though the electrode does not cause them to reclose (figure 20Ba-c). Pressure applied to the electrode, however, will cause channels to close (figure 20d; SIN gating). This would be equivalent to stretch-inactivated gating as observed in dystrophin-deficient myotubes.

A role for dystrophin in mechanosensitive-gating

Dystrophin contains a central rod-like region flanked by proline hinges, which is believed to dimerize in an antiparallel pattern, forming a "chicken wire-like" matrix within the membrane (Koenig and Kunkel, 1990). This molecular structure would make the dystrophin-network well suited to allow elasticity along one axis. Dystrophin also assoicates with actin filaments (Isobe and Shimada, 1986; Bennett, 1990; Koenig et al., 1988), which exert tension on the membrane (O'Nell et al., 1990; Lakonishok et al., 1992). Stretch-activated channels require less pressure to open when dystrophin is absent, or under conditions which depolymerize the actin-based cytoskeleton (Guharay and Sachs, 1984), it is therefore likely that the dystrophin-actin network normally imposes tension onto mechanosensitive channels at rest.

Figure 21 shows that the barrel model of mechanosensitive-gating can be made to work within the framework of the dystrophin-actin network. Under resting conditions the dystrophin-actin network imposes tension onto mechanosensitive channels, keeping them closed (figure 21a). Stretching the membrane distends the dystrophin-cytoskeletal network (figure 21b), opening channels. After a delay, the dystrophin-actin network relaxes, allowing the membrane to expand more in the direction of dystrophin's long axis (figure 21c), reclosing channels.

A role for Ca^{2+} in the relaxation of the dystrophin-actin cytoskeletal network

Several pieces of evidence support a mechanism where relaxation of the membrane-associated cytoskeleton occurs in response to membrane pressure. First, changes in membrane tension have been reported in patches of myotube membrane while under pressure (Sokabe and Sachs, 1990). Second, increasing Ca^{2+} concentration increases the elasticity modulus of cytoskeletal networks (Dembo and Harlow, 1986; Nossal, 1988). This effect is thought to be mediated by a class of Ca^{2+}-activated, actin-binding proteins which depolymerize actin filaments (Weeds, 1982). Specifically, two proteins known as gelsolin (Yin and Stossel, 1979; Ishikawa, et al., 1989) and villin (Bretscher and Weber, 1980; Northrop et al., 1986) promote actin depolymerization in a Ca^{2+}-dependent manner. Other cytoskeletal proteins (tropomyosin), stabilize actin filaments (Broschat, 1990).

It is intriguing to hypothesize a mechanism whereby Ca^{2+} entry through mechanosensitive channels causes relaxation of the dystrophin-actin network either through the activation of proteins which competitively inhibit the association of actin with dystrophin, or by the depolymerization of actin filaments. Figure 22a depicts one possibility where actin filaments impose tension onto opposing dystrophin molecules, thereby keeping resting tension on the channel. Stretching the membrane in one direction increases tension on actin filaments in the opposite direction (figure 22b). Ca^{2+} entry through mechanosensitive channels (opened with stretch) would result in the depolymerization of actin filaments, increasing the expansion of the membrane in the direction of cytoskeletal relaxation (figure 22c). For such a mechanism to work, the relaxed state of the dystrophin-actin network (closed channel = no Ca^{2+} influx) must prohibit the reassembly of actin filaments, or render the dystrophin-actin binding site inaccessible. A another model could be imagined where Ca^{2+} entry through mechanosensitive channels would regulate the association of dystrophin with actin filaments. Interestingly, dystrophin has been shown to contain two putative Ca^{2+} binding sites (Ervasti and Campbell, 1993).

One could also envision an active model where contraction, rather than relaxation, of cytoskeletal elements results in channel closing (Slager et al., 1992; Yumura, 1991; see also figure 20a; channel adaptation). I, however, favor my model because it is simple, self-contained, and does not require the expenditure of metabolic energy. Simply stated, Ca^{2+} entry through the channel results in the depolymerization of actin filaments, and closing the channel causes actin filaments to reanneal by interrupting the influx of Ca^{2+}. Furthermore, a mechanism where relaxation is the induced state following pressure is observed in hair cells (Howard and Hudspeth, 1987; see also figure 19).

Adaptation in hair cells is dependent on extracellular Ca^{2+} (Assad et al., 1989; Assad and Corey, 1992). Like those reported in skeletal muscle (Franco and Lansman, 1990a,b), the mechanotransducing channels in hair cells are permeable to Ca^{2+} (Hudspeth, 1989). Could Ca^{2+}-dependent depolymerization of the cytoskeleton at the base of the hair bundle confer added flexibility? Channel adaptation in *Xenopus* oocytes, on the other hand, does not require Ca^{2+} in the patch electrode (Hamill and McBride, 1992). In this case, Ca^{2+} may be released from intracellular stores or, alternatively, channel adaptation may arise from the activation of other actin-binding proteins which do not require Ca^{2+} (Bamburg and Bray, 1987; Abe and Obinata, 1989; Abe et al., 1990; Cao et al., 1992).

The salient features of my model are as follows: 1). The dystrophin-actin network imposes tension onto mechanosensitive channels at rest, keeping them closed. 2). Stretch applied to the membrane opens channels, and concomitantly increases tension on actin filaments coupled to dystrophin molecules. 3). Depolymerization of actin filaments relaxes tension on the dystrophin network. 4). Membrane expansion in the direction of cytoskeletal relaxation, closing channels.

Implications of the barrel model for stretch-inactivated-gating

Why is it that channels become tonically open when dystrophin is absent? In dystrophin-deficient muscle cells, stretch-activated channels require less pressure to open

due to the loss of the opposing tension imposed by the dystrophin-actin network. Accordingly, once opened there is less membrane tension acting to reclose the channel. Therefore, channels should open more easily, and remain open for longer when the membrane is stretched. However, this alone is not sufficient to keep the channel open. Channels often displayed normal stretch-activated gating just prior to tonic activation, suggesting that irreversible changes in membrane properties are associated with channel conversion (figure 13). We interpret these results to indicate that dystrophin contributes to a larger cytoskeletal network that is weakened when dystrophin is absent, and that further dissolution of the remaining cytoskeleton results in channels becoming tonically active.

Depolarization may cause channel dipoles to shift, increasing the electrostatic repulsion between neighboring subunits. We show that opening the channel with depolarization is also sufficient to cause tonic channel activation and subsequent suppression with pressure (figure 14). It thus appears the opening the channel by any manner can cause irreversible changes in membrane properties. However, the inactivation of channel activity following tonic activation is specific for stretch, as depolarization only increases channel activity.

How is it that channels which are tonically open, close when pressure is applied to the electrode? Other forces on the channel are relatively uneffected by the absence of the dystrophin-actin network. I argue that the relative distribution of membrane tension when dystrophin is absent is similar to that when the dystrophin-actin network is fully relaxed. Therefore, the channel will close when pressure is applied to the electrode, i.e. stretch-inactivated gating.

A distinction must be made at this point. The reversible nature of stretch-inactivated gating is due to the inherent elastic properties of the membrane. In this case the favored energetic state of the channel is open, and stretching the membrane reversibly closes the channel. On the other hand, during channel adaptation, channel closure is due to the committed relaxation of the dystrophin-actin network while the membrane is being

stretched. In the adapted state (membrane stretched), the favored energetic state of the channel is closed, and releasing stretch does not reopen the channel, but instead reestablishes the resting conformation of the cytoskeleton (channel closed). Since the energetics of channel adaptation can not be examined in the absence of channel activation, a relationship between stretch-inactivation and channel adaptation can only be assumed.

The ability of stretch to overcome the forces keeping the channel closed would be the threshold for mechanosensitive-gating. A lower threshold for stretch-activated gating in myotubes lacking the dystrophin-actin network supports this interpretation. A still lower threshold for stretch-inactivated gating agrees with the interpretation that further dissolution of the membrane cytoskeleton leads to channel conversion. The energy required to pull the channel subunits through the membrane phospholipid would be the sensitivity of the channel to pressure (i.e., the slope of the Boltzmann relationship). Although gating thresholds differ for stretch-activated and stretch-inactivated gating, the slopes of their Boltzmann relationships are similar. This is consistent if one agrees that the energy required to pull the channel subunits through the membrane phospholipid does not differ in stretch-activated and stretch-inactivated conditions.

The expression of stretch-inactivated channels in other cell types

Stretch-inactivated channels have been also described in molluscan growth cones (Morris and Sigurdson, 1989). The integrity of the membrane cytoskeleton in growth cones is known to be in a state of constant change (Letourneau et al.,1987; Mitchison and Kirschner, 1988; Smith, 1988). Neuronal growth cones may, therefore, recapitulate a dystrophic-like condition in a non-muscle tissue. There are some interesting similarities between the channel types observed in molluscan neurons (figure 23b) and dystrophic skeletal muscle (figure 23a; Morris, 1990). One of the most obvious is that the stretch-inactivated gating is shifted to lower pressures relative to stretch-activated gating. In addition, both channel types appear to be equally sensitive to suction as suggested from the

slopes of their pressure relationships. Finally, in all cases stretch-inactivated channels are known to coexist within the same cell with stretch-activated channels.

Effects of the extracellular matrix on the activity of mechanosensitive channels.

One of the best described events preceding myoblasts fusion is the influx of extracellular Ca^{2+} (Shainberg et al., 1969; David and Higginbotham, 1981). The fact that the density of mechanosensitive channels is highest in myoblasts prior to fusion supports a role for mechanosensitive channels in myogenesis (Franco and Lansman, 1990b; Chapter 1). Laminin induces the proliferation and subsequent differentiation of myoblasts in culture (Ocalan et al., 1988). Here I show that the activity of mechanosensitive channels is higher in muscle cell cultures grown in the presence of laminin (figure 16). It is possible that the mitogenic effects of laminin are mediated through increases in the activity of mechanosensitive channels and are dependent upon subtrate-induced changes in tension.

Mechanosensitive and voltage-sensitive gating in FDB fibers

Compared to *mdx* myotubes, *mdx* FDB fibers express relatively mild alterations in mechanosensitive-gating. The response of stretch-activated channels in *mdx* FDB fibers is only reduced when compared to wild type fibers (figure 5). On the other hand, voltage-dependency (figure 7), and resting channel activity (figures 2 and 3) does not differ significantly between wild type and *mdx* FDB fibers.

The reduced pressure-sensitivity of mechanosensitive channels in *mdx* FDB fibers may reflect differences in the composition of the membrane-associated cytoskeleton, rather than the specific deletion of dystrophin. Recently it has been shown that utrophin, an autosomal homologue of dystrophin (Tinsley et al., 1992), substitutes for dystrophin in small caliber fibers of the *mdx* mouse foot (Matsumura et al., 1992). Myoblasts were isolated from the hind limb musculature, which shows progressive degeneration in the *mdx* mouse (Bulfield et al., 1984; DiMario et al., 1991), but not the replacement of utrophin for

dystrophin (Matsumura et al., 1992). The relatively minor alterations in mechanosensitive-gating, as well as, the absence of degeneration in *mdx* FDB fibers may reflect the ability of utrophin to compensate for the lack of dystrophin. It remains to be determined if intact fibers from other muscle groups lacking both dystrophin and utrophin show alterations in mechanosensitive-gating more similar to those expressed in myotubes.

The membranes of *mdx* FDB fibers are more distensible than those of wild type fibers (Hutter et al., 1991). Membrane tension is a function of the applied pressure multiplied by the radius of curvature (LaPlace's law). Figure 24 shows that the membranes of *mdx* FDB fibers should experience less tension, simply because of the smaller radius of curvature of the membrane bleb held within the electrode while under pressure (Sokabe et al., 1991). This may also indicate that *mdx* FDB membranes flow more readily into the lumen of the electrode while suction is being applied to the electrode (Sokabe and Sachs, 1990).

The suppression of resting channel activity following suction (figure 6), may also be accounted for on the basis of membrane compliance. If the residual tension on the membrane, as a result of electrode seal formation, is greater than the tension imposed by the cytoskeleton onto the channel, the channel will open (if my model is correct). This is most likely the basis for resting channel activity. If during suction extra membrane is taken up into the electrode, the membrane will slacken when the pressure is released. Accordingly, resting channel activity in the absence of suction will also decrease. Because of the greater mobility of the membrane, more compliant membranes should be drawn up into the electrode in greater amounts during the application of suction (see figure 24). It is therefore understandable that highly complaint membranes should display suppressions of resting channel activity following suction. Since myoblasts also display this phenomenon, they should also posses compliant membranes (figure 15). By analogy, the membranes of dystrophin-deficient myotubes should also be highly compliant.

In conclusion, in this chapter I shows two examples of how membrane properties can influence the gating of mechanosensitive channels. First, the state of the membrane-associated cytoskeleton can directly influence the gating mechanism of mechanosensitive channels. This would be analogous to the expression of stretch-inactivated channels in dystrophin-deficient myotubes. Second, differences in the mechanical properties of the membrane may influence how the channels respond to stretch. This may be the situation that is observed in *mdx* FDB fibers.

Table 3-1

Single-channel conductances of mechanosensitive channels in wild type and *mdx* muscle cells.

	Physiological Saline			110 mM $BaCl_2$			110 mM $CaCl_2$		
	γ (pS)	E_{rev} (mV)	n	γ (pS)	E_{rev} (mV)	n	γ (pS)	E_{rev} (mV)	n
Myotubes									
***mdx*; low activity**	25.0 ± 2.0	14.0 ± 7.0	6	18.5 ± 2.0	18.0 ± 8.0	5	8.0 ± 3.0	38.0 ±11.0	3
***mdx*; high activity**	24.0 ± 2.0	16.0 ± 8.0	6	19.0 ± 3.0	18.0 ± 8.0	9	7.0 ± 2.0	40.0 ± 0.5	4
wild type	26.0 ± 1.0	10.0 ± 2.0	2	19.0 ± 2.0	20.5 ± 6.0	4	10.0 ± 1.0	32.0 ± 11.0	3
FDB fibers									
mdx	25.0 ± 2.0	9.0 ± 2.0	7	17.0 ± 0.5	15.0 ± 2.0	3			
wild type				16.0 ± 0.5	20.0 ± 2.5	8	8.0 ± 1.0	27.0 ± 3.0	3

γ, single-channel conductance; E_{rev}, reversal potential; n, number of experiments; ± S.D.

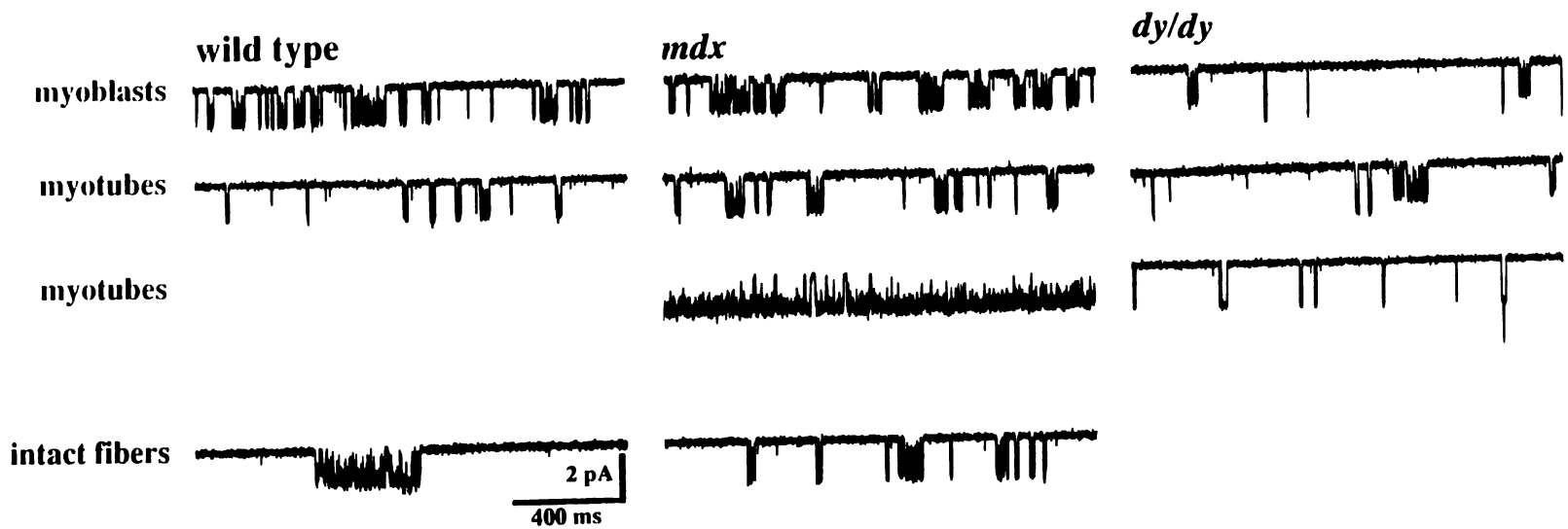
wild type
mdx
dy/dy
myoblasts
myotubes
myotubes
intact fibers
2 pA
400 ms

Figure 3-1. Channel openings of extremely long duration are detected in *mdx* myotubes. Channel activity recorded from wild type (**Left**), *mdx* (**Middle**) and *dy/dy* (**Right**) mice from myoblasts, myotubes and intact fibers; *dy/dy* intact fibers were not included in the analysis (see Methods). Records were chosen for clarity of channel transitions and may not be representative of mean open probability for a given condition. All recordings were made at a constant holding potential of -60 mV in this and all other experiments except where otherwise indicated. Single-channel records were filtered at 2kHz and sampled at 5 kHz in this and all other experiments except where otherwise indicated.

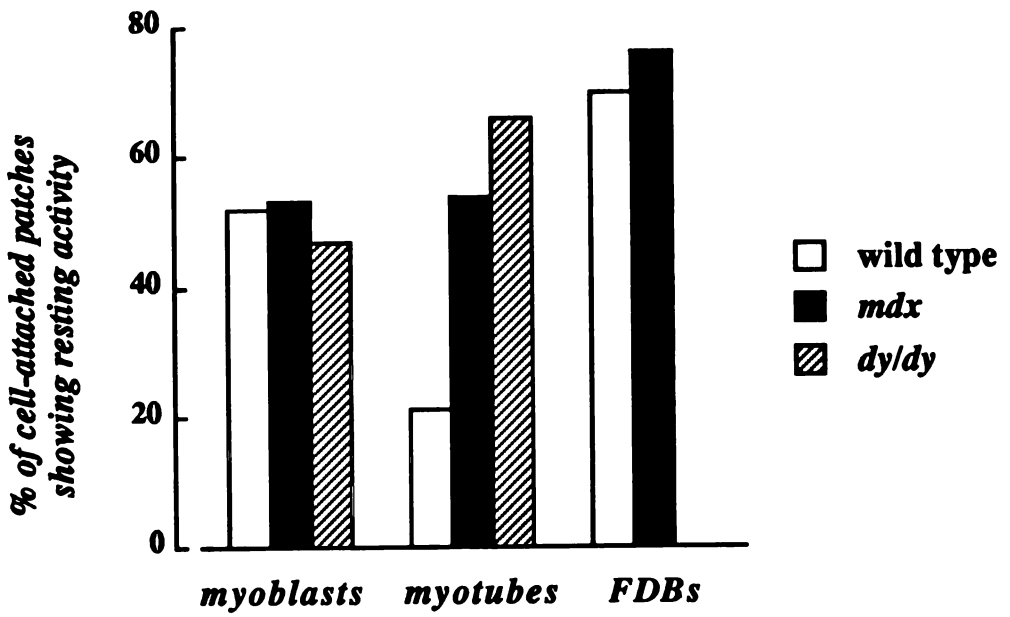

Figure 3-2. Fraction of cell-attached patches showing channel activity under resting conditions. Resting activity was detected in ~52% (wild type), ~53% (*mdx*) and ~47% (*dy/dy*) of cell-attached patches from the surface of myoblasts and in ~21% (wild type), ~54% (*mdx*) and ~66% (*dy/dy*) of cell-attached patches from myotubes. For FDB fibers the fraction of cell-attached patches showing resting channel activity was ~70% (wild type) and ~76% (*mdx*).

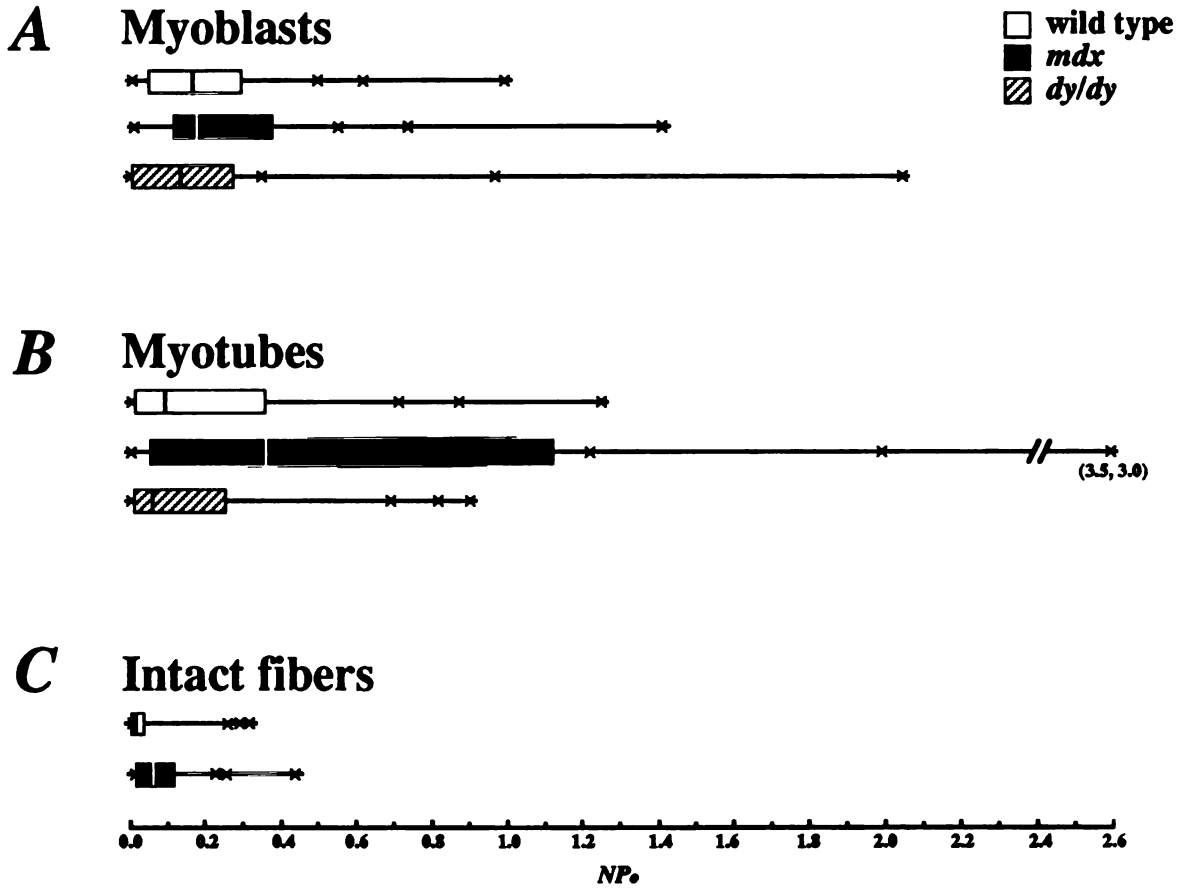
A
Myoblasts
wild type
mdx
dy/dy
B
Myotubes
(3.5, 3.0)
C
Intact fibers
0.0
0.2
0.4
0.6
0.8
1.0
1.2
1.4
1.6
1.8
2.0
2.2
2.4
2.6
NPo

Figure 3-3. *Mdx* myotubes showed the highest levels of resting channel activity. Channel activity recorded from myoblasts, myotubes and FDB fibers under resting conditions. Resting NP_os are shown in the form of box plots. In this form of analysis the center line through the box represents the median value of the data set and the values at which one quarter of the observations lie above and below define its outer margins. The outlying points represent the three highest values and the single lowest value of each data set.

Resting activity of mechanosensitive channels only varied significantly between classes of myotube. In recordings from myoblasts, the mean values of channel activity were 0.24 ± 0.06 (wild type; n=18), 0.30 ± 0.09 (*mdx*; n=16) and 0.28 ± 0.13 (*dy/dy*; n=15). In myotubes, the mean values of channel activity were 0.25 ± 0.07 (wild type; n=24), 0.73 ± 0.21 (*mdx*; n=29) and 0.17 ± 0.04 (*dy/dy*; n=44). For FDB fibers the mean values of channel activity were 0.045 ± 0.02 (wild type; n=35) and 0.075 ± 0.02 (*mdx*; n=38). The range in the data are given as standard errors.

mdx FDB fiber

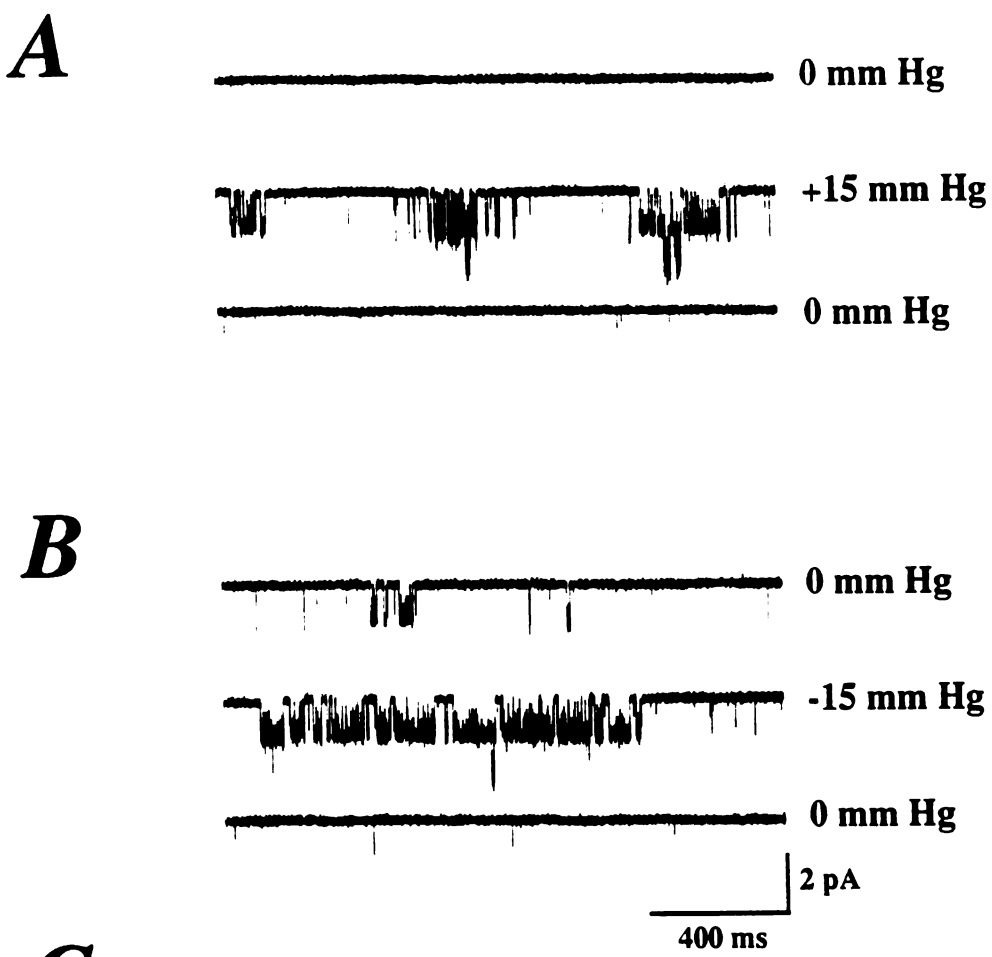

Figure 3-4. Positive (blowing) or negative (suction) pressure applied to the patch electrode opens stretch-activated channels. Channel activity elicited with positive (**A**) or negative (**B**) pressure in a recording from a *mdx* FDB fiber. **C**). Channel activity as a function of positive and negative pressure on channel activity for the recording shown above. The increase in channel activity with positive or negative pressures were both fit with Boltzmann relationships. For channel activity elicited with negative pressure, $P_{1/2}$ = -21.0 mm Hg and π = -6.0. For channel activity elicited with positive pressure, $P_{1/2}$ = 24.0 mm Hg and π = 5.0.

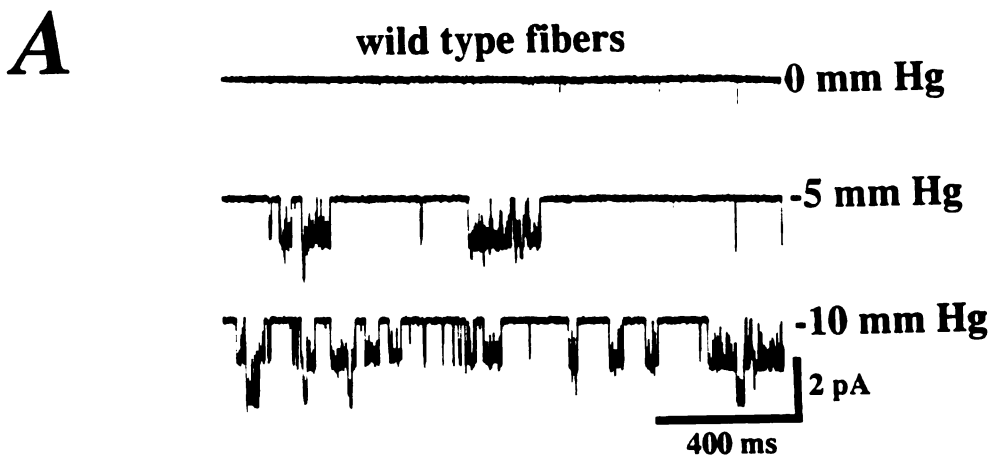
A
wild type fibers
0 mm Hg
-5 mm Hg
-10 mm Hg
2 pA
400 ms

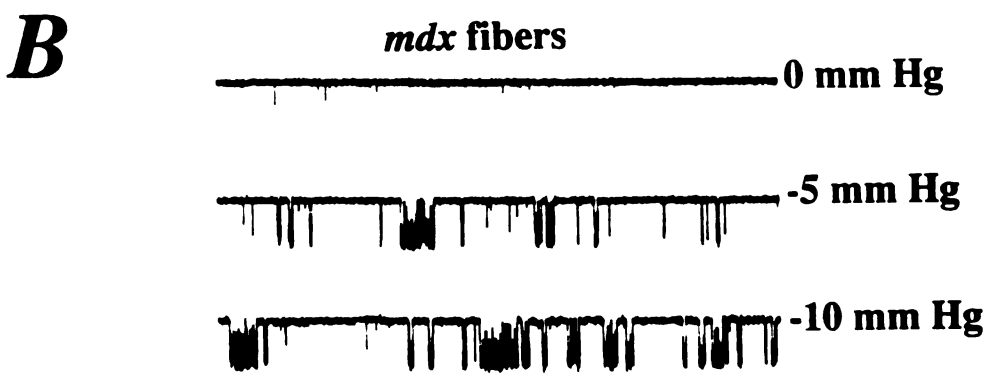
B
mdx fibers
0 mm Hg
-5 mm Hg
-10 mm Hg

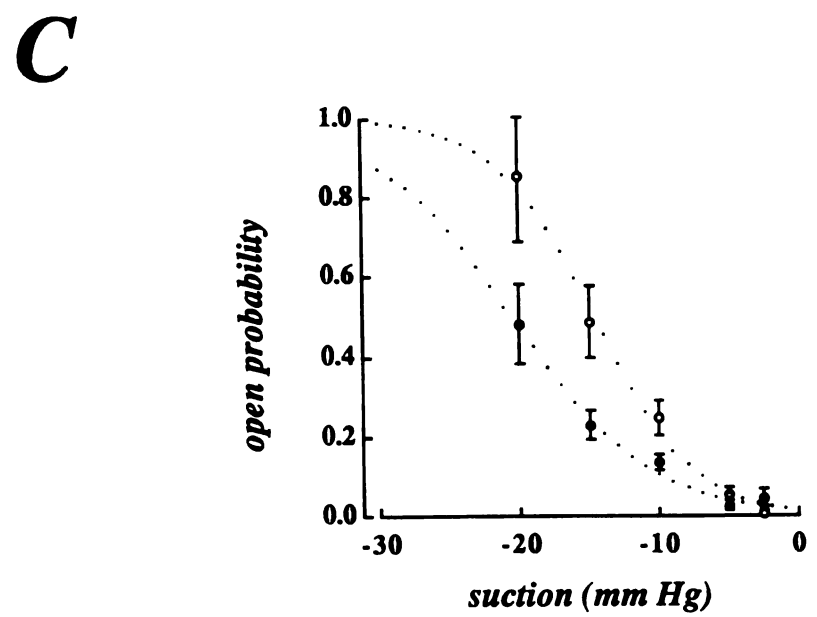
C
1.0
0.8
0.6
0.4
0.2
0.0
open probability
-30
-20
-10
0
suction (mm Hg)

Figure 3-5. Suction applied to the electrode opens channels in wild type and *mdx* FDB fibers. Channel activity recorded from a wild type (A) and *mdx* (B) FDB fiber at the indicated pressures. Channel activity from both wild type and *mdx* FDB fibers increased with pressure applied to the electrode. C). Averaged effects of the amount of suction applied to the patch electrode on channel openings from wild type (open circles; n=22) and *mdx* (solid circles; n=25) FDB fibers. In comparison to mechanosensitive channels from wild type FDB fibers, mechanosensitive channels from *mdx* FDB fibers showed smaller responses to comparable amounts of suction. The data was fit to Boltzmann relationships (dotted lines) with $P_{1/2}$'s = -14.0 and -20.0 mm Hg and π's (steepness) = -3.0 and -5.0, for wild type and *mdx* fibers, respectively. Error bars represent ± standard error of the mean.

The incidence of stretch-activated channels is similar in both wild type and *mdx* FDB fibers. Of 69 (wild type) and 62 (*mdx*) cell-attached patches showing channel activity, 17% (n=12) and 22% (n=14) failed to respond to suction while 82% (n=57) and 78% (n=48) showed stretch-activated gating, respectively.

Channels which are unresponsive to suction applied to the electrode may represent channels which are newly inserted into the membrane and not yet coupled to the tension sensing apparatus of the cell or may indicate channels which are unable to perceive changes in tension due to the configuration of the membrane bleb within the patch electrode. However, these channels have identical single-channel conductances and similar responses to depolarization as channels which showed clear responses to membrane tension (Franco and Lansman, 1990b; also see Chapter 1).

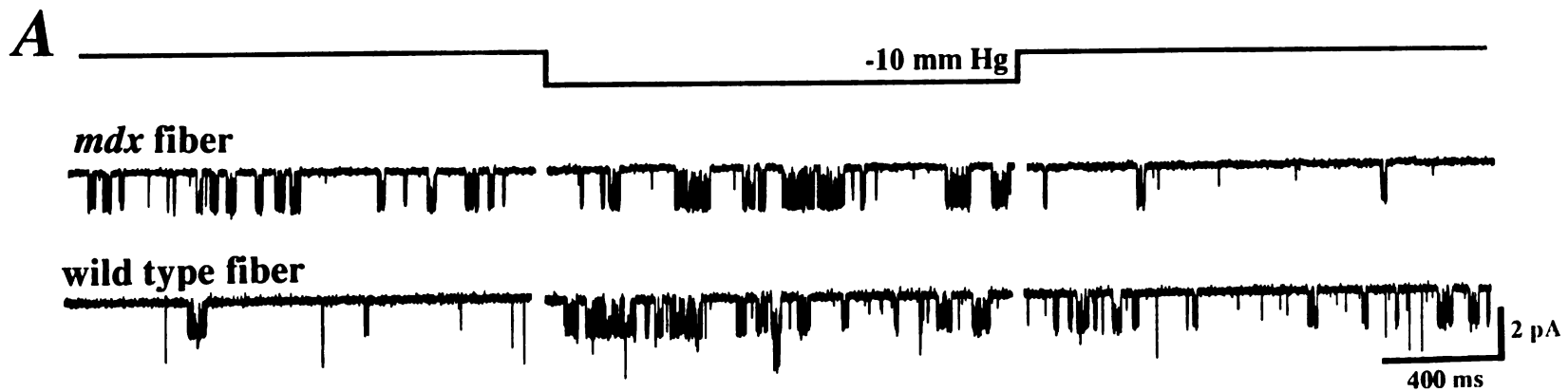
A
-10 mm Hg
mdx fiber
wild type fiber
2 pA
400 ms

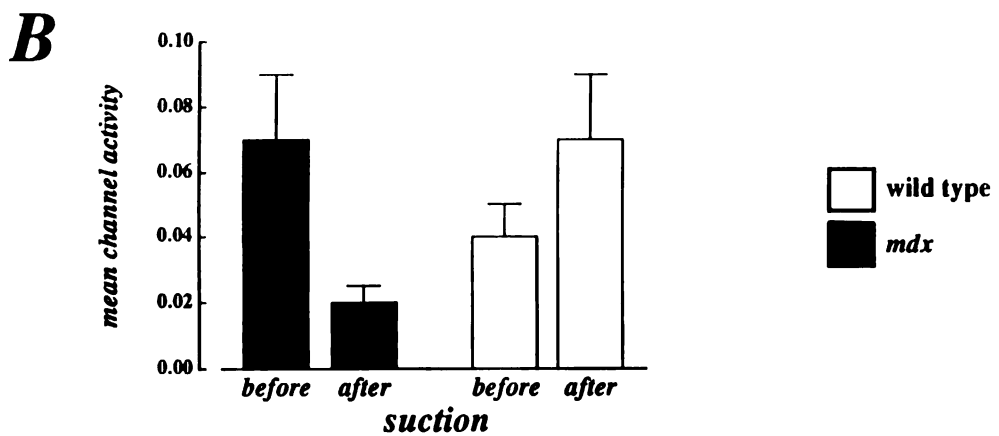
B
mean channel activity
0.10
0.08
0.06
0.04
0.02
0.00
before
after
before
after
suction
wild type
mdx

Figure 3-6. Residual tension on the membrane could suppress channel activity in *mdx* FDB fibers. Changes in resting activity following the application of suction in FDB fibers. **A**). Representative records of channel activity before, during and after suction was applied to the patch electrode for the first time. -10 mm Hg suction was used because it is comparable in magnitude to that used in forming a seal between the electrode and the membrane. Channel activity was reduced after suction in ~73% of patches (n=30) from *mdx* fibers. On the other hand, channel activity increased following suction in ~65% patches (n=31) from wild type fibers. **B**). Mean channel activity before and after suction. The mean values of channel activity were 0.07 ± 0.02 (*mdx*; n=30) and 0.04 ± 0.01 (wild type; n=31) before suction and 0.02 ± 0.005 (*mdx*) and 0.07 ± 0.02 (wild type) after suction. Error bars represent ± standard error of the mean. Significance = 0.176 (wild type) and 0.013 (*mdx*).

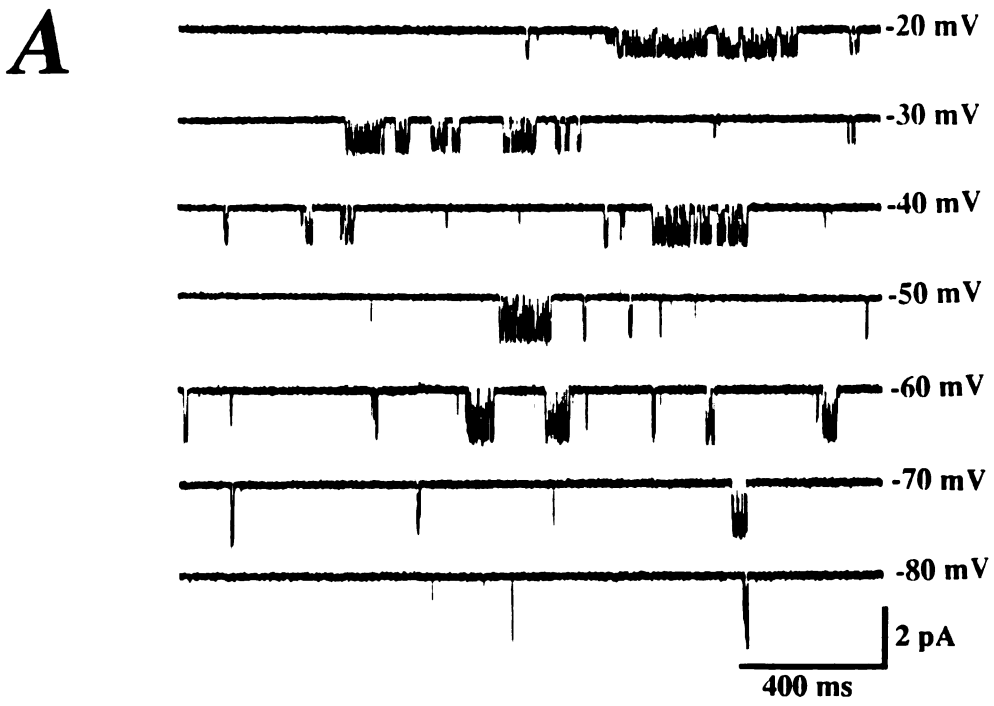
A
-20 mV
-30 mV
-40 mV
-50 mV
-60 mV
-70 mV
-80 mV
2 pA
400 ms

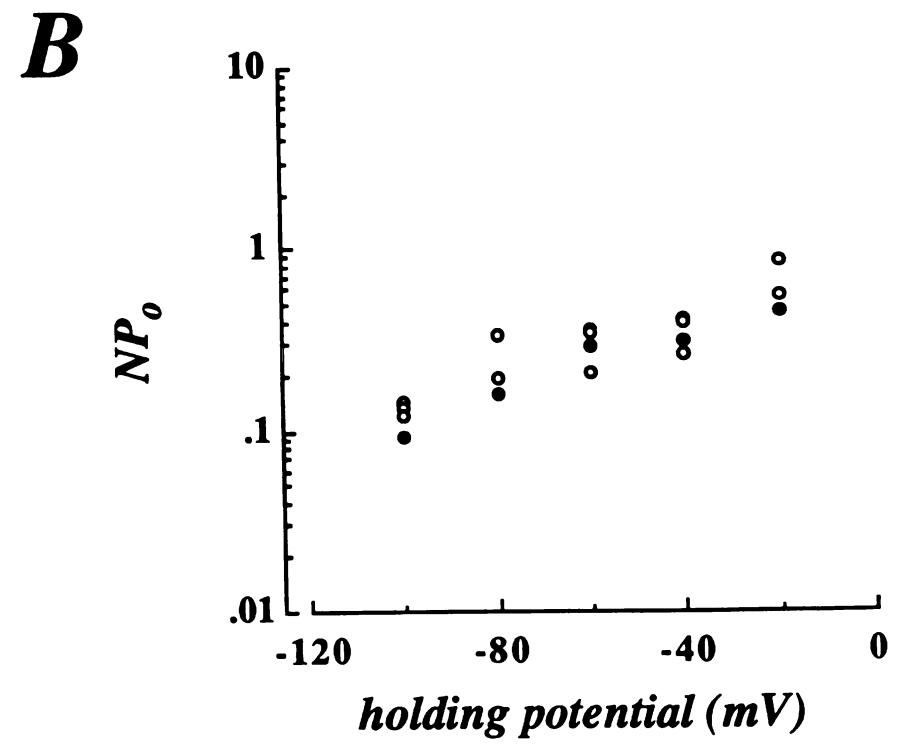
B
10
1
.1
.01
NP0
-120
-80
-40
0
holding potential (mV)

Figure 3-7. Depolarization of the patch membrane potential increases stretch-activated channel activity in both wild type and *mdx* FDB fibers. **A).** Representative records of channel activity from a *mdx* fiber at the indicated patch potentials. **B).** Effect of membrane potential on channel activity in recordings from wild type (open circles) and *mdx* (filled circle) FDB fibers. Channel activity increased *e*-fold for ~56 ± 5 mV (SD, n=3) and ~53 mV (n=1) depolarization for channels activity recorded from wild type and *mdx* fibers.

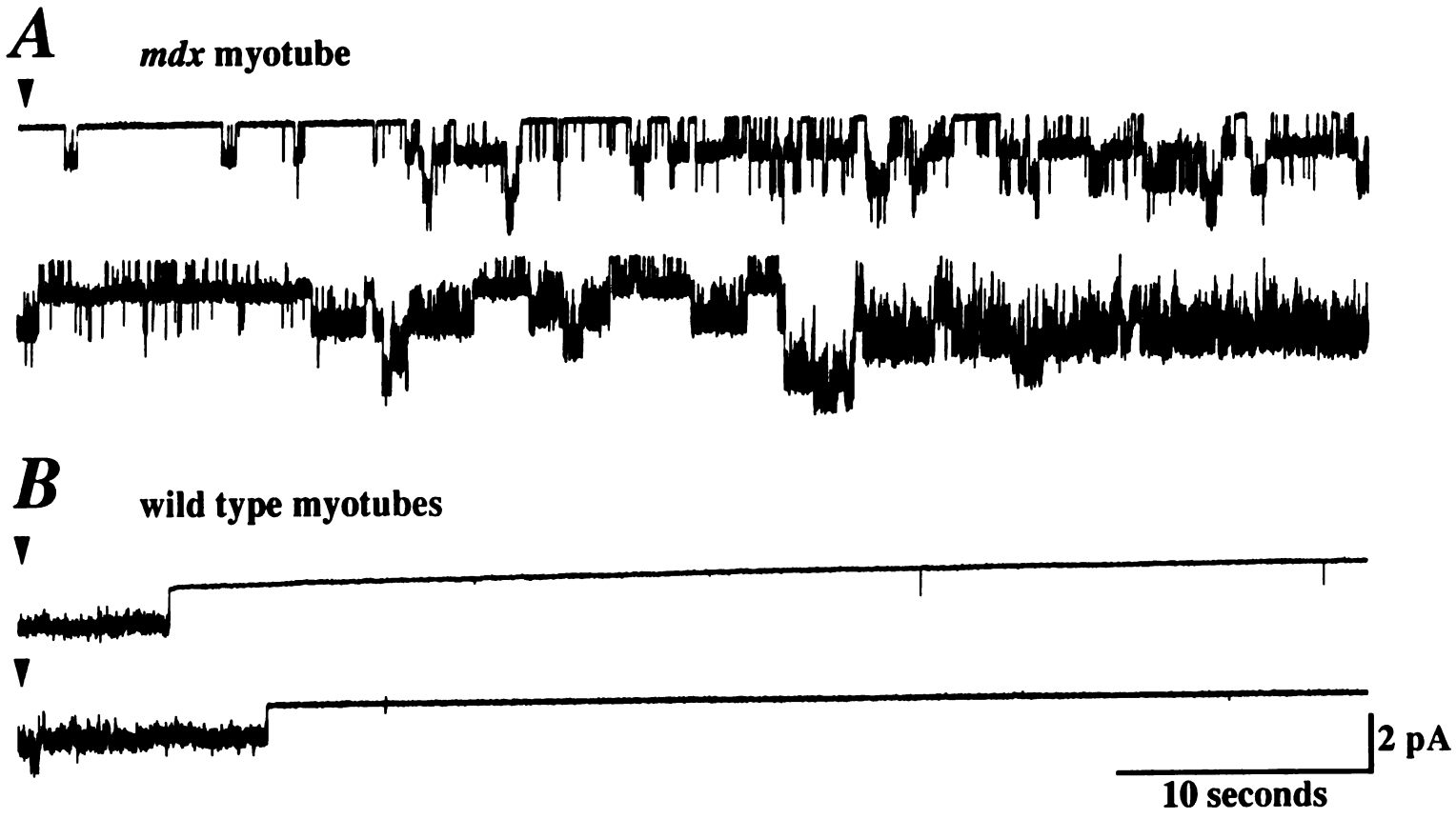
A
mdx myotube
B
wild type myotubes
2 pA
10 seconds

Figure 3-8. The level of resting activity often increased following electrode seal formation with the membrane in dystrophin-deficient myotubes. A). Example of the increase in channel activity following seal formation in a *mdx* myotube. Consecutive single-channel records beginning immediately after starting recording. Increases in channel activity after seal formation were observed in ~10% (*mdx* myotubes) and ~0.5% (wild type myotubes) of cell-attached recordings. **B).** Two examples of the decrease in channel activity immediately following seal formation in wild type myotubes. Arrows indicate when single-channel recordings were begun (~30-45 seconds after seal formation). Single-channel records were filtered at 0.5 kHz and sampled at 1.25 kHz.

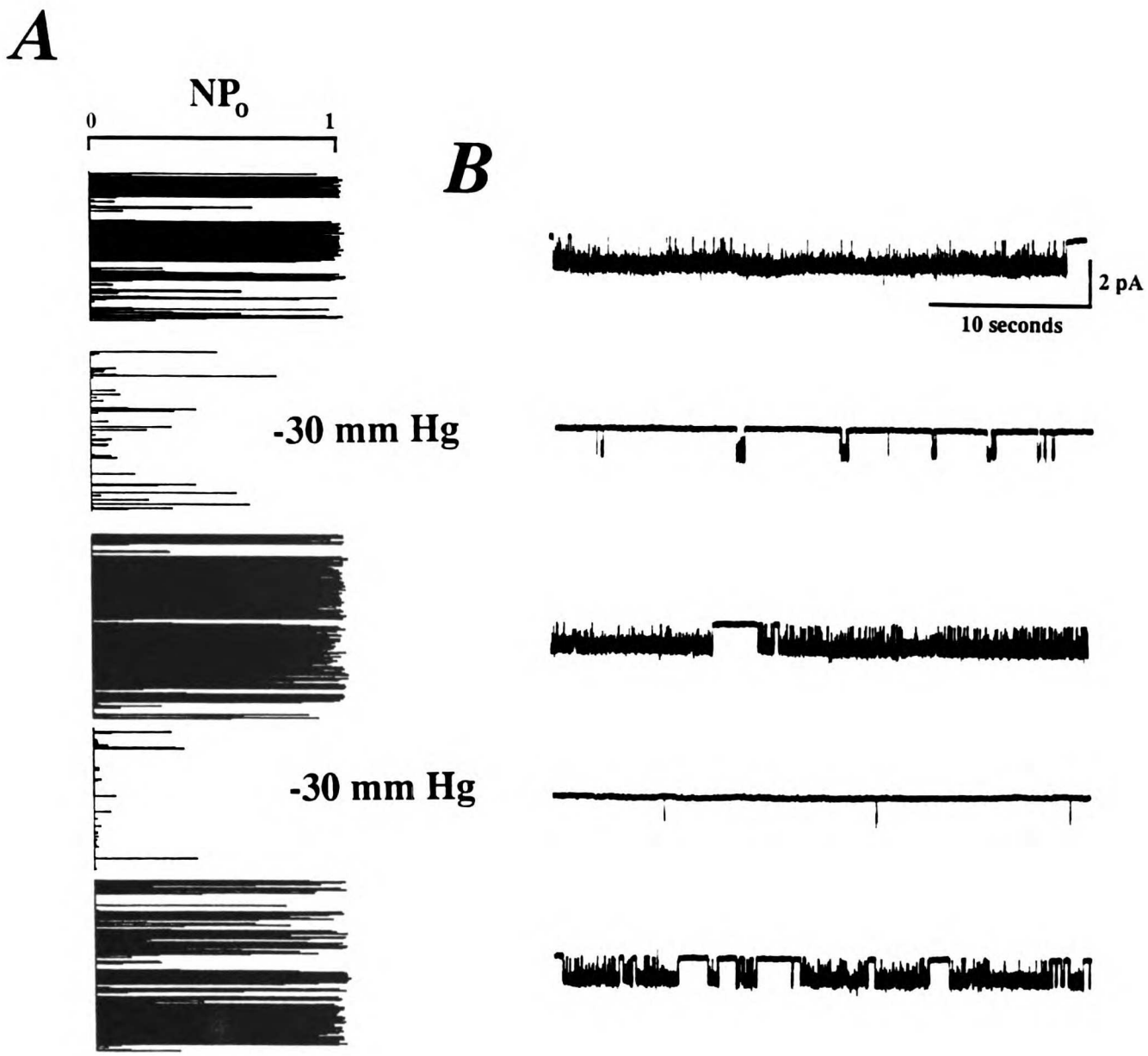
A
NP0
0
1
B
2 pA
10 seconds
-30 mm Hg
-30 mm Hg

Figure 3-9. The effects of suction on stretch-inactivated channel activity were reversible. **A**). Channel open probability per 1 second interval for a recording of ~13 minutes duration. Suction (-30 mm Hg) was applied to the electrode at the indicated times and was released at all other times. 1st interval without suction, NP_o=~54% (143 seconds); 2nd interval with suction, NP_o=~4% (153 seconds); 3rd interval without suction, NP_o=~85% (155 seconds), 4th interval with suction, NP_o=~1% (137 seconds); 5th interval without suction, NP_o=~63% (163 seconds). **B**) Representative current records for the indicated periods. Single-channel records were filtered at 0.5 kHz and sampled at 1.25 kHz.

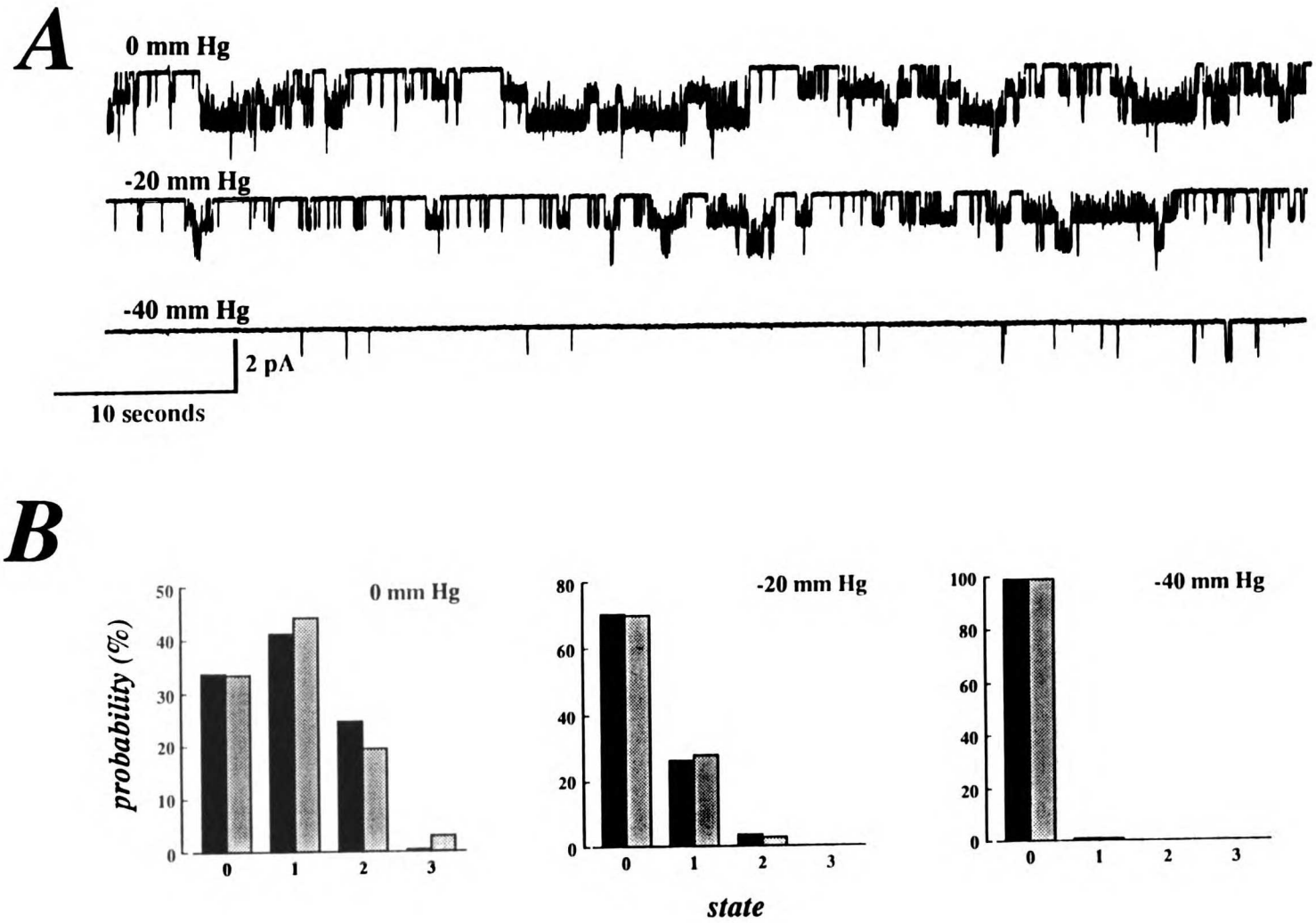
A
0 mm Hg
-20 mm Hg
-40 mm Hg
2 pA
10 seconds
B
0 mm Hg
-20 mm Hg
-40 mm Hg
probability (%)
state

Figure 3-10. Stretch-inactivated channels respond to suction in a graded manner. **A)** Single-channel records from a cell-attached patch recording from a *mdx* myotube containing three stretch-inactivated channels at 0, -20 and -40 mm Hg suction. **B).** Effect of suction on independent openings of stretch-inactivated channels for the recording shown above. At all pressures, the predictions for channel openings in the 1, 2 or 3 opening levels from the binomial distribution (hatched bars) are in good agreement with the experimentally measured values (solid bars). Single-channel records were filtered at 0.5 kHz and sampled at 1.25 kHz.

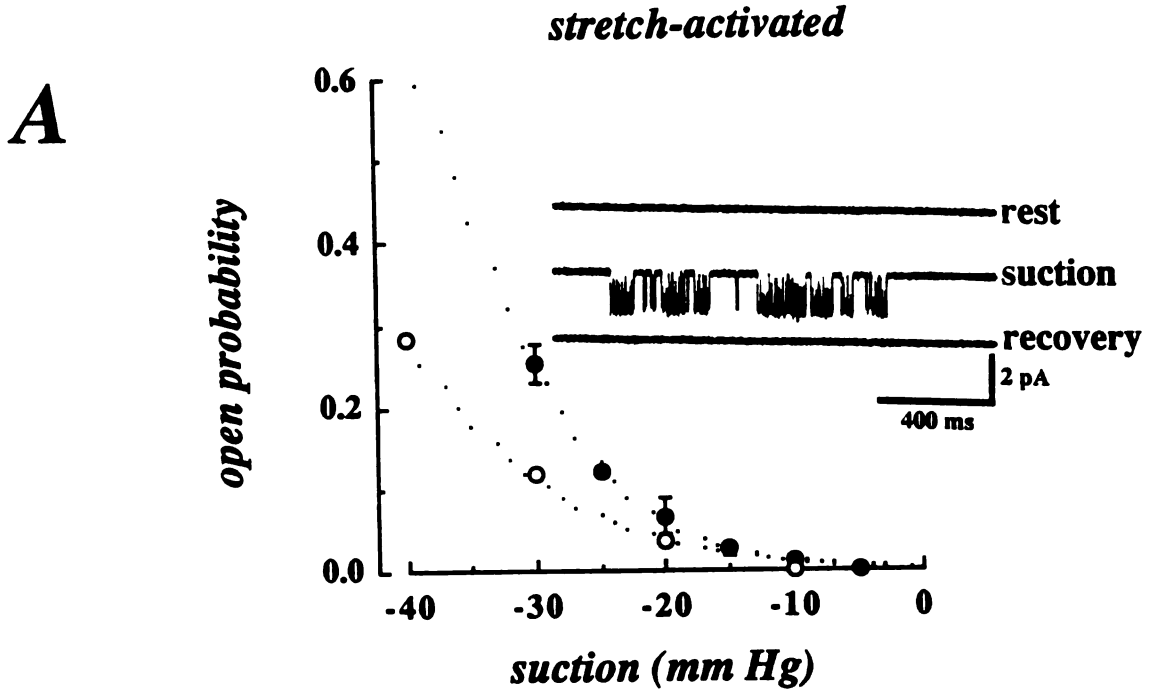
A
stretch-activated
0.6
0.4
0.2
0.0
open probability
rest
suction
recovery
2 pA
400 ms
-40
-30
-20
-10
0
suction (mm Hg)

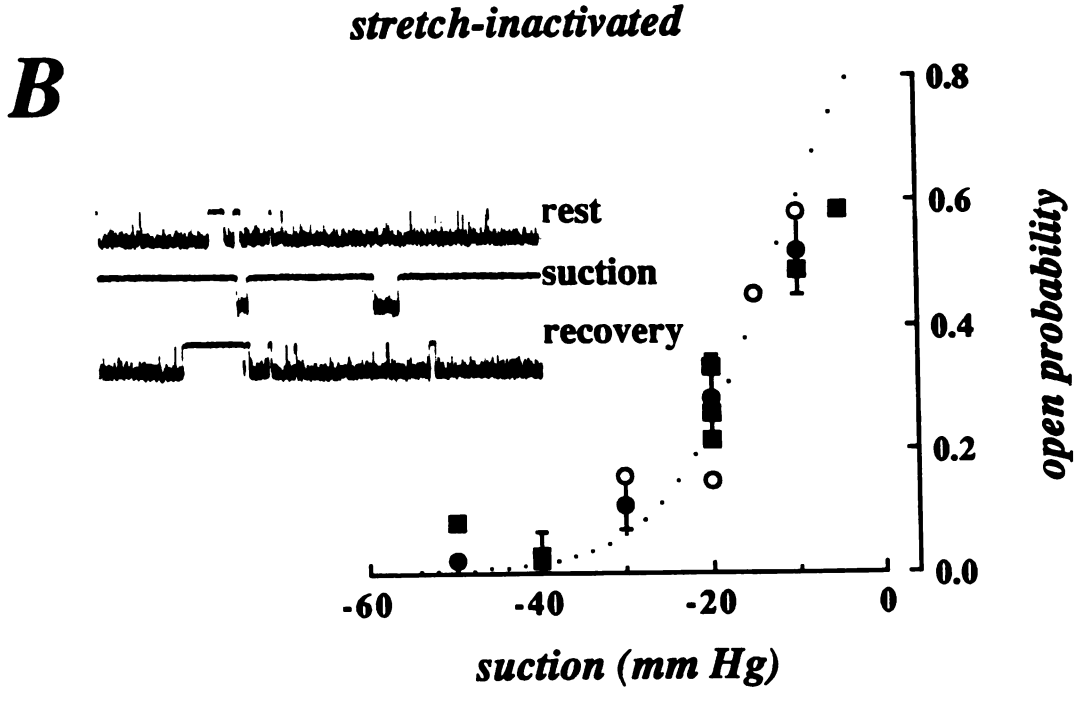
B
stretch-inactivated
rest
suction
recovery
0.8
0.6
0.4
0.2
0.0
open probability
-60
-40
-20
0
suction (mm Hg)

Figure 3-11. Stretch-inactivated and stretch-activated channels respond with similar sensitivity to pressure in dystrophin-deficient myotubes. Effects of the amount of suction applied to the patch electrode on stretch-activated (**A**) and stretch-inactivated (**B**) channels from *mdx* (solid circles) and wild type (open circles) myotubes. The solid squares are from channels in *mdx* myotubes that underwent an irreversible change in gating sensitivity to pressure during the course of a recording (see results; *Irreversible change of mechanosensitive-gating in mdx myotubes*.). The data points represent the average responses of 6 and 14 recordings channels showing stretch-activated and stretch-inactivated gating, respectively, in *mdx* myotubes. I show only single examples of a stretch-activated and stretch-inactivated channels in wild type myotubes. Dotted lines represent non-linear, least-squares fits to a Boltzmann equation as described in Methods. For stretch-activated channels in *mdx* myotubes $P_{1/2}$ = -37 mm Hg and the steepness of the relationship, π= -6.0. For stretch-activated channels in wild type myotubes $P_{1/2}$ = -48 mm Hg and the steepness of the relationship, π= -8. For stretch-inactivated channels $P_{1/2}$ = -13 mm Hg and π = 6.5. Error bars represent ± standard error of the mean. **Insets**). Single-channel current traces showing the opposing effects of suction (-20 mm Hg) on stretch-activated (**A**) and stretch-inactivated channels from *mdx* myotubes (**B**).

Stretch-inactivated channels were almost exclusively detected in dystrophin-deficient myotubes. Of 57 cell-attached patches containing channels from wild type myotubes, 26% (n=15) failed to respond to suction , 70% (n=40) showed stretch-activated gating and 2% (n=1) showed stretch-inactivated gating. Of 44 cell-attached patches containing channels from *mdx* myotubes, 39% (n=17) did not respond to suction, 25% (n=11) showed stretch-activated gating, and 20% (n=9) showed stretch-inactivated gating. The remaining channels (2% (n=1), wild type; 16%, (n=7) *mdx*) underwent an irreversible change in gating behavior during the course of the single-channel recording.

The channels showing the highest levels of resting activity were stretch-inactivated channels. The mean channel open probability for stretch-activated and stretch-inactivated channels in *mdx* myotubes was 0.012 ± 0.004 (S.E.M., n=24) and 0.72 ± 0.27 (S.E.M., n=23), respectively. The mean channel open probability for stretch-activated and stretch-inactivated channel(s) in wild type myotubes was 0.015 ± 0.08 (S.E.M., n=19) and 0.45 (n=1), respectively.

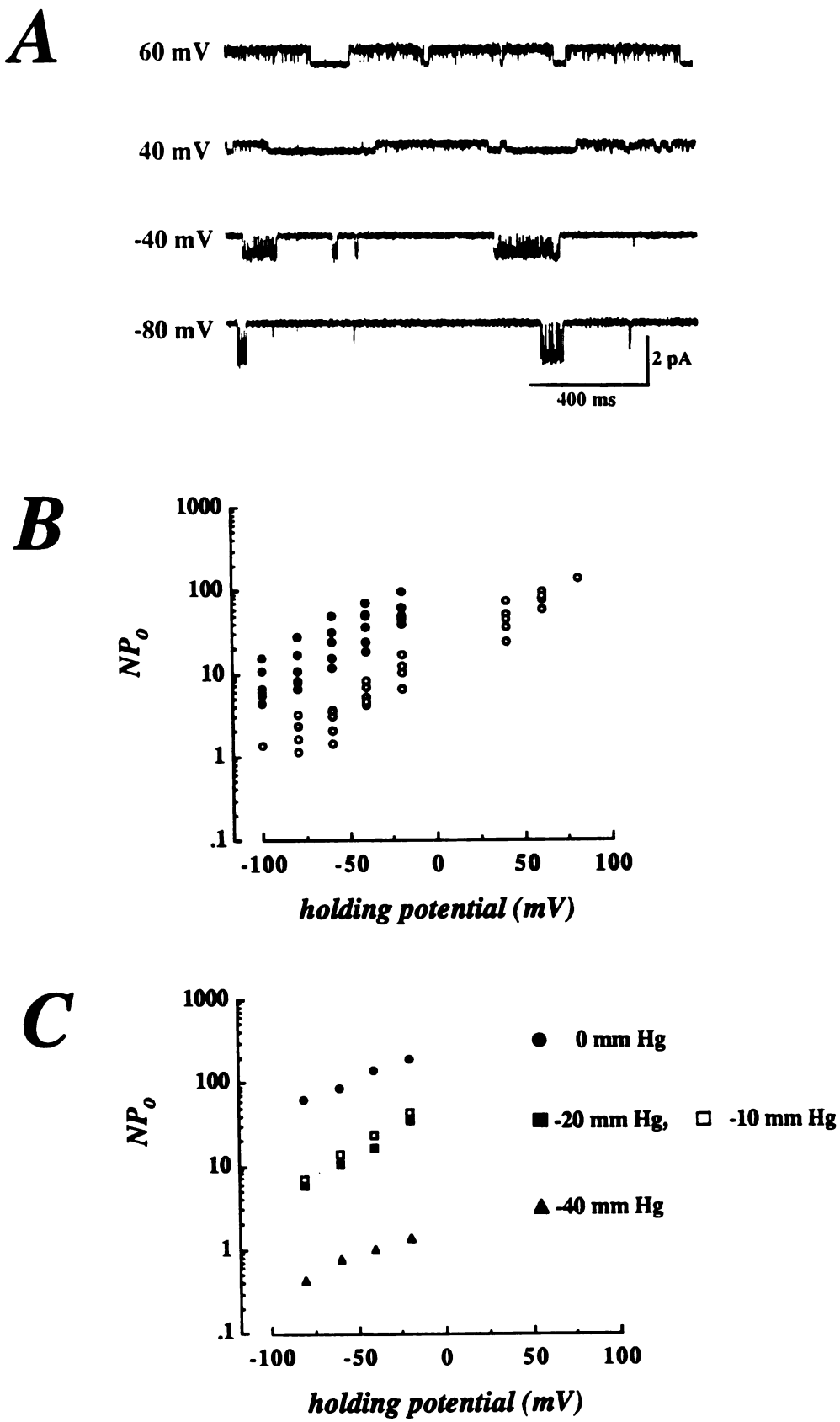
A
60 mV
40 mV
-40 mV
-80 mV
2 pA
400 ms
B
1000
100
10
1
.1
NP_o
-100
-50
0
50
100
holding potential (mV)
C
1000
100
10
1
.1
NP_o
0 mm Hg
-20 mm Hg,
-10 mm Hg
-40 mm Hg
-100
-50
0
50
100
holding potential (mV)

Figure 3-12. Depolarization of the patch membrane potential increases both stretch-activated and stretch-inactivated channel activity. **A).** Representative current traces from a *mdx* myotube at the indicated patch potentials. The upper two traces show outward current through the channel, while the lower two traces show inward current through the channel. **B).** The modulation of channel activity with holding potential for recordings showing high (filled circles) and low (open circles) channel activity from *mdx* myotubes. In *mdx* myotubes, channel open probability increased *e*-fold for ~36 ± 7 mV (SD, n=6) and ~38 ± 5 mV (SD, n=5) depolarization for channels showing high and low activity, respectively. At positive potentials where channel activity increased dramatically, patches already showing high activity at negative potentials could not be analyzed. Note that the relationship for stretch-activated channels is linear over the range where single-channel current reverses direction, suggesting that both inward and outward currents are carried by the same channel (Franco and Lansman, 1990b; also see Chapter 1). **C).** The effect of suction on voltage-sensitive gating of stretch-activated and stretch-inactivated channels. Suction was maintained throughout the range of patch membrane potentials. The solid symbols represent a recording from a *mdx* myotubes which contained several stretch-inactivated channels at the indicated pressures. In the presence of 0 (solid circles), -20 (solid squares) and -40 (solid triangles) mm Hg suction channel activity increased *e*-fold per ~50, ~38 and ~40 mV depolarization, respectively. The experiment shown in open symbols represents a recording from a *mdx* myotube which contained a stretch-activated channel that was closed at rest, but opened when suction was applied to the electrode. In the presence of -10 mm Hg suction (open squares) channel activity increased *e*-fold per ~37 mV depolarization.

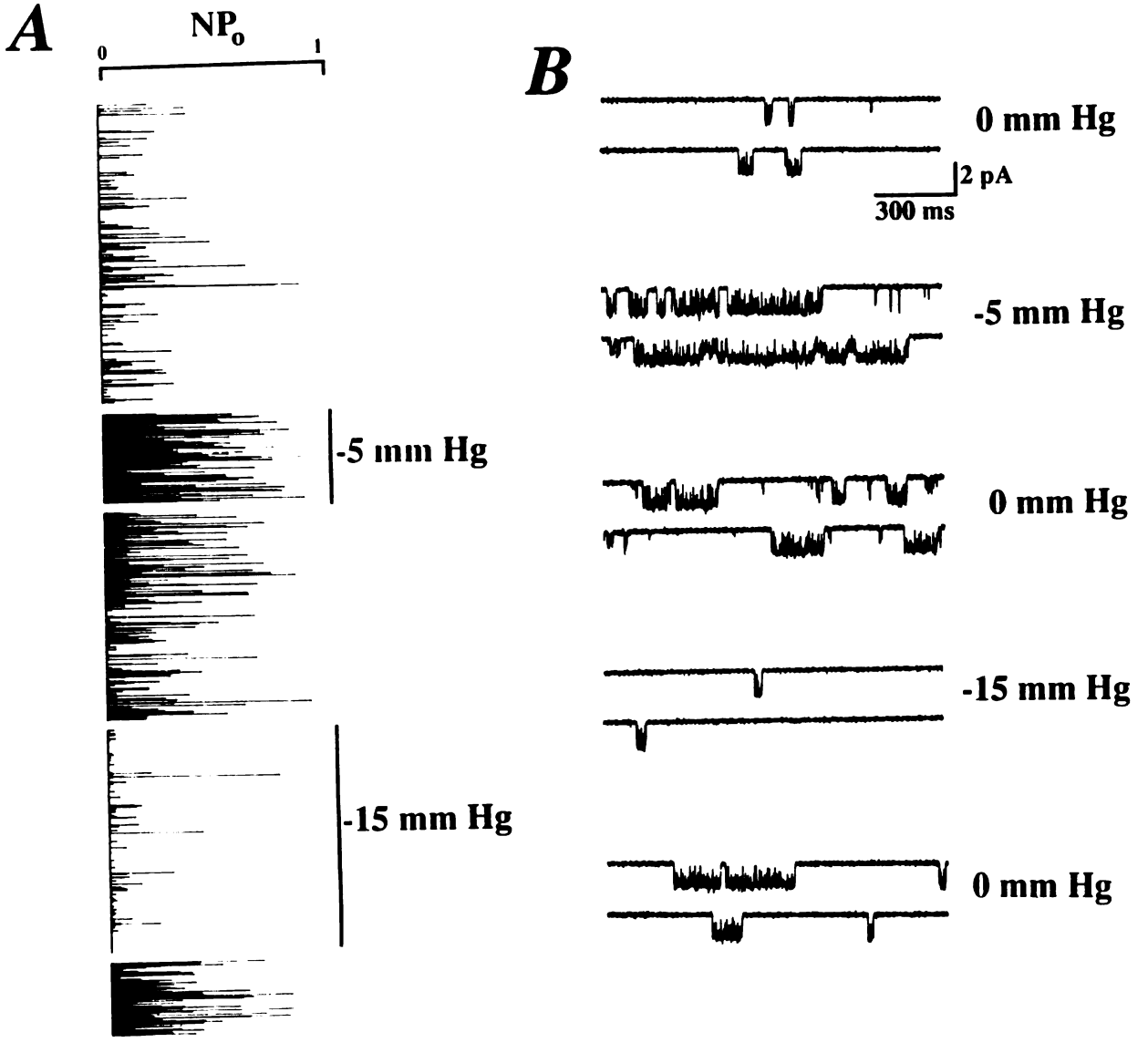
A
NP$_o$
0
1
-5 mm Hg
-15 mm Hg
B
0 mm Hg
2 pA
300 ms
-5 mm Hg
0 mm Hg
-15 mm Hg
0 mm Hg

Figure 3-13. Membrane deformation sometimes causes irreversible changes in channel gating behavior in *mdx* myotubes. **A)** Channel open probability per 200 ms interval. There were three channels within the patch that converted during the recording. The bars indicate the time during which the indicated amount of suction was applied to the patch electrode. At all other times, no suction was applied to the electrode. **B)** Representative current records obtained (from top to bottom) at the beginning of the experiment (NP_o=~4%) before applying suction (0 mm Hg), while applying -5 mm Hg of suction to the electrode (NP_o=~20%), after releasing the suction (0 mm Hg, NP_o=~15%), after applying -15 mm Hg of suction during which time channel activity was suppressed (NP_o=~1%), and after releasing the suction again (0 mm Hg) whereupon channel activity returned to a high level (NP_o=~10%).

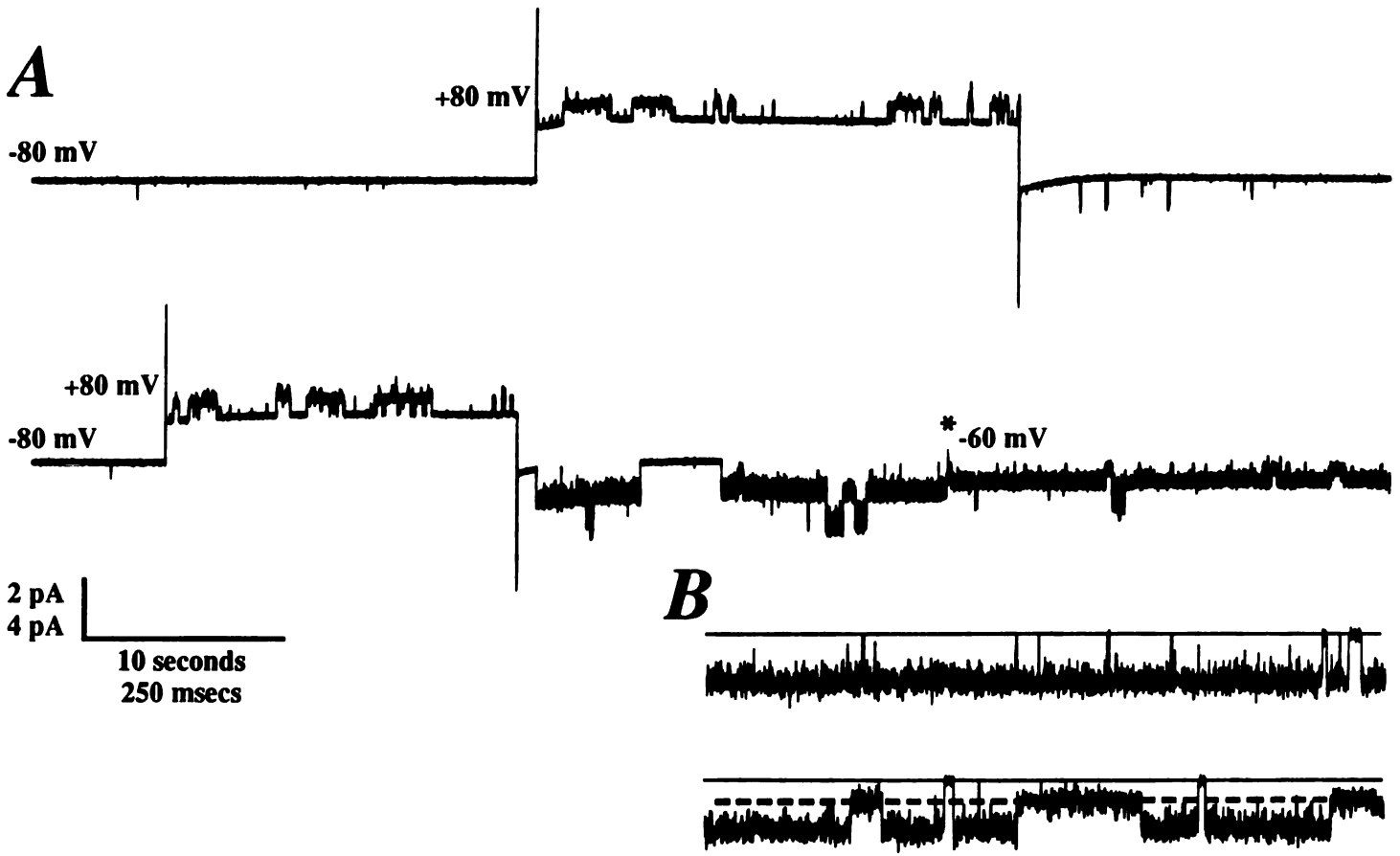
A
+80 mV
-80 mV
+80 mV
-80 mV
*-60 mV
2 pA
4 pA
10 seconds
250 msecs
B

Figure 3-14. Stretch-inactivated channel activity can be induced without membrane deformation. **A**). Voltage pulses were applied to a cell-attached patch from a holding potential of -80 mV, to a test potential of +80 mV and then repolarized back to -80 mV. At the star the holding potential was changed to -60 mV for comparison with previous current records. The records show that long duration channel openings were induced after the second voltage-pulse in a recording from a *mdx* myotube. Single-channel records were filtered at 0.5 kHz and sampled at 1.25 kHz. **B**). Expansion of the current records shown in **A** at a holding potential of -60 mV. Single-channel records were filtered at 2 kHz and sampled at 5 kHz. The vertical scale bar represents 2 picoamps for **A** and 4 picoamps for **B**. The horizontal scale bar represents 10 seconds for **A** and 250 milliseconds for **B**.

Subconducting states have been previously reported in stretch-activated channels (Sachs, 1988). We also see subconductance states associated with mechanosensitive channels in wild type and dystrophic muscle cells. The appearance of subconductance states becomes much more evident when the channels are open for longer periods, as in stretch-inactivated channels. Figure 14b (bottom trace) shows an example of a sub-conductance state in a channel that became tonically active. The fully closed channel level is indicated by the solid line, and the subconducting current level is shown with the dashed line.

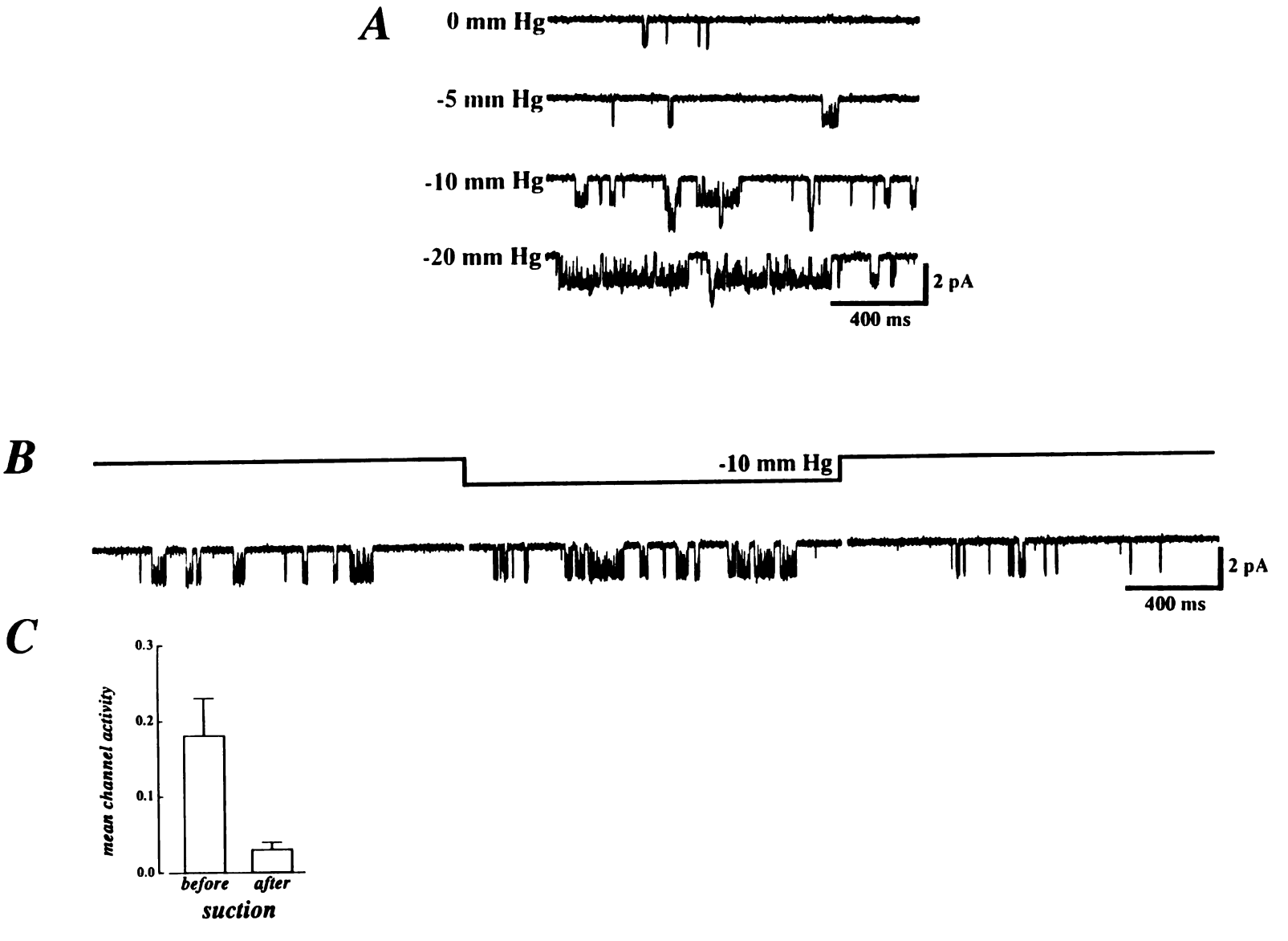
A
0 mm Hg
-5 mm Hg
-10 mm Hg
-20 mm Hg
2 pA
400 ms
B
-10 mm Hg
2 pA
400 ms
C
mean channel activity
0.3
0.2
0.1
0.0
before
after
suction

Figure 3-15. Mechanosensitive-gating in myoblasts is similar to that in dystrophin-deficient myotubes. A) Channel activity recorded from a *mdx* myoblast at the indicated pressures. For stretch-activated channels in myoblasts $P_{1/2}$ = -30 mm Hg and the steepness of the relationship, π = -6.0 (n=4). B). Changes in resting activity following the application of suction in wild type myoblasts. Representative records of channel activity before, during and after suction (-10 mm Hg) was applied to the patch electrode for the first time. Channel activity was reduced after suction in ~93% (n=15) of cell-attached patches from the surface of wild type myoblasts. C). Mean channel activity before and after suction. The mean values of channel activity were 0.18 ± 0.05 before suction and 0.03 ± 0.01 after suction. Error bars represent ± standard error of the mean. Significance = 0.009.

Stretch-inactivated channels were observed less frequently in myoblasts than in dystrophin-deficient myotubes. Of 22 cell-attached patches containing channels from wild type myoblasts, 23% (n=5) failed to respond to suction , 73% (n=16) showed stretch-activated gating and 5% (n=1) showed stretch-inactivated gating. Of 29 cell-attached patches containing channels from *mdx* myoblasts, 21% (n=6) did not respond to suction, 73% (n=21) showed stretch-activated gating, 3% (n=1) showed stretch-inactivated gating and 3% (n=1) underwent a switch from stretch-activated to stretch-inactivated gating in response to suction.

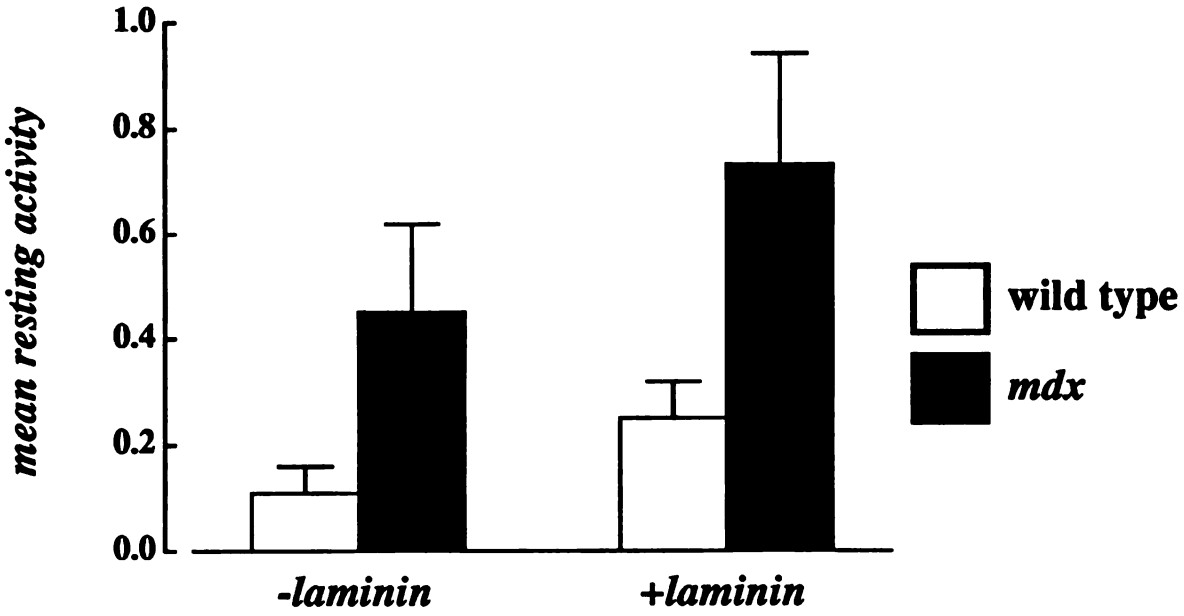

Figure 3-16. Laminin increases the level of resting channel activity in both wild type and *mdx* myotubes. A). Mean values of resting activity with and without laminin. The mean values of channel activity were 0.25 ± 0.07 (wild type; s.e.m., n=24) and 0.73 ± 0.21 (*mdx*; n=29) for myotubes grown in the presence of laminin and 0.11 ± 0.05 (wild type; n=20) and 0.41 ± 0.17 (*mdx*; n=35) for myotubes grown in the absence of laminin. Error bars represent ± standard error of the mean.

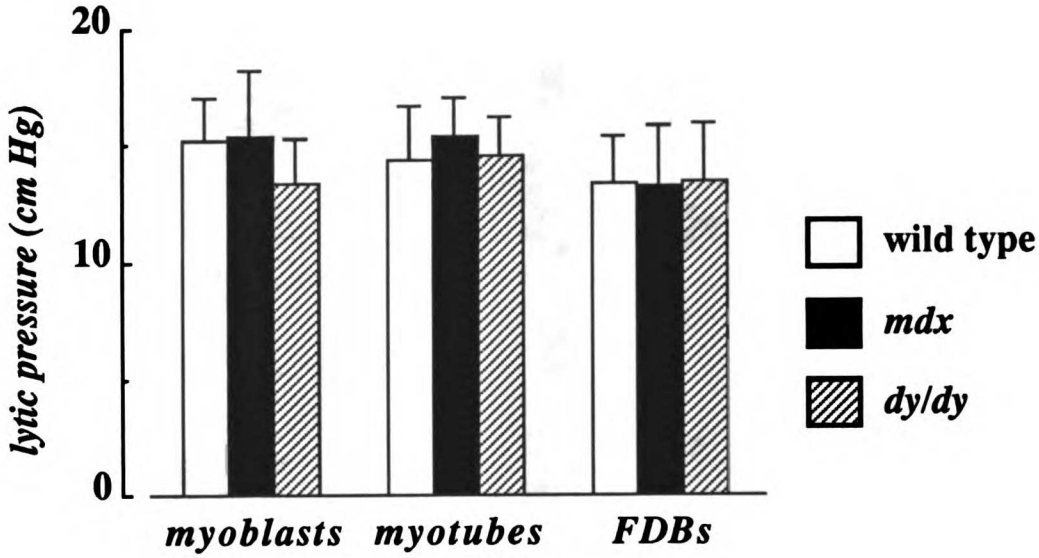

Figure 3-17. Muscle membranes lacking dystrophin are not mechanically more fragile than wild type muscle membranes. Pressure applied to the patch electrode to rupture the membrane of wild type, *mdx* and *dy* mouse myoblasts, myotubes and intact fibers. Measurements from wild type (open bars), *mdx* (solid bars) and *dy/dy* muscle cells (hatched bars). The number of measurements for were; myoblasts 26 (wild type), 25 (*mdx*) and 21 (*dy/dy*); myotubes 37 (wild type), 24 (*mdx*) and 41 (*dy/dy*); intact fibers 21 (wild type), 23 (*mdx*) and 26 (*dy/dy*). Error bars represent ± standard deviation.

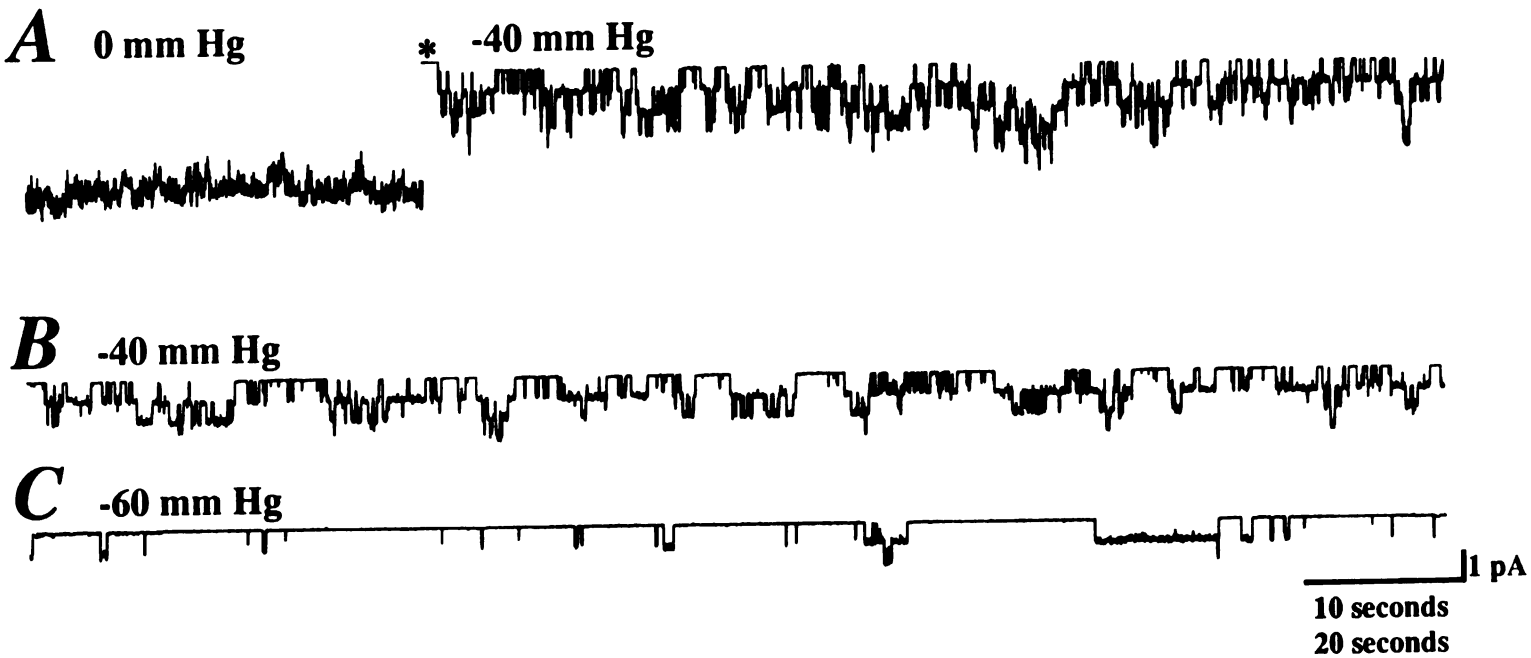
A
0 mm Hg
*
-40 mm Hg
B
-40 mm Hg
C
-60 mm Hg
1 pA
10 seconds
20 seconds

Figure 3-18. "Hot spot" of stretch-inactivated channels from the surface of a *mdx* myotube. The patch membrane potential was held at -40 mV. The zero current level is indicated by the star (*). **A**). Current records before and after the application of -40 mm Hg suction to the electrode. **B**). Current records in the presence of -40 mm Hg suction. **C**). Current records in the presence of -60 mm Hg suction. Relieving suction through the electrode in all cases resulted in channel activity returning to high levels. Single-channel records were filtered at 0.5 kHz and sampled at 1.25 kHz. The horizontal scale bar represents 10 seconds for **A** and 20 seconds for **B** and **C**.

Sachs (1988) has calculated that the optimal density for mechanosensitive channels to gather mechanical energy is ~1.5 per μm^2. In agreement with his results, I find an average of ~1.5 channels per 1-2 μm^2 in both wild type and *mdx* myotubes (see results; *Channel density*). However, "hot spots" of mechanosensitive channels have not before been described, and where thought not to exist (Morris, 1990). Since stretch-inactivated channels are open for long periods, it is possible that areas of high channel density that were before undetected become revealed.

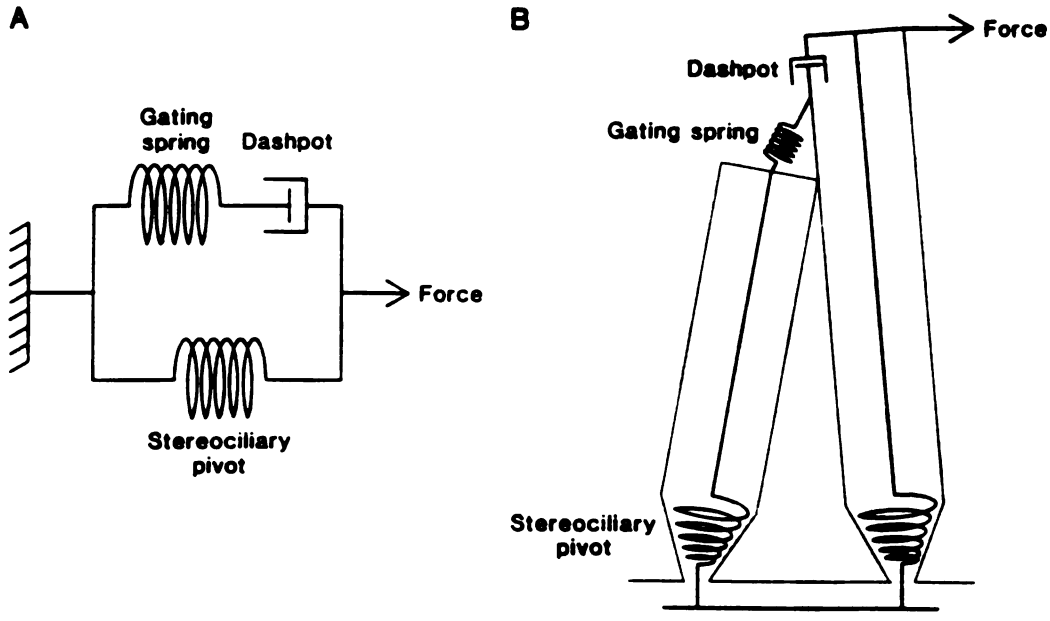

Figure 3-19. Howard and Hudspeth model of mechanotransduction in the bullfrog saccular hair cell (Adapted from Howard and Hudspeth, 1987). The transduction channels are thought to lie at one or both ends of the gating spring and to be gated by tension in that spring.

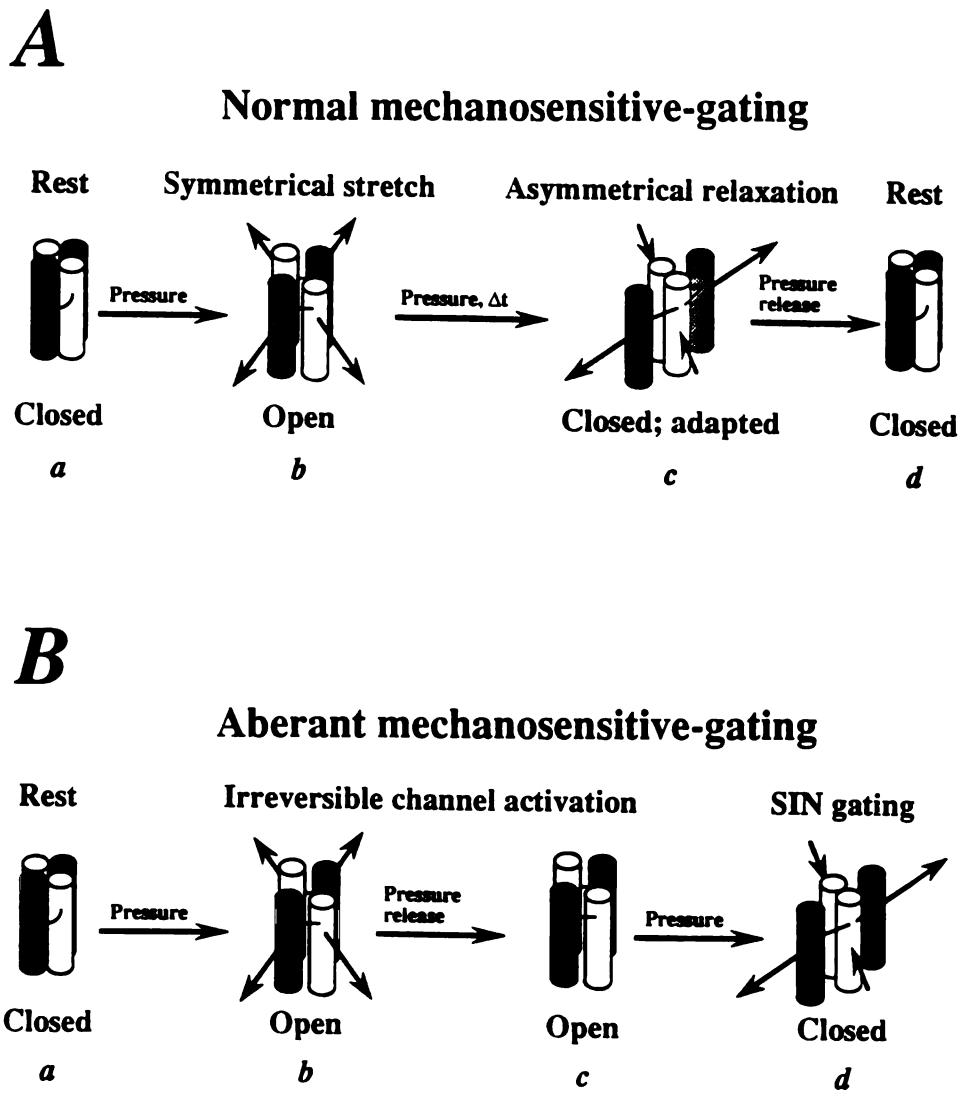

Figure 3-20. Four-barreled model of mechanosensitive gating. Aa-Ad). Normal mechanosensitive-gating. **Aa**). Resting state of the membrane. **Ab**). Pressure applied to the electrode symmetrically stretches the membrane, opening the channel. **Ac**). Asymmetrical relaxation of the membrane in the direction of the shaded barrels recloses the channel. **Ad**). Releasing pressure through the electrode reestablishes the resting state of the channel. **Ba-Bd**). Aberrant mechanosensitive-gating as in dystrophin-deficient myotubes. After opening (**Bb**), the channel remains open (**Bc**), even after releasing pressure through the electrode. Applying pressure to the electrode, however, closes the channel (**Bd**). Shaded barrels do not indicate heterogeneity between channel subunits.

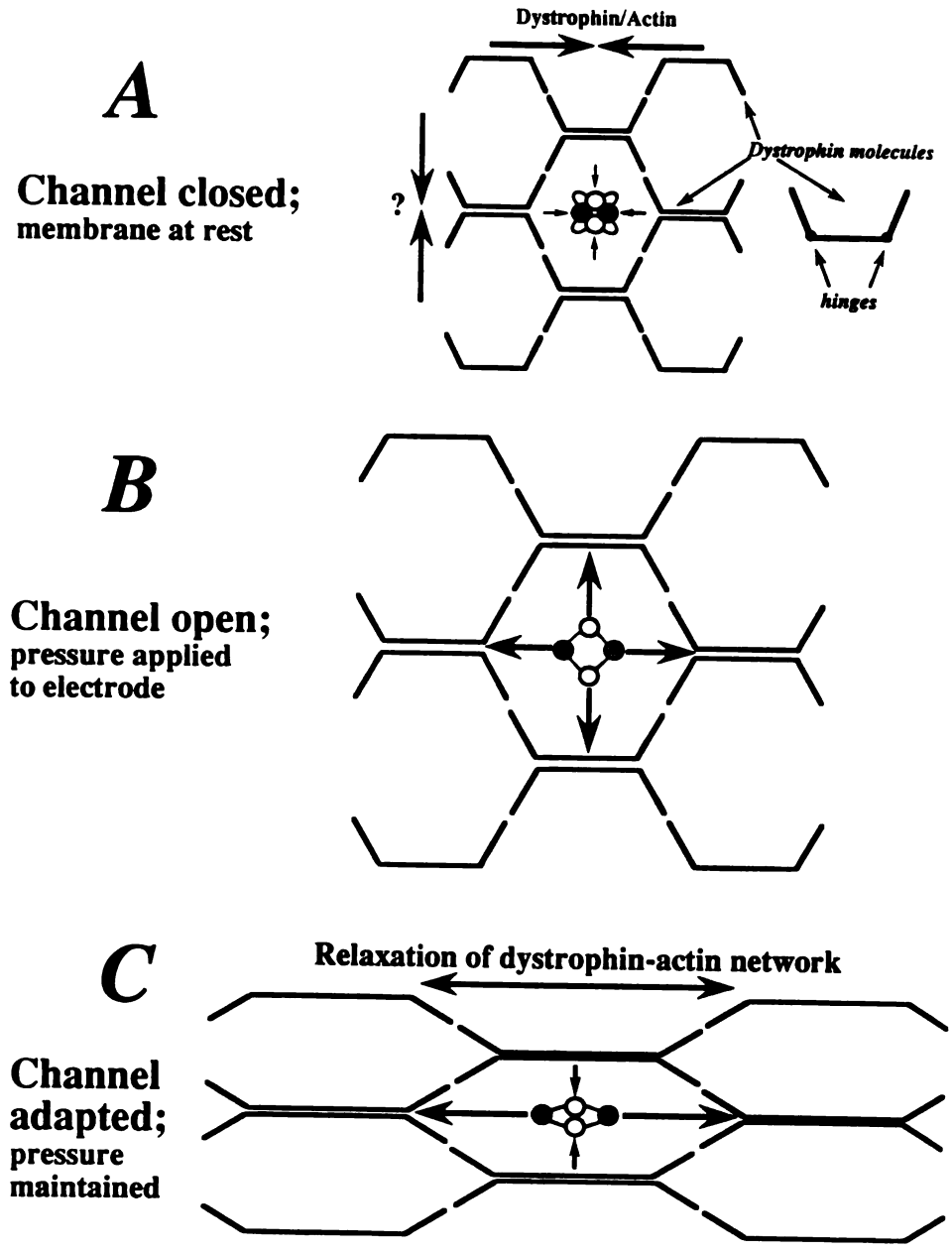

Figure 3-21. Barrel model of mechanosensitive-gating in the context of the dystrophin-actin cytoskeletal network. A "bird's eye" view of the mechanosensitive channel as (proposed to be) situated in the dystrophin-actin membrane lattice. A). The tension imposed by the dystrophin-actin network on the channel keeps it closed at rest. B). Symmetrical stretch of the membrane opens the channel. C). Asymmetrical relaxation of the dystrophin-actin network recloses the channel. The configuration of the dystrophin network was adapted from Koenig and Kunkel (1990).

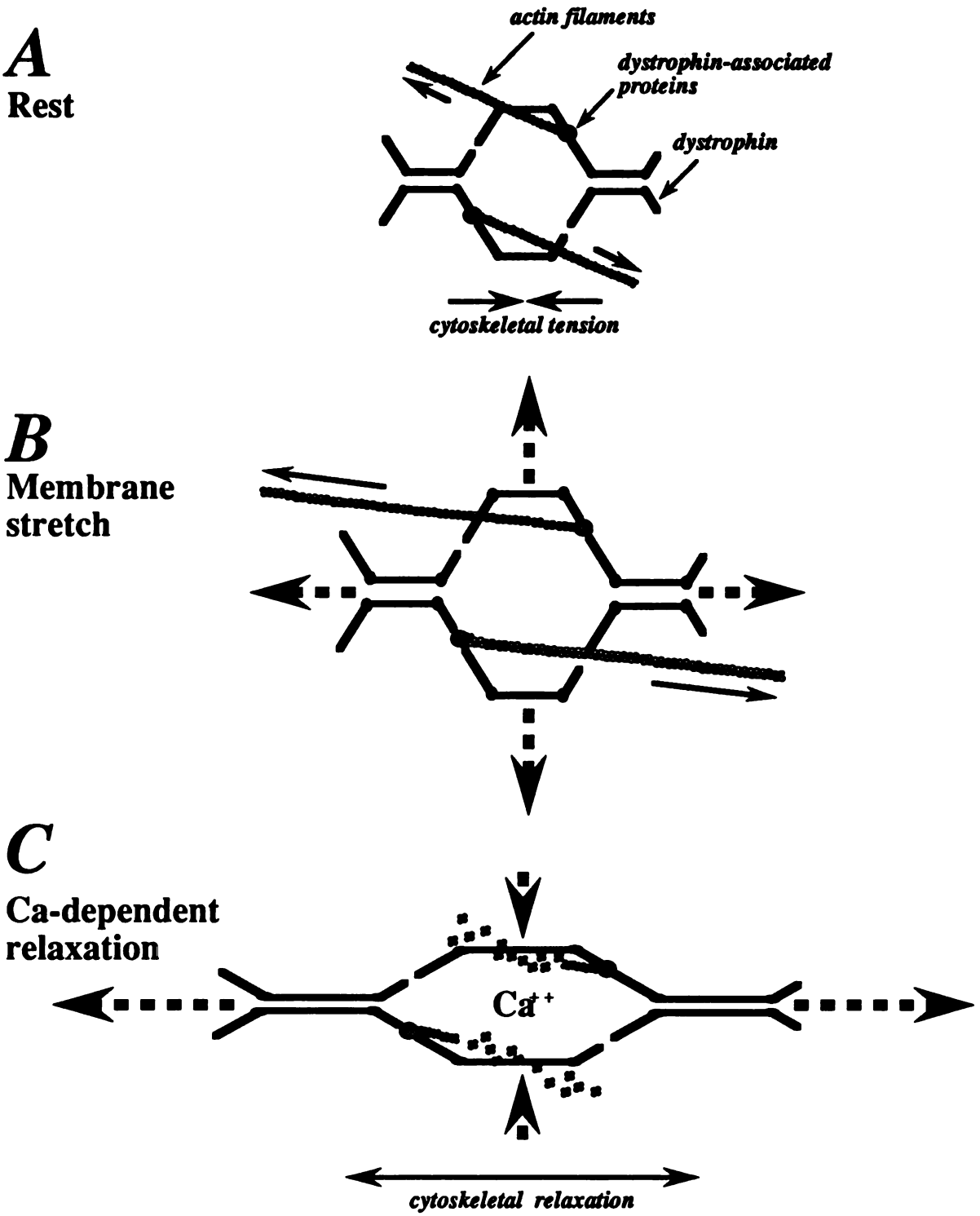
A
Rest
actin filaments
dystrophin-associated proteins
dystrophin
cytoskeletal tension
B
Membrane stretch
C
Ca-dependent relaxation
Ca++
cytoskeletal relaxation

Figure 3-22. Relaxation of the dystrophin-actin network may arise from the influx of Ca^{2+} through mechanosensitive channels. A). Dystrophin-actin network at rest membrane tension. B). Symmetrically stretching the membrane imparts tension onto the actin filaments coupled to dystrophin. Solid and dashed arrows indicate the direction and magnitude of tension on actin filaments and of membrane movement, respectively. C). Ca^{2+} influx through mechanosensitive channels results in the depolymerization of actin filaments and subsequent relaxation of the dystrophin-actin network. For clarity only half of the dystrophin-actin network is shown.

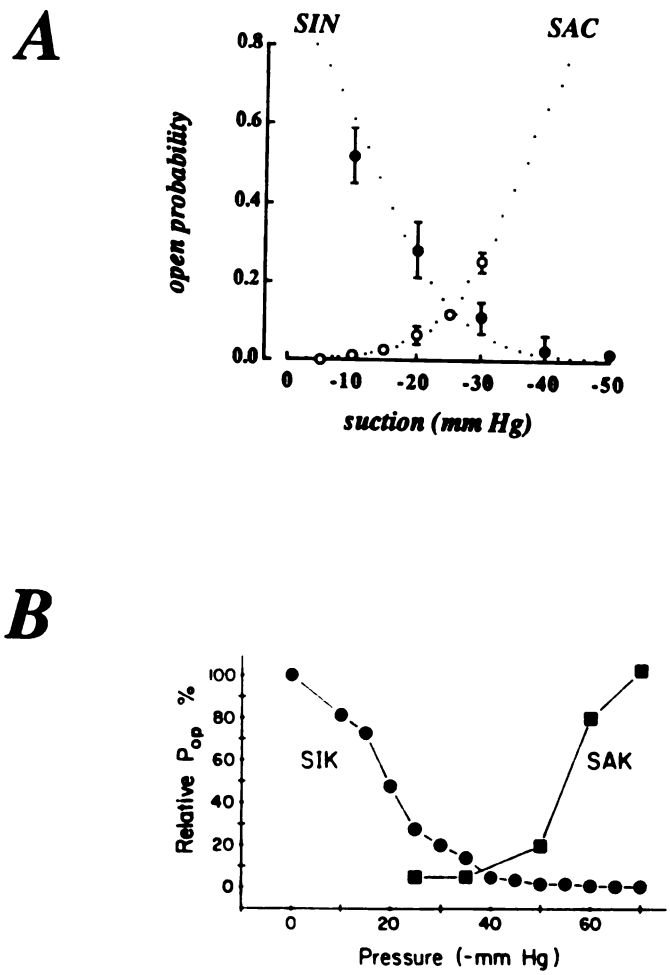

Figure 3-23. Stretch-activated and stretch-inactivated gating are displaced relative to each other along the pressure axis. A). Pressure relationships for stretch-activated and stretch-inactivated channels in *mdx* myotubes. Stretch-inactivated channels achieved half maximal inactivation at ~-13 mm Hg (for details see figure 11). Stretch-activated channels achieved half maximal activation at ~-37 mm Hg. **B).** Pressure relationships for stretch-activated and stretch-inactivated channels in molluscan growth cones (Adapted from Morris, 1990).

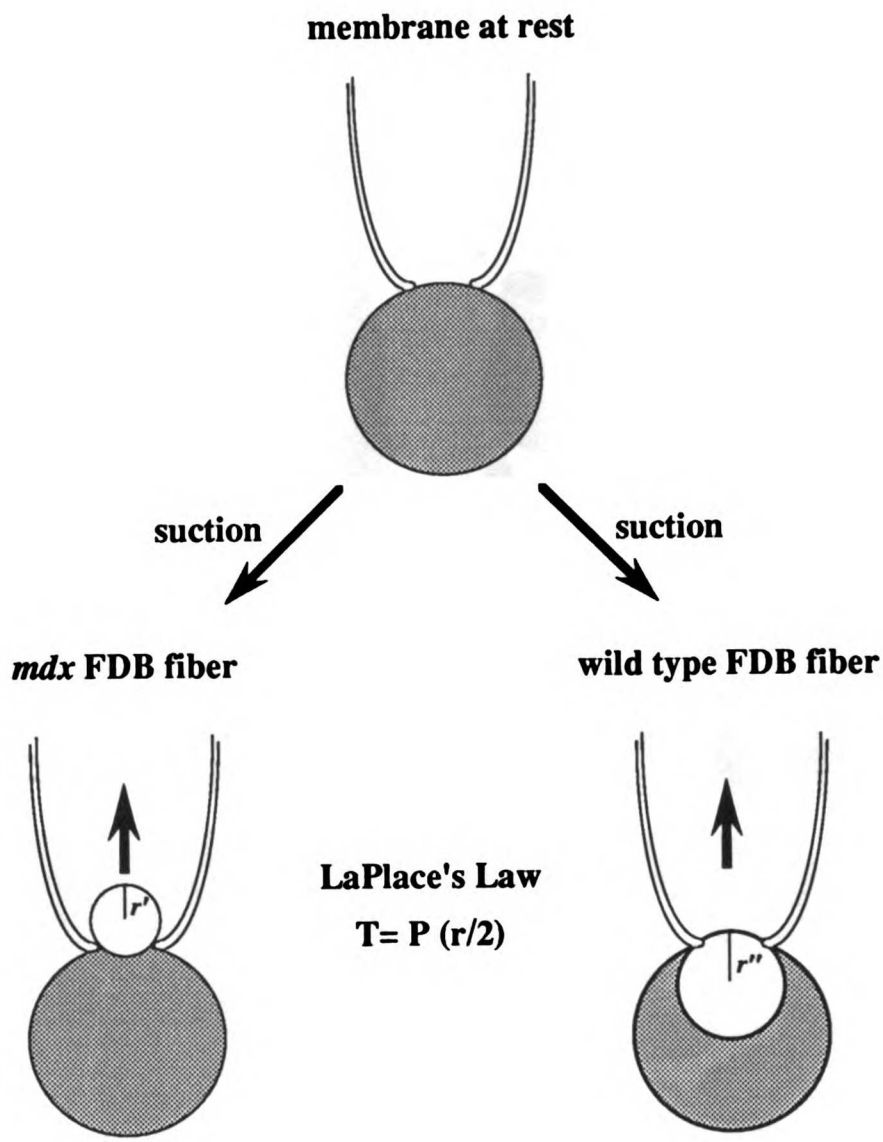

Figure 3-24. The membranes of *mdx* FDB fibers experience less membrane tension in response to electrode pressure. Side view of the membrane bleb held within an electrode at rest (top) and in response to pressure applied to the electrode (bottom). LaPlace's law states that the tension (**T**) perceived by the membrane is a function of the electrode pressure (**P**) multiplied by the radius of curvature (**r**), divided by 2. Since the membranes of *mdx* FDB fibers are more distensible than those of wild type FDB fibers, they should experience less tension (smaller radius of curvature) in response to suction applied to the electrode. The arrows indicate the direction of pressure through the electrode.

A
B
C
D

Plate 3-1. None of the histological abnormalities typically associated with the dystrophic condition were evident in FDB fibers from *mdx* mice. Photomicrographs showing longitudinal and cross-sections through FDB fibers removed from wild type (A and C) and *mdx* (B and D) mice. Histology was performed on FDB fibers acutely removed from 6 week old mice in the same manner as those prepared for single-channel recording. In *mdx* mice characteristic features of degenerating fibers are vesiculation of the sarcoplasmic reticulum, disorganization of the sarcomeres and focal lesions of the sarcolemma (Bulfield et al., 1984; DiMario et al., 1991). Scale bar = 50 μm. Magnification =210x.

Chapter 4

Open channel block by gadolinium ion of the stretch-inactivated ion channel in *mdx* myotubes.

Introduction

Skeletal muscle myotubes from *mdx* mice, an animal model for human X-linked muscular dystrophy (Bulfield et al., 1984) possess a novel type of mechanotransducing ion channel that is open for seconds at the resting membrane potentials and closes when the membrane is stretched by applying suction to the patch electrode (Franco and Lansman, 1990a). Like stretch-activated channels in both normal muscle (Guharay and Sachs, 1984; Franco and Lansman, 1990b) as well as *mdx* muscle cells (Franco and Lansman, 1990a), stretch-inactivated channels are permeable to both monovalent and divalent cations. The single-channel conductance, however, is smaller when divalent cations carry charge, suggesting that divalent cations bind more strongly than do monovalent cations to a site within the channel pore during ion transport.

Lanthanide cations have been useful as transition state analogues for studying the Ca^{2+} binding sites of ion channels (cf Lansman, 1990). Lanthanides have ionic radii close to that of Ca^{2+} and, like Ca^{2+}, they form primarily ionic complexes with oxygen donor groups (Nieboer, 1975). The lanthanide cation gadolinium (Gd) has an ionic radius of 0.105 nm, close to Ca^{2+} which has an ionic radius of 0.106 nm at a coordination number of eight (Shannon, 1976). Gd, moreover, inhibits unitary currents through stretch-activated channels with an affinity in the micromolar range (Yang and Sachs, 1989; Franco and Lansman, 1990b).

In this paper, I describe the results of experiments which investigated the blocking actions of Gd on currents through single stretch-inactivated ion channels in *mdx* myotubes, taking advantage of the exceptionally long open time of the stretch-inactivated channel to resolve discrete blocking and unblocking events. I show that the blocking kinetics are well described with a simple two-state model of open channel block. I also show that the blocking kinetics are independent of the extent of channel inactivation produced by the mechanosensitive gating mechanism, suggesting that the reduction in channel open probability produced by deforming the membrane does not alter the structure of the pore as probed by the blocking ion.

Methods

The methods for preparing primary cultures of *mdx* myotubes have been described previously (Chapter 2; Franco and Lansman, 1990b). Recordings of single-channel activity were made from cell-attached patches following the method of Hamill et al. (1981). Patch electrodes were made from Boralex hematocrit glass (Rochester Scientific, Rochester, New York) and had a resistance of ~2 MΩ with standard saline in the electrode and isotonic potassium aspartate in the bath. The junction potential between the electrode and the bathing solution was zeroed before forming a seal and rechecked at the end of each experiment. Current signals were recorded with a List EPC-7 amplifier with a 50 GΩ feedback resistor. Currents were filtered with an eight-pole, low pass Bessel filter at 2 kHz (-3dB) and sampled at 10 kHz. Recordings were made at room temperature (20-24 °C).

Solutions

The patch electrode filling solution was a standard saline solution containing 150 mM NaCl, 5 mM KCl, 2 mM $CaCl_2$, 1 mM $MgCl_2$, 10 mM glucose, and 5 mM Hepes. The pH was adjusted to 7.5 with NaOH. Gadolinium (>99.9% purity, Aldrich Chemical Co., Milwaukee, WI) was added to the electrode filling solution directly as the chloride salt. Hydrolysis of gadolinium occurs at pH 7.5 (Smith and Martell, 1976), but because of the uncertainties in the determination of lanthanide affinity constants, the concentration of free trivalent was not calculated (see Lansman, 1990 for discussion).

The bathing solution (K-Asp) contained 150 mM aspartic acid, 150 mM KOH, 5 mM $MgCl_2$, 60 mM Glucose, 1 mM EGTA and 10 mM Hepes. The pH was adjusted to 7.4 with KOH. The isotonic KAsp bathing solution was used to zero the cell membrane potential so that the patch potential would be equal to the voltage command applied through the patch clamp

amplifier. Comparing the single-channel current-voltage relation measured before and after excising the patch from the cell surface indicated a maximum voltage error of ~5 mV.

Measurement of the duration of open and blocked times

Open times were corrected for missed blockages when greater than 20% of the events were missed. The correction followed the method described by Colquhoun and Sigworth (1983) and Blatz and Magelby (1986) for the case when only blockages are missed. Because individual openings separated by a missed blocked period would be detected as a single event, the exponential fit to the open time histogram gives a mean open time that is larger than the true mean open time. The ratio of the number of missed blockages to the total number of blockages is given by

$$1-\exp(-D/\mu_C) \qquad (1)$$

where D is the dead time of the recording system and μ_C is the mean closed time obtained from the time constant of the exponential fit to the lifetime histogram. Mean open times were corrected by multiplying the uncorrected mean open time by the ratio of the detected to the total number of blocking events and then subtracting the sum of the duration of all missed closings.

Analysis of the distribution of current amplitudes

At negative membrane potentials, the rate of unblocking became very fast. To obtain the rate constants for blocking and unblocking I analyzed the distribution of current amplitudes by fitting it to a beta function (FitzHugh, 1983; Yellen, 1984). The amplitude distribution, which included the blocking and unblocking events within a channel burst, was measured and compared to the theoretical beta function derived for a two-state process which is obtained by specifying the transition rates and the filter cut-off frequency. The numerically generated beta function was convolved with a Gaussian function fit to the closed channel noise and the

transition rates changed to obtain the best fit by eye (Winegar and Lansman, 1990) Current records were refiltered with a low cut-off frequency (100-200 Hz) so that blocking kinetics would be in a range, relative to the system bandwidth, where the single-pole filter approximation used to derive the beta distribution would be valid (see Yellen, 1984).

Power spectra of current fluctuations

Power density spectra of open channel current fluctuations produced by Gd blocking and unblocking were measured from records filtered at 2 kHz. The power spectrum of the closed channel noise in each experiment was subtracted from the power spectrum of the current fluctuations produced by Gd. The subtracted spectra were fit with a single Lorentzian function. For a simple transition between an open and blocked channel the Lorentzian should have a single time constant

$$t = 2\pi f^{-1}_c \qquad (2)$$

where f_c is the corner frequency. For a two-state blocking reaction, the reciprocal of the time constant is the sum of the blocking and unblocking rates where

$$2\pi f_c = k_{off} + k_{on}[B] \qquad (3)$$

and k_{off} is the unblocking rate and $k_{on}[B]$ is the product of the blocking rate and the blocking ion concentration. No correction was made for the filtered variance in the net power spectra (Ogden and Colquhoun, 1985).

Results

Concentration dependence

Figure 1 shows the effects of adding increasing concentrations of Gd to the patch electrode which contained physiological saline. The records are from different recordings from cell-attached patches in which the electrode contained the indicated concentration of Gd. As the concentration of Gd in the electrode was increased, the number of rapid transitions between the open and closed channel levels increased. This behavior is consistent with a simple two-state model of open channel block in which Gd enters and exits the channel pore, blocking the flow of permeant ions during the time it resides within the channel (cf Neher and Steinbach, 1978; Lansman et al., 1986).

The two state model predicts that the distribution of open and closed times within a burst of openings are exponentially distributed. In addition, the rate of blocking should increase with the concentration of blocker, while the rate of unblocking should be independent of the concentration of blocker. These predictions were tested in figure 2. Figure 2a shows the open and closed time histograms from two experiments in which the electrode contained either 2.5 (top) or 7.5 μM (bottom) Gd. In both experiments, the histograms of open and closed times were well fit with a single exponential. The mean open time and closed times were obtained from the maximum likelihood fit to a single exponential and are indicated in the figure. The mean open time decreased from 1.9 ms in the presence of 2.5 μM Gd to 0.8 ms in the presence of 7.5 μM Gd. On the other hand, the mean closed time was ~0.6 ms in the presence either concentration of Gd.

Figure 2 shows the concentration dependence of the blocking kinetics from a number of experiments. Figure 2b shows the inverse of the mean open time (blocking rate) plotted as a function of the concentration of Gd in the electrode. As predicted by the two-state blocking model, the blocking rate depended linearly on the concentration of Gd. The slope of the

relation between the blocking rate and the concentration of Gd gave a second-order rate coefficient of ~2.3 x10^8 $M^{-1}s^{-1}$. As shown in figure 2c, the unblocking rate was independent of the concentration of Gd in the electrode. The results support the interpretation that Gd produces the rapid transitions between the open and closed channel levels by rapidly entering and exiting the channel.

Voltage dependence

To determine whether the blocking site is within the channel (Woodhull, 1973), I investigated the effects of the patch potential on the kinetics of the current fluctuations produced by a fixed concentration of Gd. Figure 3a shows records obtained in the presence of 5.0 μM Gd at -40, -80, -120, and -160 mV. At -40 and -80 mV, discrete transitions between the open and blocked states can be seen. At the more extreme hyperpolarized potentials, the blockages became quite brief.

At negative membrane potentials where the duration of the individual blocked times became to brief to detect as discrete events, I fit the distribution of current amplitudes with a beta function (see methods). I measured the amplitude of the current in the presence of Gd during extended openings. Figure 4a shows the amplitude distribution of the current in the presence of Gd at -60 (top) and -120 mV (bottom) in the same patch. In these figures, the amplitude distribution represents the filtered blocking and unblocking of the open channel. The fit to a theoretical beta function is shown by the solid line. At -60 mV, the fit to a beta function gave a blocking rate of 2250 s^{-1} and an unblocking rate of 1400 s^{-1}. In four experiments with 5 μM Gd in the electrode, amplitude distribution analysis gave a mean blocking rate of 2,425 ± 132 s^{-1} and a mean unblocking rate of 1,350 ± 526 s^{-1} (± S.D.). At -120 mV (figure 4a, bottom), the unblocking rate increased to 2,175 s^{-1}, while the blocking rate did not change significantly (2,400 s^{-1}). The analysis suggests that the blocking rate does not depend on membrane potential, whereas unblocking becomes faster as the patch potential is made more negative.

The two-state blocking model predicts that the power density spectra of the current fluctuations produced by the blocking ion should be fit by a single Lorentzian function in which the corner frequency is proportional to the sum of the blocking and unblocking rates. The power spectra were measured from the same experiment from which the amplitude distributions were analyzed and are shown in figures 4b. The power spectra were well fit with a single Lorentzian, as expected for a simple two-state blocking process. In four experiments, the corner frequency for block produced by 5 μM Gd at -60 mV was 310 ± 45 Hz.

I compared the expected corner frequency predicted by the blocking and unblocking rates obtained from the amplitude distribution analysis with that measured directly by noise analysis to check the correspondence between these two measurements. The fit of the amplitude distribution measured at -60 mV predicts a corner frequency of ~580 Hz compared with that measured experimentally of 360 Hz. At -120 mV, the fit to a beta distribution predicts a corner frequency of 728 Hz, whereas the fit of a single Lorentzian to the power spectrum gave a time constant of 510 Hz. Although the rates obtained from the analysis of the amplitude distribution predict a corner frequency that is larger than that measured directly, the general agreement is good considering the methods used to analyze the blocking kinetics are different.

I also compared the blocking and unblocking rate constants obtained directly from the mean open and closed times within a burst over the range of -40 to -80 mV where individual events could be resolved. Like the open and closed time histograms shown in figure 2a for records measured at -60 mV, both were well fit with single exponentials suggesting the existence of a single open and blocked state over this voltage range. The inverse of the mean open time (blocking rate) and the blocked time (unblocking rate) were plotted as a function of the patch potential in figure 5 (filled squares). The rate constants obtained from the fit of the amplitude distribution to a beta function over the entire voltage range (-40 to -160 mV, open circles) are also plotted in figure 5. Figure 5a shows that the blocking rate is independent of membrane potential over a wide range of voltages. Figure 5b, on the other hand, shows that

the unblocking rate increases with hyperpolarization (~*e*-fold per 85 mV). In both cases, there was good agreement between the measurement of the blocking rate constants by the fit of the amplitude distribution to a beta function and the direct measurement of the open and blocked times. The results indicate that the voltage dependence of channel block results solely from the voltage-dependent increase in the rate of unblocking.

The blocking kinetics are independent of mechanosensitive gating

The open probability of the stretch-inactivated channel is reduced by applying suction to the patch electrode (Franco and Lansman, 1990a). To determine whether mechanosensitive gating alters the structure of the open channel, I examined the effects on the blocking kinetics of applying suction to the patch electrode. Figure 6 shows the currents recorded in an experiment in which the patch electrode contained 5 μM Gd. In the absence of applied suction (0 mm of Hg), the rapid blocking and unblocking by Gd of the open channel appeared as long bursts of activity. Suction was subsequently applied to the electrode to inactivate the channel. Applying suction reduced in a graded and reversible manner the overall duration of the long channel burst. This can be seen in figure 6 as a shortening of the apparent burst duration with the amount of suction applied to the electrode.

The relationship between the amount of suction applied to the electrode and the mean channel open probability in the presence of Gd is shown in figure 7a. In this experiment, each period during which suction was applied to the electrode was followed by a control period in which the suction was released. Channel open probability at each pressure was normalized to that measured during the subsequent return to zero applied pressure as a control for any slow rundown of channel activity. The normalized open probability decreased as the amount of suction applied to the electrode was increased as shown in figure 7a. The smooth line through the experimental points was drawn to a Boltzmann distribution with a half-inactivation = -17 mm Hg and steepness = 6 mm Hg. This compares with the stretch-inactivation curve measured in the absence of blocking ion in which half-inactivation = -13 mm Hg and the

steepness = 6.3 mm Hg (Franco-Obrégon and Lansman, 1992). Apparently, steady-state stretch-inactivation is not altered by the presence of the blocker.

The blocking and unblocking rates were measured for records like those shown in figure 6, in which different amounts of suction applied to the electrode to produce different degrees of inactivation. Figure 7b shows the result of this experiment in which the blocking rate (filled circles) and unblocking rate (open triangles) are plotted as a function of the amount of suction applied to the electrode. As can be seen in figure 7b, the rate constants for blocking and unblocking did not depend on the extent of channel inactivation over a wide range of channel open probability.

Discussion

The use of the transition state analogue of Ca^{2+} allowed us to observe directly the blocking and unblocking of open mechanosensitive ion channels at the single-channel level. I find that Gd inhibits current through stretch-inactivated channels by entering and occluding the channel pore. The main new finding presented here is that the residence time of the blocking ion within the channel is not altered when the patch membrane is deformed by applying suction to the electrode. Apparently, mechanosensitive gating does not produce major modifications of the structure of the channel pore as probed by the blocking ion.

Mechanism of block

Channel block produced by Gd depends on membrane potential in such a way that hyperpolarization enhances the rate of unblocking. The effect of membrane potential on unblocking suggests that Gd can transverse the channel and exit to the cell under the influence of the applied membrane field. The block by Gd is similar to the block of single voltage-gated Ca^{2+} channels by Ca^{2+} and Lanthanide cations (Lansman et al., 1986; Lansman, 1990). Block of the stretch-inactivated channel by Gd, however, is much more sensitive to membrane potential than block of voltage-gated Ca^{2+} channels (~*e*-fold/85 mV vs. ~*e*-fold/25 mV, respectively). If it is assumed that Gd substitutes for Ca^{2+} at its channel binding site(s), then the difference in the sensitivity of the rate of unblocking to membrane potential suggests that the location of the Ca^{2+} complexation site within the channel also differs.

I find that the blocking rate is extremely rapid (~2.3×10^8 $M^{-1}s^{-1}$) and near the limit of the rate of diffusion of the ion in free solution (Diebler et al., 1969). That the blocking rate was independent of membrane potential is consistent with a diffusion-limited process which would be expected to lie outside the membrane field. The absolute value of the blocking rate is

similar to that reported by Yang and Sachs (1989) for the block of the stretch-activated channel in *Xenopus* oocytes (1.6×10^8 $M^{-1}s^{-1}$).

My results show that Gd does not alter the relationship between channel open probability and pressure, consistent with the results of Yang and Sachs (1989) who found that the sensitivity of the stretch-activated channel to pressure in *Xenopus* oocytes was not greatly altered in the presence of Gd. On the other hand, the block of the stretch-inactivated channel described here differs from the block of the stretch-activated channel (Yang and Sachs, 1989; Franco and Lansman, 1990b) in that Gd does not reduce the amplitude of the unitary current over a range in concentrations (figure 1). Information on the kinetics of blocking and unblocking of both stretch-activated and stretch-inactivated channels will be helpful for understanding the structural features of the permeation pathway of mechanosensitive channels.

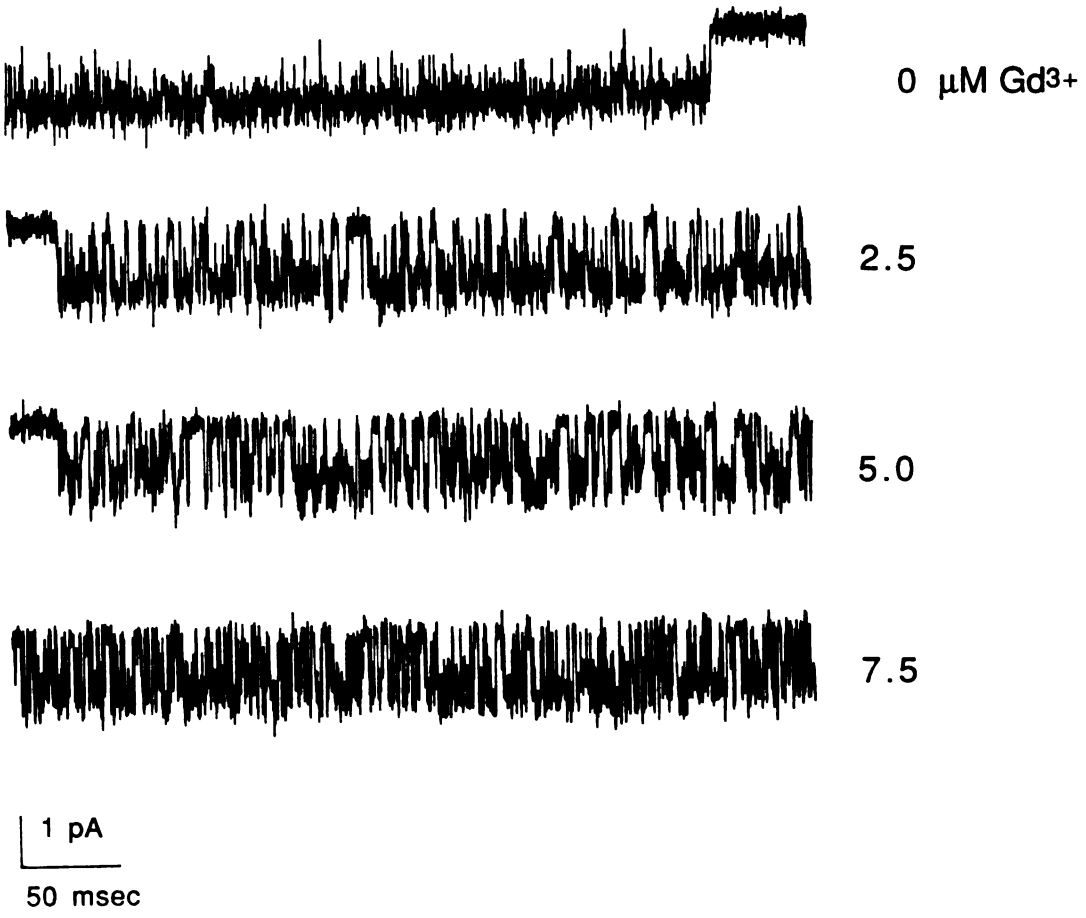

Figure 4-1. Gadolinium blocks single-channel current through stretch-inactivated channels. The unitary current in the presence of different concentrations of Gd in the electrode. Each record of channel activity is from a different patch with the indicated concentration of Gd in the electrode. Holding potential was -60 mV. Currents were filtered a 2kHz.

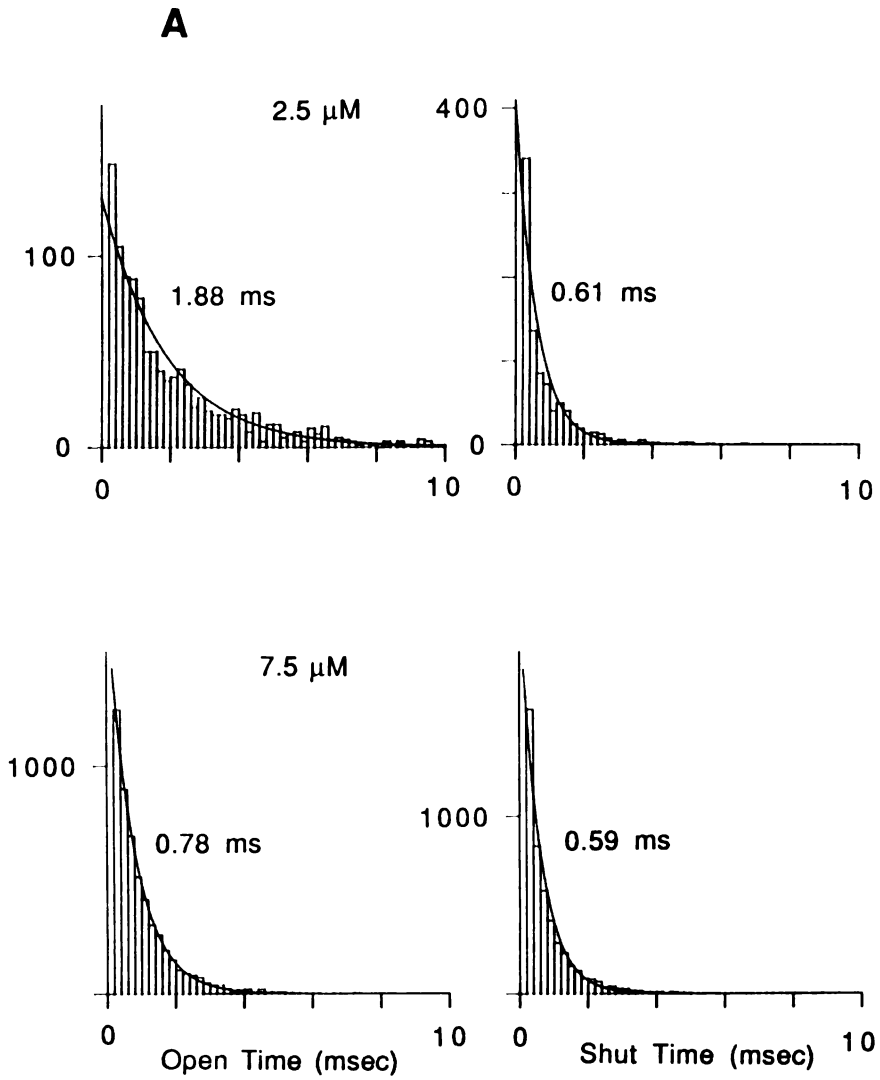
A
2.5 μM
400
100
1.88 ms
0.61 ms
0
0
0
10
0
10
7.5 μM
1000
1000
0.78 ms
0.59 ms
0
10
0
10
Open Time (msec)
Shut Time (msec)

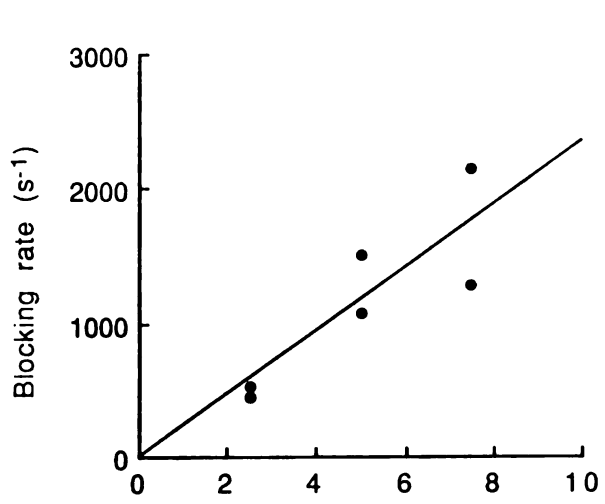
B
3000
2000
1000
0
Blocking rate (s-1)
0
2
4
6
8
10

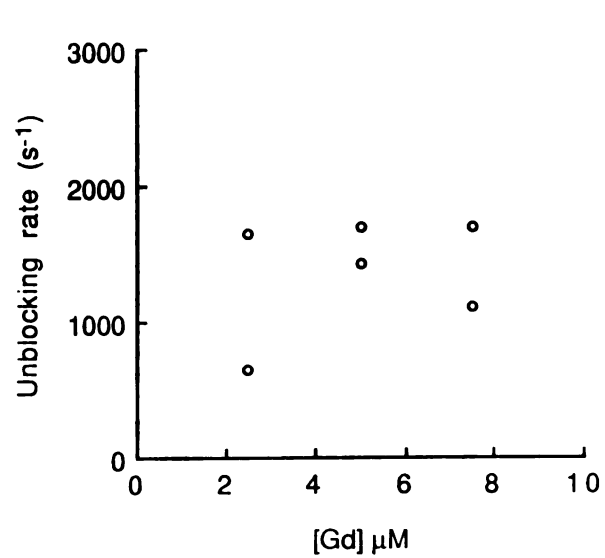
C
3000
2000
1000
0
Unblocking rate (s-1)
0
2
4
6
8
10
[Gd] μM

Figure 4-2. Analysis of the concentration-dependence of the blocking kinetics. A) Histograms of the durations of the open and closed times within a burst obtained from records like those shown in figure 1. Smooth curve through the histogram is the maximum likelihood fit with a single exponential. With 2.5 μM Gd (top), the mean open time was 1.88 ms and the mean closed time was 0,61 ms; with 7.5 μM Gd (bottom), the mean open time was 0.78 ms and the mean closed time was 0.59 ms. B) The dependence of the blocking rate (1/mean open time) on the concentration of Gd in the electrode. The line through the experimental points is the least-squares linear regression line (r=0.86) the slope of which gives a second-order rate coefficient of $2.5 \times 10^8\ M^{-1}s^{-1}$. C) The dependence of the unblocking rate (1/mean closed time) on the concentration of Gd in the electrode.

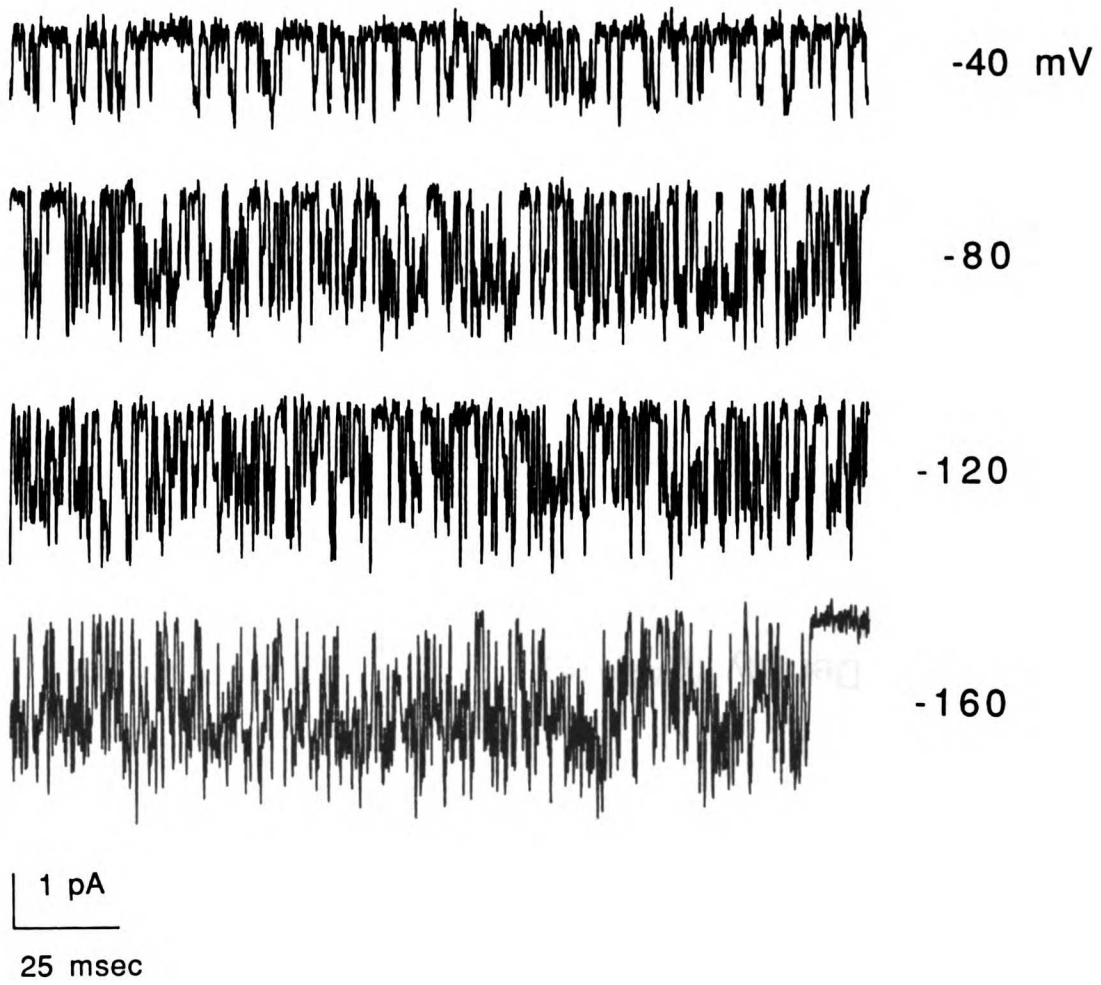

Figure 4-3. Voltage-dependence of gadolinium block. A) Records from a single recording from a cell-attached patch with 5.0 μM Gd in the electrode at the indicated patch potentials. The conductance in the presence of 5.0 μM Gd was 18 ± 4 pS (S.D.; n=13), compared with 24 ± 2 pS (S.D.; n=5) in the absence of Gd.

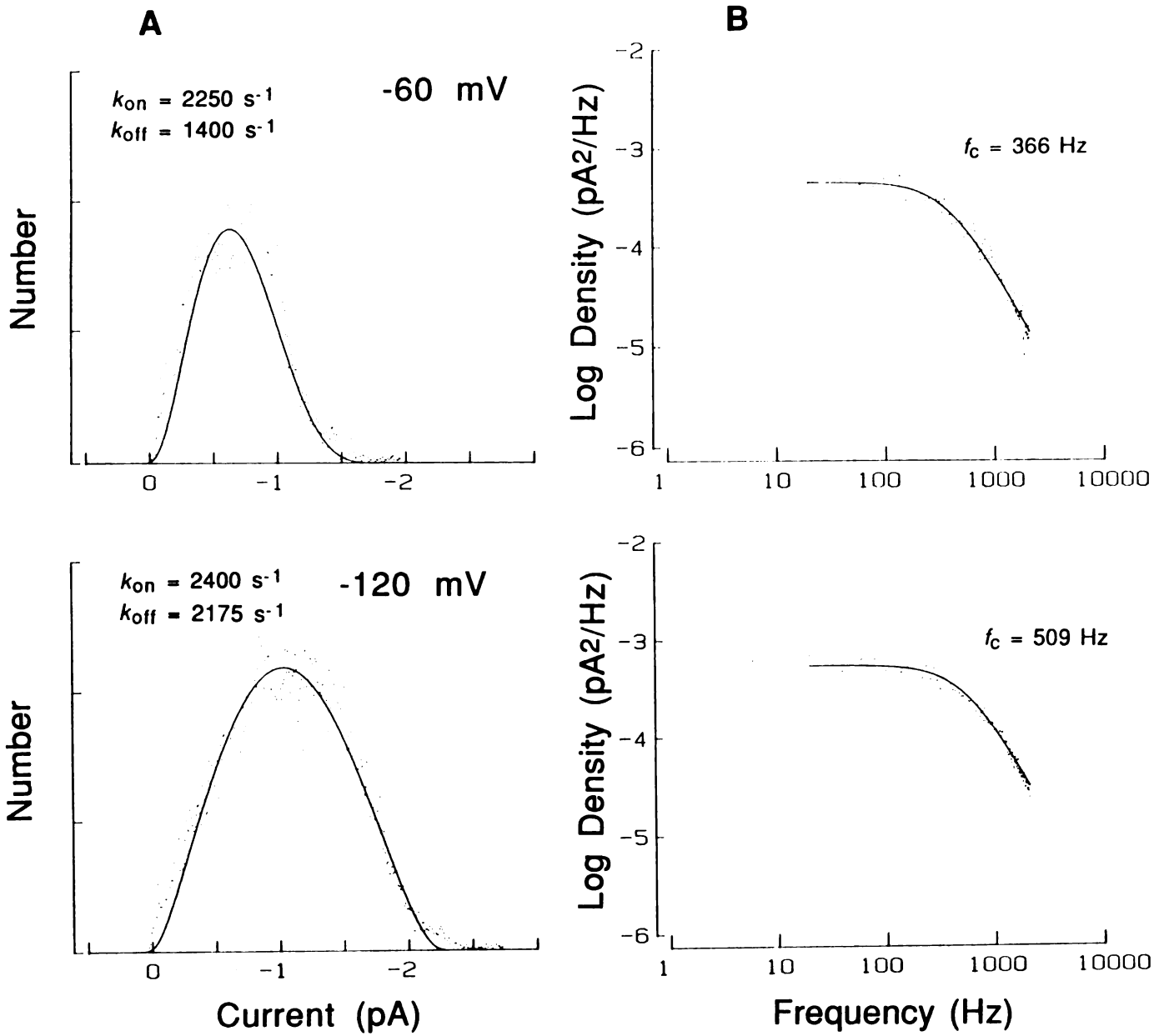
A
B
k_{on} = 2250 s^{-1}
k_{off} = 1400 s^{-1}
-60 mV
Number
0
-1
-2
Log Density (pA^2/Hz)
f_c = 366 Hz
-2
-3
-4
-5
-6
1
10
100
1000
10000
k_{on} = 2400 s^{-1}
k_{off} = 2175 s^{-1}
-120 mV
Number
Current (pA)
f_c = 509 Hz
Log Density (pA^2/Hz)
Frequency (Hz)

Figure 4-4. Blocking rate does not depend on membrane potential. Kinetic analysis of the voltage-dependence of the block by Gd. **A)** amplitude distributions of the current during a burst in the presence of 5 μM Gd at -60 (top) and -120 mV (bottom). The smooth curve through the experimental points is the fit to a numerically-generated beta distribution with blocking rates of 2250 and 2400 s^{-1} and unblocking rates of 1400 and 2175 s^{-1} at -60 and -120 mV, respectively. Current records were filtered at 100 or 200 Hz before measuring the distribution of current amplitudes. **B)** Power density spectra of the current fluctuations in the presence of 5.0 μM Gd at -60 (top) and -120 mV (bottom). The smooth curve was drawn to a single Lorentzian of the form

$$S(f) = S(0)/1+ (f/f_c)^2$$

where the corner frequency f_c = 366 and 509 at -60 and -120 mV, respectively.

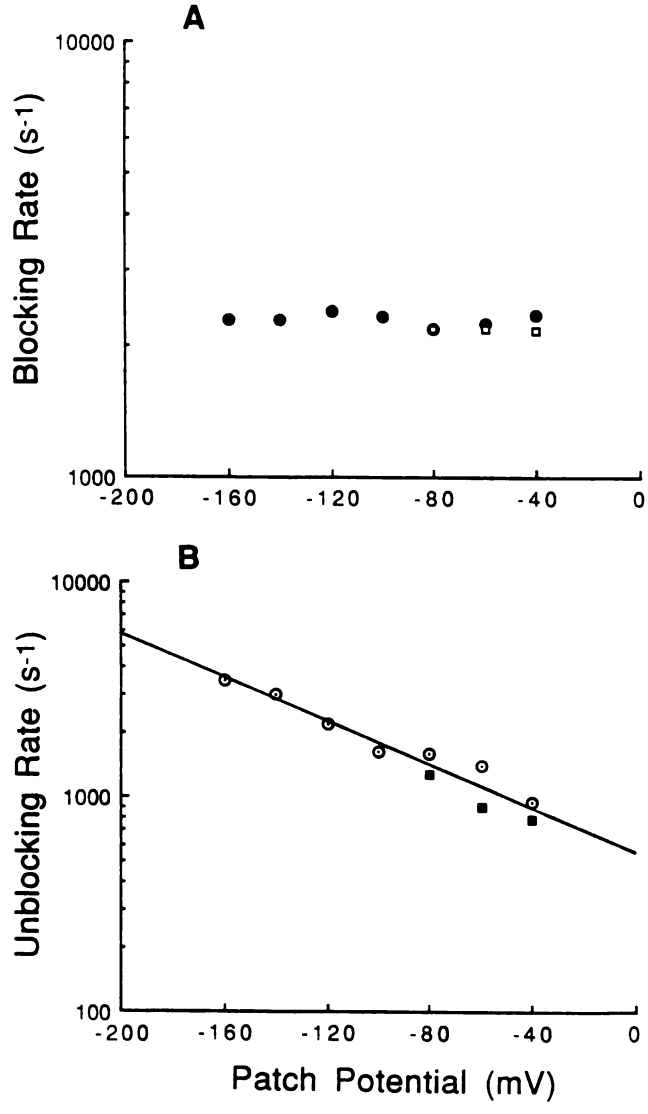

Figure 4-5. Dependence of the blocking and unblocking rates on membrane potential. A) Dependence of the blocking rate on the patch potential. Open squares represent the inverse of the mean open time obtained from the single exponential fit to the histogram of open times. Filled circles are the rates obtained from the amplitude distribution analysis. B) Dependence of the unblocking rate on the patch potential. Filled squares represent the inverse of the mean blocked time obtained from the exponential fit to the histogram of closed times. Open circles are the rates obtained from the amplitude distribution analysis. The line through the experimental points is the non-linear least squares fit to a single exponential. The unblocking rate change e-fold/85 mV.

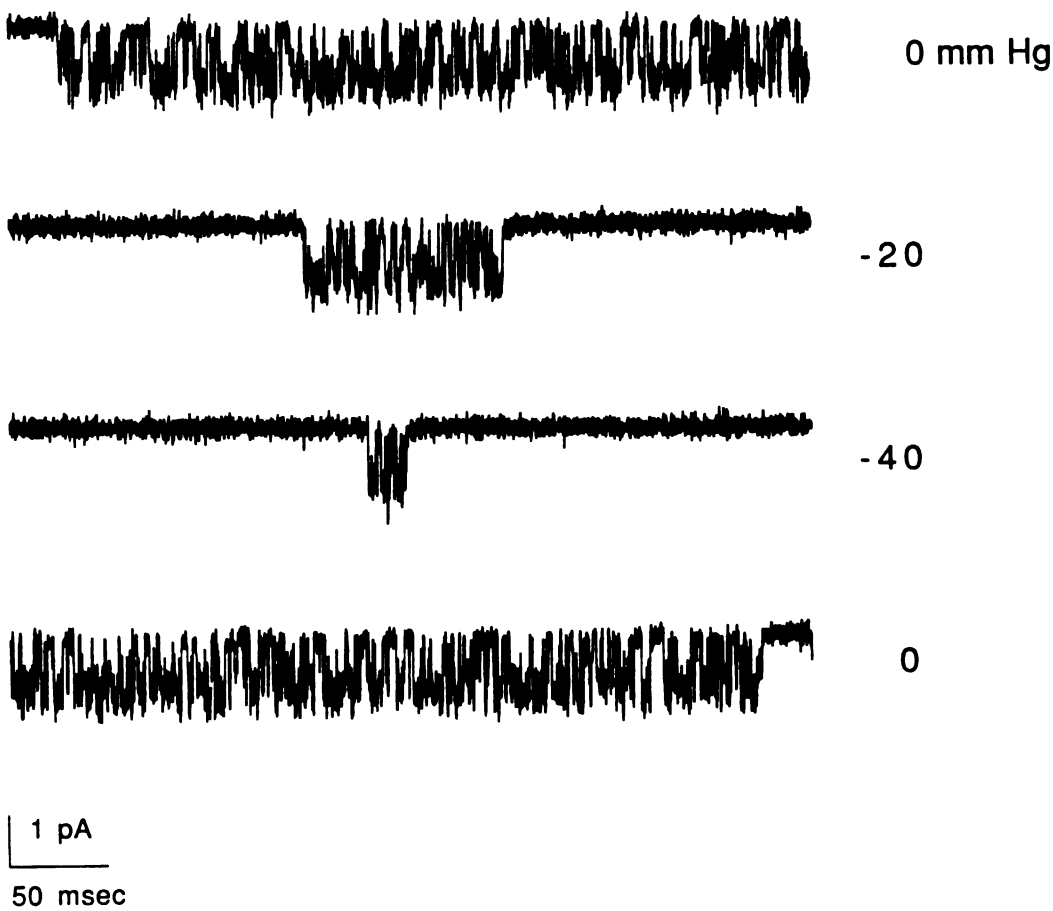

Figure 4-6. Suction applied to the electrode reduces the activity of stretch-inactivated channels in the presence of gadolinium. Records are from an experiment in which suction was applied to the patch electrode. The amount of suction applied is indicated next to the record. Holding potential was -60 mV. Current records were filtered at 2 kHz.

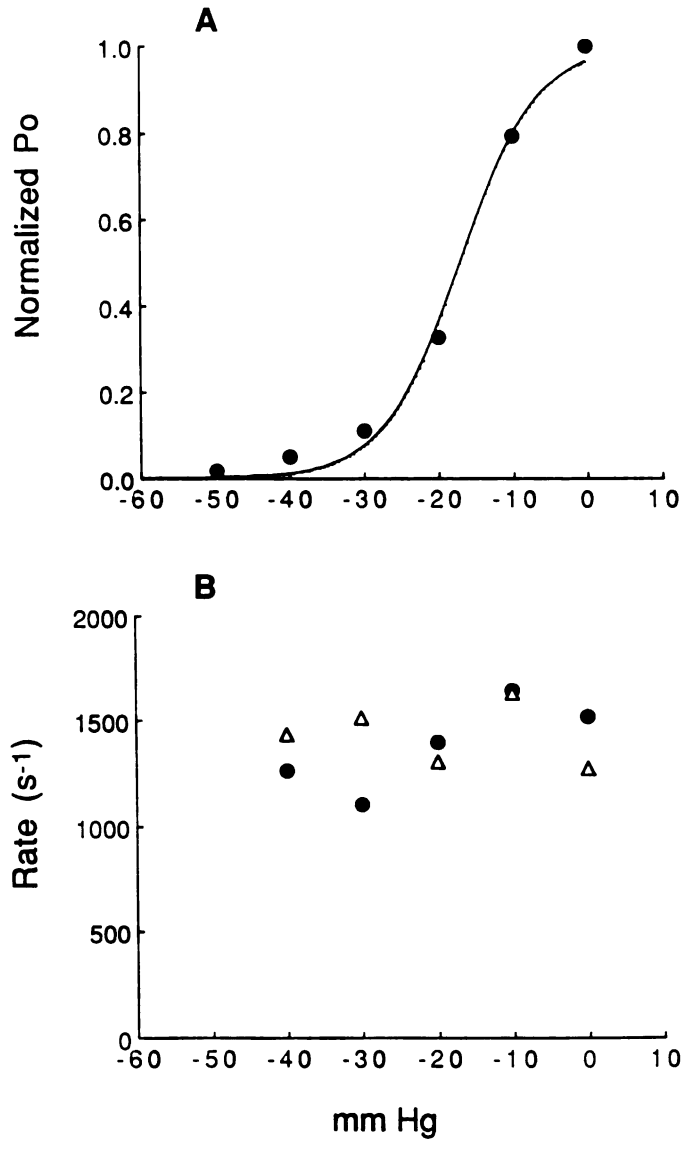

Figure 4-7. Block by gadolinium does not alter stretch-inactivated gating. Dependence of the blocking kinetics on the extent of steady-state inactivation by stretch. Holding potential was -60 mV. Current records were filtered at 2kHz. A) The dependence of channel open probability on the amount of suction applied to the electrode. The smooth curve was draw to a Boltzmann relation with $P_{1/2}$ = -17 mm Hg and Steepness 6.0 mm Hg. B) The blocking rate (filled circles) and the unblocking rate (open triangles) plotted as a function of the amount of suction applied to the electrode. Comparison with (A) shows that the blocking kinetics were independent of the extent of channel inactivation by suction.

Conclusion

The activity of mechanosensitive channels can be detected at all stages of early myogenesis, and in intact skeletal muscle fibers acutely removed from adult animals. Their activity is also observed in muscle cells from mice of different genetic backgrounds (Franco and Lansman, 1990a; Chapters 2 and 3), as well as, mouse muscle cell lines (Franco and Lansman, 1990b; Chapter 1). They have also been described in avian (Guharay and Sachs, 1984, 1985) and amphibian skeletal muscle (Brehm et al., 1984). At all stages of muscle development, and in skeletal muscle of all species, mechanosensitive channels posses similar single-channel conductances, voltage-sensitive gating mechanisms and mechanosensitive gating mechanisms. These results indicate that mechanosensitive channels are common features of skeletal muscle cells.

In most cases the physiological role of mechanosensitive channels remains obscure (Howard et al., 1988; Sachs, 1988, 1989; Morris, 1990). Skeletal muscle development and function requires Ca^{2+} (see **Background**). I propose that mechanosensitive channels provide a pathway for resting Ca^{2+} influx into skeletal muscle. The progression from proliferative myoblasts to myoblasts that are fusing to form multinucleated myotubes requires extracellular extracellular Ca^{2+}, which is consistent with the density of mechanosensitive channels being greatest in myoblasts prior to fusion (Franco and Lansman, 1990b; Chapter 1). Skeletal muscle force generation (contraction) requires the release of Ca^{2+} from intracellular stores. In adult skeletal muscle, Ca^{2+} entry through mechanosensitive channels may be required to maintain myoplasmic Ca^{2+} stores. The discovery of specific blockers for mechanosensitive channels would be of great importance in definitively determining their physiological role (Franco et al., 1991; cf Hamill et al., 1992; cf Lane et al., 1991; Chapter 4).

The integrity of the membrane-associated cytoskeleton is necessary for mechanosensitive channel to function properly (Guharay and Sachs, 1984; Sokabe et al., 1991). In mouse muscle cells which lack the cytoskeletal protein, dystrophin (Bulfield et al., 1984; Hoffman et al., 1987; Arahata et al., 1988; Watkins et al., 1988), the gating of mechanosensitive channels is altered (Franco and Lansman, 1990a; Chapters 2 and 3). On the other hand, other properties of mechanosensitive channels, such as, single-channel conductance and voltage-sensitive gating, do not differ from that observed in wild type skeletal muscle. This suggest that the absence of dystrophin has specific consequences on the pressure-sensitive component of mechanosensitive-gating, which may not alter the structure of the channel protein(s) directly.

There has been some dispute as to whether mechanosensitive channels are an artifact of patch clamp recordings (Morris and Horn, 1991). However, the highly consistent and quantitative behavior of mechanosensitive channels argues against this interpretation (Chapter 3). The fact that mechanosensitive channels can be detected throughout myogenesis with relatively little difference in channel gating, suggests that they are important for normal muscle development and function. We may not know what makes mechanosensitive channels work, but they are certainly real.

References

Abe, H. & Obinata, T. (1989). An actin-depolymerizing protein in embryonic chicken skeletal muscle: purification and characterization. *Journal of Biochemistry* **106**, 172-180.

Abe, H., Endo, T., Yamamoto, K. & Obinata, T. (1990). Sequence of cDNAs encoding actin depolymerizing factor and cofilin of embryonic chicken skeletal muscle: two functionally distinct actin-regulatory proteins exhibit high structural homology. *Biochemistry* **29(32)**, 7420-7425.

Adams, D.J., Dwyer, T.M. & Hille, B. (1980). The permeability of endplate channels to monovalent and divalent metal cations. *Journal of General Physiology* **75**,493-510.

Anglister, L., McMahan, U.J. & Marshall, R.M. (1985). Basal Lamina directs acetylcholinesterase accumulation at synaptic sites in regenerating muscle. *The Journal of Cell Biology* **101**, 735-743.

Arahata, K., Ishiura, S., Ishiguro, T., Tsukahara, T., Suhara, Y., Eguchi, C., Ishihara, T., Nonaka, I., Ozawa, E. & Sugita, H. (1988). Immunostaining of the skeletal and cardiac muscle surface membrane with antibody against Duchenne muscular dystrophy peptide. *Nature* **333**, 861-863.

Ashby, P.R., Pincon-Raymond, M. & Harris, A.J. (1993). Regulation of myogenesis in paralyzed muscled in the mouse mutants *peroneal muscular atrophy* and *muscular dysgenesis*. *Developmental Biology*, **156** (In press).

Ashmore, C. R., Hitchcock, L. & Lee, Y. B. (1988). Passive stretch of adult chicken muscle produces a myopathy remarkably similar to hereditary muscular dystrophy. *Experimental Neurology* **100**, 341-353.

Assad, J.A. & Corey, D.P. (1992). An active motor model for adaptation by vertebrate hair cells. *The Journal of Neuroscience* **12(9)**, 3292-3309.

Assad, J.A., Hacohen, N. & Corey, D.P. (1989). Voltage dependence of adaptation and active bundle movement in bullfrog saccular hair cells. *Proceedings of the National Academy of Science of the U.S.A.* **86**, 2918-2922.

Bamburg, J.R. & Bray, D. (1987). Distribution and cellular localization of actin depolymerizing factor. *The Journal of Cell Biology* **105**, 2817-2825.

Beam, K.G. & Knudson, C.M. (1988a). Calcium currents in embryonic neonatal mammalian skeletal muscle. *The Journal of General Physiology* **91**, 781-798.

Beam, K.G. & Knudson, C.M. (1988b). Effect of postnatal development on calcium currents and slow charge movement in mammalian skeletal muscle. *The Journal of General Physiology* **91**, 799-815.

Beam, K.G., Knudson, C.M., & Powell, J.A., (1986). A lethal mutation in mice eliminates the slow calcium current in skeletal muscle cells. *Nature* **320**, 168-170.

Bekoff, A. & Betz, W.J. (1977). Physiological properties of dissociated muscle fibers obtained from innervated and denervated adult rat muscle. *Journal of Physiology* **271**, 25-40.

Benham, C.D. & Tsien, R.W. (1986). Calcium-permeable channels in vascular smooth muscle: voltage-activated, receptor-operated and leak channels. In *Cell Calcium and the Control of Membrane Transport*, editors Mandel, L.J. and Eaton, D.C., New York: The Rockefeller University Press.

Bennett, V. (1990). Spectrin-based membrane skeleton: A multipotential adaptor between plasma membrane and cytoplasm. *Physiological Reviews* **70**, 1029-1065.

Blatz, A.L. & Magleby, K.L. (1988). Correcting single channel data for missed events. *Biophysical Journal* **49**, 967-980.

Bodensteiner, J.B. & Engel, A.G. (1978). Intracellular calcium accumulation in Duchenne dystrophy and other myopathies: A study of 567,000 muscle fibers in 114 biopsies. *Neurology* **28**, 439-446.

Bonilla, E., Samitt, C. E., Miranda, A. F., Hays, A. P., Saliviati, G., Dimuro, S., Kunkel, L. M., Hoffman, E. P. & Rowland, L. P. (1988). Duchenne muscular dystrophy: Deficiency of dystrophin at the muscle surface. *Cell* **54**, 447-452.

Bray, G.M. & Banker, B.Q. (1970). An ultrastructural study of degeneration and necrosis of muscle in the dystrophic mouse. *Acta Neuropathologica* **15**, 34-44.

Bregestovsky, P.D., Miledi, R., & Parker, I. (1979). Calcium conductance of acetylcholine-induced endplate channels. *Nature* **279**, 638-639.

Brehm, P., Kullberg, R. & Moody-Corbett, F. (1984). Properties of non-junctional acetylcholine receptor channels on innervated muscle of Xenopus Laevis. *Journal of Physiology* **350**, 631-648.

Bretscher, A. & Weber, K. (1980). Villin is a major protein of the microvillus cytoskeleton which binds both G and F actin in a calcium-dependent manner. *Cell* **20**, 839-847.

Brochat, K.O. (1990). Tropomyosin prevents depolymerization of actin filaments from the pointed end. *The Journal of Biological Chemistry* **265(34)**, 21323-21329.

Brum, G., Stefani, E. & Rios, E. (1987). Simultaneous measurements of Ca^{2+} currents and intracellular Ca^{2+} concentrations in single skeletal muscle fibers of the frog. *Canadian Journal of Physiological Pharmacology* **65**, 681-685.

Bulfield, G., Siller, W.G., Wight, P.A.L. & Moore, K.J. (1984). X chromosome-linked muscular dystrophy (mdx) in the mouse. *Proceedings of the National Academy of Science of the U.S.A.* **81**, 1189-1192.

Caffrey, J.M., Brown, A.M. & Schneider, M.D. (1987) Mitogens and oncogenes can block the induction of specific voltage-gated ion channels. *Science* **236**, 570-573.

Campbell, K. & Kahl, S.D. (1989). Association of dystrophin and an integral membrane glycoprotein. *Nature* **338**, 259-262.

Cao, L., Babcock, G.C., Rubenstein, P.A. & Wang, Y. (1992). Effects of profilin and profilactin on actin structure and function in living cells. *The Journal of Cell Biology* **117(5)**, 1023-1029.

Carpenter, S. & Karpati, G. (1984). Diseases of skeletal muscle. In *Pathology of Skeletal Muscle*, New York, Edinburgh, London and Melbourne: Churchil Livingstone.

Chatfield, C. (1983). Appendix D. In *Statistics for technology*, third edition, London and New York: Chapman and Hall

Cognard, C., Lazdunski, M. & Romey, G. (1986). Different types of Ca^{2+} channels in mammalian skeletal muscle cells in culture. *Proceedings of the National Academy of Sciences of the U.S.A.* **83**, 517-521.

Colquhoun, D. & Sigworth, F.J. (1983). Fitting and statistical analysis of single-channel records. In *Single Channel Recordings*, editors Sakmann, B. and Neher, E., New York: Plenum Press.

Cooper, K.E., Tang, J.M., Rae, J.L., & Eisenberg, R.S. (1986) A cation channel in frog lens epithelia responsive to pressure and calcium. *Journal of Membrane Biology* **93**, 259-269.

Cooper, B.J. & Hamill, O.P. (1989). Patch clamp measurements of the visoelastic properties and mechanoelectric transduction in dystrophic muscle membrane. *Society for Neuroscience Abstracts* **15**, 1034.

Dangain, J. & Vrbova, G. (1987). Response of skeletal muscles from normal and dystrophic mice (C57Bl/6J dy^{2j}) to a local decrease in Ca^{2+}. *Journal of Physiology* **394**, 21P.

Dangain, J. & Vrbova, G. (1990). Response of a fast muscle from normal and dystrophic (dy^{2j}) mice to a local decrease in extracellular Ca^{2+} induced at different stages of postnatal life. *Journal of Neurological Sciences* **95**, 271-282.

David, J.D. & Higginbothham, C. (1981). Fusion of chick embryo skeletal myoblasts: interactions of Prostaglandins E1, Adenosine 3':5' Monophosphate, and Calcium influx. *Developmental Biology* **82**, 308-316.

David, J.D., Faser, C.R. & Perrot, G.P. (1990). Role of Protein Kinase C in chick embryo myoblast fusion. *Developmental Biology* **139**, 89-99.

David, J.D., See, W.M. & Higginbothham, C. (1981). Fusion of chick embryo skeletal myoblasts: role of Calcium influx preceding fusion. *Developmental Biology* **82**, 297-307.

Decker E.,R. & Dani, J.A. (1990). Calcium permeability of the Nicotinic Acetylcholine Receptor: The single-channel Calcium influx is significant. *The Journal of Neuroscience* **10(10)**, 3413-3420.

Delaporte, C., Dehaupas, M. & Fardeau, M. (1984). Comparison between the growth pattern of cell cultures from normal and Duchenne dystrophy muscle. *Journal of the Neurological Sciences* **64**, 149-160.

Dembo, M. & Harlow, F. (1986). Cell motion, contractile networks, and the physics of interpenetrating reactive flow. *Biophysical Journal* **50**, 109-121.

DeWitt, M.T., Handley, C.J., Oakes, B.W. & Lowther, D.A. (1984). *In vitro* response of chondrocytes to mechanical loading. The effect of short term mechanical tension. *Connective Tissue Research* **12**, 97-109.

Diebler, H.M., M. Eigen, G. Illgenfritz, G. Maas, & Winkler, R. (1969). Kinetics and mechanism of reactions of main group metal ions with biological carriers. *Pure and Applied Chemistry* **20**, 93-115.

DiMario, J.X., Uzman, A. & Strohman, R.C. (1991). Fiber regeneration is not persistent in dystrophic (mdx) mouse skeletal muscle. *Developmental Biology* **148**, 314-321.

Dubreuil, R.R. (1991). Structure and Evolution of the actin crosslinking proteins. *BioEssays* **13**, 219-226.

Eisenberg, R.S., McCarthy, R.T. & Milton, R.L. (1983). Paralysis of frog skeletal muscle fibres by the calcium antagonist D-600. *Journal of Physiology* **341**, 495-505.

Emery, A.E.H. & Burt, D. (1980). Intracellular calcium and pathogenesis and antenatal diagnosis of Duchenne muscular dystrophy. *British Medical Journal* **48**, 355-361

Endo, T. & Nadal-Ginard, B. (1987). Three types of muscle-specific gene expression in fusion-blocked rat skeletal muscle cells: translational control in EGTA-treated cells. *Cell* **49**, 515-526.

Engel, A.G., Lambert, E.H., Mulder, D.M., Torres, C.F., Sahashi, K., Bertorini, T.E. & Whitaker, J.N. (1982). A newly recognized cogenital myasthenic syndrome attributed to the prolonged open time of the acetylcholine-induced ion channel. *Annals of Neurology* **11**, 553-569.

Entwistle, A., Warner, A. & Zalin, R. (1983) Is avian myoblast fusion controlled by voltage-dependent calcium entry? *Journal of Physiology* **341**,21P.

Entwistle, R., Zalin, R.J., Bevan, S. & Warner, A.E. (1988a). The control of chick myoblast fusion by ion channels operated by prostaglandins and acetylcholine. *The Journal of Cell Biology* **106**, 1693-1702.

Entwistle, R., Zalin, R.J., Warner, A.E. & Bevan, S. (1988b). A role for acetylcholine receptors in the fusion of chick myoblasts. *The Journal of Cell Biology* **106**, 1703-1712.

Ervasti, J.M. & Campbell, K.P. (1991). Membrane organization of the dystrophin-glycoprotein complex. *Cell* **66**, 1121-1131.

Ervasti, J.M. & Campbell, K.P. (1993). Dystrophin and the membrane cytoskeleton. *Current Opinion in Cell Biology* **5**, 82-87.

Ervasti, J.M., Ohlendieck, K., Kahl, S.D., Gaver, M.G. & Campbell, K.P. (1990). Deficiency of a glycoprotein component of the dystrophin complex in dystrophic muscle. *Nature* **345**, 315-319.

Fingerman, E., Campisi, J. & Pardee, A. B. (1984). Defective Ca^{2+} metabolism in Duchenne muscular dystrophy: Effects on cellular and viral growth. *Proceedings of the National Academy of Science of the U.S.A.* **81**, 7617-7621.

FitzHugh, R. (1983). Statistical properties of the asymmetric random telegraph signal with applications to single-channel analysis. *Mathematical Bioscience* **64**, 75-89.

Fong, P., Turner, P.R., Denetclaw, W.F. & Steinhardt, R.A. (1990). Increased activity of calcium leak channels in myotubes of Duchenne human and *mdx* mouse origin. *Science* **250**, 673-675.

Ford, L.E., Huxley, A.F. & Simmons, R.M. (1977). Tension responses to sudden length change in stimulated frog muscle fibers near slack length. *Journal of Physiology* **269**, 441-515.

Franco, A. & Lansman, J.B. (1990a). Calcium entry through stretch-inactivated ion channels in *mdx* myotubes. *Nature* **344**, 670-673.

Franco, A. & Lansman, J.B. (1990b). Stretch-sensitive ion channels in developing muscle cells from a mouse cell line. *Journal of Physiology* **427**, 361-380.

Franco, A., Weingar, B.D. & Lansman, J.B. (1991). Open channel block by gadolinium ion of the stretch-inactivated ion channel in *mdx* myotubes. *Biophysical Journal* **59**, 1164-1170.

Gonzalez-Serratos, H., Valle-Aguilera, R., Lanthrop, D.A., & Garcia, M. (1982). Slow inward calcium currents have no obvious role in muscle excitation-contraction coupling. *Nature* **298**, 292-294.

Guharay, F. & Sachs, F. (1984). Stretch-activated single ion channel currents in tissue-cultured embryonic chick skeletal muscle. *Journal of Physiology* **352**, 685-701.

Guharay, F. & Sachs, F. (1985). Mechanotransducer ion channels in chick skeletal muscle: The effects of extracellular pH. *Journal of Physiology* **363**, 119-134.

Gustin, M.C., Zhou, X., Martinac, B. & Kung, C. (1988). A mechanosensitive ion channel in the yeast plasma membrane. *Science* **242**, 762-765.

Hamill, O.P. & McBride, D.W. (1992). Rapid adaptation of single mechanosensitive channels in *Xenopus* oocytes. *Proceedings of the National Academy of Science of the U.S.A.* **89**, 7462-7466.

Hamill, O.P. & Sakmann, B. (1981). Multiple conductance states of single acetylcholine receptor channels in embryonic muscle cells. *Nature* **294**, 462-464.

Hamill, O.P., Lane, J.W. & McBride, D.W. (1992). Amiloride: a molecular probe for mechanosensitive channels. *Trends in Pharmacological Sciences* **13**, 373-376.

Hamill, O.P., Marty, A., Neher, E., Sakmann, B. & Sigworth , F.J. (1981). Improved patch-clamp techniques for high resolution current recordings from cells and cell-free membrane patches. *Pflügers Archiv* **391**, 85-100.

Hart, Z.H., Sahashi, K., Lambert, E.H., Engel, A.G. & Lindstrom, J.M. (1979). A congenital, familial myasthenic syndrome caused by a presynaptic defect of transmitter resynthesis or mobilization. *Neurology (Abstract)* **29**, 556-557.

Hoffman, E. P., Fischbeck, K. H., Brown, R. H., Johnson, M., Medori, R., Loike, J. D., Harris, J. B., Waterston, R., Brooke, M., Specht, L., Kupsky, W., Chamberlain, J., Caskey, T., Shapiro, F. & Kunkel, L. M. (1988). Characterization of dystrophin in muscle-biopsy specimens from patients with Duchenne's or Becker's muscular dystrophy. *The New England Journal of Medicine* **318**, 1363-1368.

Hoffman, E.P. & Kunkel, L.M. (1989). Dystrophin abnormalities in Duchenne/Becker muscular dystrophy. *Neuron* **2**, 1019-1029.

Hoffman, E.P., Brown, R.H., Jr. & Kunkel, L.M. (1987a). Dystrophin: the protein product of the Duchenne muscular dystrophy locus. *Cell* **51**, 919-928.

Hoffman, E.P., Monaco, A.P., Feener, C.C., & Kunkel, L.M. (1987b). Conservation of the Duchenne muscular dystrophy gene in mice and humans. *Science* **238**, 347-350.

Howard, J. & Hudsepth, A.J. (1987). Mechanical relaxation of the hair cell bundle mediates adaptation in the mechanoelectrical transduction by the bullfrog's saccular hair cell. *Proceedings of the National Academy of Science of the U.S.A.* **84**, 3064-3068.

Howard, J., Roberts, W.M. & Hudspeth, A.J. (1988). Mechanoelectrical transduction by hair cells. *Annual Reviews in Biophysics and Biophysical Chemistry* **17**, 99-124.

Howlett, S.E. & Hoekman, T.B. (1988). Responsiveness of normal and dystrophic avian muscle to acetylcholine, carbamylcholine and *d*-turbocurarine. *General Pharmacology* **19(5)**, 697-701.

Hudspeth, A.J. (1989). How the ear's works work. *Nature* **341**, 397-404.

Hutter, O.F., Burton, F.L. & Bovell, D.L. (1991). Mechanical properties of normal and *mdx* mouse sarcolemma: bearing on function of dystrophin. *Journal of Muscle Research and Cell Motility* **12**, 585-589.

Hymel, L., Inui, M., Fleischer, S., & Schindler, H., (1988). Purified ryanodine receptor of skeletal muscle sarcoplasmic reticulum forms Ca^{2+}-activated oligomeric Ca^{2+} channels in planar bilayers. *Proceedings of the National Academy of Sciences of the U.S.A.* **85**, 441-445.

Ibraghimov-Beskrovnaya, O., Ervasti, J.M., Leveille, C.J., Slaugther, C.A., Sernett, S.W. & Campbell, K.P. (1992). Primary structure of dystrophin-associated glycoproteins linking dystrophin to the extracellular matrix. *Nature* **355**, 696-702.

Inestrosa, N.C., Miller, J.B., Silberstein, L., Ziskind-Conheim, L. & Hall, Z.W. (1983) Developmental regulation of 16S acetylcholinesterase and acetylcholine receptors in a mouse muscle cell line. *Experimental Cell Research* **147**,393-405.

Ishikawa, R., Yamashiro, S. & Matsumura, F. (1989). Annealing of gelsolin-severed actin fragments by tropomyosin in the presence of Ca^{2+}. *The Journal of Biological Chemistry* **264(28)**, 16764-16770.

Isobe, Y. & Shimada, Y. (1986). Cytoskeleton of embryonic skeletal muscle cells. *BioEssays* 4, 167-171.

Jackson, M.B. (1984). Spontaneous openings of the acetylcholine receptor channel. *Proceedings of the National Academy of Sciences of the U.S.A.* **81**, 3901-3904.

Jackson, M.B. (1986). Kinetics of unliganded acetylcholine receptor channel gating. *Biophysical Journal* **49**, 663-672.

John, H.A. & Jones, K.W. (1988).Cell biology in relation to neuromuscular disease. In *Disorders of voluntary muscle*, editor Walton, J., Edinburgh London and New York: Churchill Livingstone.

Kakulas, B.A. & Adams, R.D. (1985). Muscular Dystrophies. In *Diseases of Muscle: Pathological Foundations of Clinical Myology*, Philadelphia: Harper and Row, Publishers.

Kano, M., Wakuta, K. & Satoh, R. (1989). Two components of calcium channel current in embryonic chick skeletal muscle cells developing in culture. *Developmental Brain Research* **47**, 101-112.

Karpati, G., Carpenter, S. & Prescott, S. (1988). Small-caliber skeletal muscle fibers do not suffer necrosis in mdx mouse dystrophy. *Muscle and Nerve* **11**, 795-803.

Kerr, L.M. & Sperelakis, N. (1983). Membrane alterations in skeletal muscle fibers of dystrophic mice. *Muscle and Nerve* **6**, 3-13.

Kieny, M., Boutineau, A., Pautou, M. & Goetinck, P.F. (1988). Muscular dysgenesis in fowl: Ultrastructural study of skeletal muscle in the crooked neck dwarf (*cn/cn*) mutant. *Biological Structures and Morphogenesis* **1(1)**, 15-27.

Knudsen, K.A. & Horwitz, A.F. (1977). Tandem events in myoblasts fusion. *Developmental Biology* **54**, 328-338.

Knudson, C. M., Hoffman, E. P., Kahl, S. D., Kunkel, L. M. & Campbell, K. P. (1988). Evidence for the association of dystrophin with the transverse tubular system in skeletal muscle. *Proceedings of the National Academy of Science of the U.S.A.* **263**, 8480-8484.

Koenig, M., Hoffman, E.P., Bertelson, C.J., Monaco, A.P., Feener, C. & Kunkel, L.M. (1987). Complete cloning of the Duchenne muscular dystrophy (DMD) cDNA and preliminary genomic organization of the DMD gene in normal and affected individuals. *Cell* **50**, 509-517.

Koenig, M., Monaco, A.P., & Kunkel, L.M. (1988). The complete sequence of dystrophin predicts a rod-shaped cytoskeletal protein. *Cell* **53**, 219-228.

Kojima, I., Nishimoto, I., Iiri, T., Ogata E. & Rosenfeld, R. (1988). Evidence that type II insulin-like growth factor receptor is coupled to calcium gating system. *Biochemical and Biophysical Research Communications* **154**, 9-19.

Konieczny, S.F., McKay, J. & Coleman, J.R. (1982). Isolation an characterization of terminally differentiated chicken and rat skeletal muscle myoblasts. *Developmental Biology* **91**, 11-26.

Lai, A.F., Erickson, H.P., Rousseau, E., Liu, Q., & Meissner, G., (1988). Purification and reconstitution of the calcium release channel from skeletal muscle. *Nature* **331**, 315-319.

Lakonishok, M., Muschler, J. & Horwitz, A.F. (1992). The $\alpha_5\beta_1$ integrin associates with dystrophin-containing lattice during muscle development. *Developmental Biology* **152**, 209-220.

Lane, J.W., McBride, D.W. & Hamill, O.P. (1991). Amiloride block of the mechanosensitive cation channel in *Xenopus* oocytes. *Journal of Physiology* **441**, 347-366.

Lansman, J.B. (1990). Blockade of current through single calcium channels by trivalent lanthanide cations. Effect of ionic radius on the rates of ion entry and exit. *Journal of General Physiology* **95**, 679-696.

Lansman, J.B., P. Hess, & Tsien, R.W. (1986). Blockade of current through single calcium channels by Cd^{2+}, Mg^{2+}, and Ca^{2+}. Voltage and concentration dependence of calcium entry into the pore. *Journal of General Physiology* **88**, 321-347.

Lee, K.S. & Tsien, R.W. (1984) High selectivity calcium channels in single dialysed heart cells of the guinea-pig. *Journal of Physiology* **354**,253-272.

Leonard, J.P. & Salpeter, M.M. (1979). Agonist-induced myopathy at the neuromuscular junction is mediated by calcium. *The Journal of Cell Biology* **82**, 811-819.

Leonard, J.P. & Salpeter, M.M. (1982). Calcium-mediated myopathy at neuromuscular junctions of normal and dystrophic muscle. *Experimental Neurology* **76**, 121-138.

Letourneau, P.C., Shattuck, T.A. & Ressler, A.H. (1987). "Pull" and "Push" in neurite elongation: Observations on the effects of different concentrations of Cytochalasin B and Taxol. *Cell Motility and the Cytoskeleton* **8**, 193-209.

Lev, A.A., Feener, C.C., Kunkel, L.M. & Brown, R.H., Jr. (1987). Expression of the Duchenne muscular dystrophy gene in cultured muscle cells. *The Journal of Biological Chemistry* **262**, 15817-15820.

Linkhart, T.A., Clegg, C.H. & Hauschka, S.D. (1981) Myogenic differentiation in permanent clonal mouse myoblast cell lines: regulation by macromolecular growth factors in the culture medium. *Developmental Biology* **86**,19-30.

Love, D.R., Hill, D.F., Dickson, G., Spurr, N. K., Byth, B.C., Marsden, R. F., Walsh, F.S., Edwards, Y.H. & Davies, K.E. (1989). An autosomal transcript in skeletal muscle with homology to dystrophin. *Nature* **339**, 55-58.

Love, D.R., Morris, G.E., Ellis, J.M., Fairbrother, U., Marsden, R.F., Bloomfield, J.F., Edwards, Y.H., Slater, C.P., Parry, D.J. & Davies, K.E. (1991). Tissue distribution of the dystrophin-related gene product and expression in the *mdx* and *dy* mouse. *Proceedings of the National Academy of Sciences of the U.S.A.* **88**, 3243-3247.

Luttgau, H.C. & Spiecker, W. (1979). The effects of calcium deprivation upon mechanical and electrophysiological parameters in skeletal muscle fibres of frog. *Journal of Physiology* **296**, 411-429.

Mancinelli, E., Sardini, A., D'Aumiller, A., Meola, G., Martucci, G., Cossu, G. & Wanke, E. (1989). Properties of acetylcholine-receptor activation in human Duchenne muscular dystrophy myotubes. *Proceedings of the Royal Society of London (B)* **237**, 247-257.

Martinac, B., Buechner, M., Delcour, A.H., Adler, J., & Kung, C. (1987) Pressure-sensitive ion channel in *Escherichia coli. Proceedings of the National Academy of Sciences (USA)* **84**, 2297-2301.

Martonosi, A. (1989). Calcium regulation in muscle diseases; the influence of innervation and activity. *Biochemica et Biophysica Acta* **991**, 155-242.

Matsumura, K., Ervasti, J.M., Ohlendieck, K., Kahl, S.D. & Campbell, K.P. (1992). Association of dystrophin-related protein with dystrophin-associated proteins in *mdx* mouse muscle. *Nature* **360**, 588-591.

McBride, D.W.& Hamill, O.P. (1992).Pressure-clamp: a method for rapid step perturbation of mechanosensitive channels.*Pflügers Archiv* **421**, 606-612.

McCully, K.K. & Faulkner, J.A. (1985). Injury to skeletal muscle fibers of mice following lengthening contractions. *Journal of Applied Physiology* **59**, 119-126.

McCully, K.K. & Faulkner, J.A. (1986). Characteristics of lengthening contractions associated with injury to skeletal muscle fibers. *Journal of Applied Physiology* **61**, 293-299.

Meier, H. & Southard, J.L. (1970). Muscular dystrophy in the mouse caused by an allele at the *dy*-locus. *Life Sciences* **9**, 137-144.

Meier, H. (1973). Effects of multiple alleles on the expression of muscular dystrophy. In *Clinical Studies in Myology*, ed. Kakulas, B.A. New York: Elsevier.

Menke, A. & Jockusch, H. (1991). Decreased osmotic stability of dystrophin-less muscle cells from the *mdx* mouse. *Nature* **349**, 69-71.

Meshul, C.K. (1989). Calcium channel blocker reverses anticholinesterase-induced myopathy. *Brain Research* **497**, 142-148.

Mishina, M., Takai, T., Imoto, K., Noda, M., Takahashi, T., Numa, S., Methfessel, C. & Sakmann, B. (1986). Molecular distinction between fetal and adult forms of muscle acetylcholine receptor. *Nature* **321**, 406-411.

Mitchison, T. & Kirschner, M. (1988). Cytoskeletal dynamics and nerve growth. *Neuron* **1**, 761-772.

Mokri, B. & Engel, A.G. (1975). Duchenne dystrophy: Electron microscopic findings pointing to a basic or early abnormality in the plasma membrane of the muscle fiber. *Neurology* **25**, 111-1120.

Monaco, A.P., Neve, R.L., Colletti-Feener, C., Bertelson, C.J., Kurnit, D.M. & Kunkel, L.M. (1986). Isolation of candidate cDNAs for portions of the Duchenne muscular dystrophy gene. *Nature* **323**, 646-650.

Mongini, T., Ghigo, D., Doriguzzi, C., Bussolino, F., Pescarmona, G., Pollo, B., Schiffer, D. & Bosia, A. (1988). Free cytoplasmic Ca^{2+} at rest and after cholinergic stimulus is increased in cultured muscle cells from Duchenne muscular dystrophy patients. *Neurology* **38**, 476-480.

Morris, C.E. & Horn, R. (1991). Failure to elicit neuronal macroscopic mechanosensitive currents anticipated by single-channel studies. *Science* **251**, 1246-1249.

Morris, C.E. & Sigurdson, W.J. (1989). Stretch-inactivated ion channels coexist with stretch-activated ion channels. *Science* **243**, 807-809.

Morris, C.E. (1990). Mechanosensitive Ion Channels. *Journal of Membrane Biology* **113**, 93-107.

Neerunjun, J.S. & Dubowitz, V. (1979). Increased calcium-activated neutral protease activity in muscles of dystrophic hamsters and mice. *Journal of the Neurological Sciences* **40**, 105-111.

Neher, E. & Steinback, J.H. (1978). Local anesthetics transiently block currents through single acetylcholine receptor channels. *Journal of Physiology* **277**, 153-176.

Nelson, W.J. & Lazarides, E. (1985). Posttranslational control of membrane-skeleton (Ankyrin and ab-Spectrin) assembly in early myogenesis. *Journal of Cell Biology* **100**, 1726-1735.

Nieboer, E. (1975). The lanthanide ions as structural probes in biological and model systems. *Structure and Bonding* **22**, 1-46.

Northrop, J., Weber, A., Mooseker, M.S., Franzini-Armstrong, C., Bishop, M.F., Dubyak, G.R., Tucker, M. & Walsh, T.P. (1986). Different calcium dependence of the capping and cutting activities of villin. *The Journal of Biological Chemistry* **261(20)**, 9274-9281.

Nossal, R. (1988). On the elasticity of cytoskeletal networks. *Biophysical Journal* **53**, 349-359.

Nudel, U., Robzyk, K. & Yaffe, D. (1988). Expression of the putative Duchenne muscular dystrophy gene in differentiated myogenic cell cultures and in the brain. *Nature* **331**, 635-638.

O'Nell, C. Jordan, P., Riddle, P. & Ireland, G. (1990). Narrow linear strips of adhesive substratum are powerful inducers of both growth and total focal contact area. *Journal of Cell Science* **95**, 577-586.

Ocalan, M., Goodman, S.L., Kuhl, U., Hauschka, S.D. & Von Der Mark, K. (1988). Laminin alters cell shape and stimulates motility and proliferation of murine skeletal myoblasts. *Developmental Biology* **125**, 158-167.

Ogden, D.C. & Colquhoun, D. (1985). Ion channel block by acetylcholine, carbachol, and suberyldicholine at the frog neuromuscular junction. *Proceedings of the Royal Society London B* **225**, 329-355.

Ohlendieck, K. & Campbell, K.P. (1991). Dystrophin-associated proteins are greatly reduced in skeletal muscle from mdx mice. *The Journal of Cell Biology* **115**, 1685-1694.

Ohlendieck, K., Ervasti, J.M., Matsumura, K., Kahl, S.D., Leveille, C.J. & Campbell, K.P. (1991a). Dystrophin-related protein is localized to neuromuscular junctions of adult skeletal muscle. *Neuron* **7**, 499-508.

Ohlendieck, K., Ervasti, J.M., Snook, J.B. & Campbell, K.P. (1991b). Dystrophin-glycoprotein complex is highly enriched in isolated skeletal muscle sarcolemma. *The Journal of Cell Biology* **112**, 135-148.

Olson, E.N., Sternberg, E., Hu, J.S., Spizz, G. & Wilcox, C. (1986) Regulation of myogenic differentiation by type ß transforming growth factor. *Journal of Cell Biology* **103**,1799-1805.

Oronzi-Scott, M., Sylvester, J.E., Heiman-Patterson, T., Shi, J.-Y., Fieles, W., Stedman, H., Burghes, A., Ray, P., Worton, R. & Fischbeck, K.H. (1988). Duchenne muscular dystrophy gene expression in normal and diseased human muscle. *Science* **239**, 1418-1420.

Pearce, G.W. & Walton, J.N. (1963). A histological study of muscle from the bar harbor strain of dystrophic mice. *Journal of Pathology and Bacteriology* **86**, 25-37.

Pringle, J.W.S. (1977). Stretch-activation of muscle: function and mechanism. *Proceedings of the Royal Society of London B* **201**, 107-130.

Roe, M.W., Hepler, J.R., Harden, T.K. & Herman, B. (1989). Platelet-derived growth factor and Angiotensin II causes increases in cytosolic free calcium by different mechanisms in vascular smooth muscle cells. *Journal of Cellular Physiology* **139**, 100-108.

Rojas, L. & Zuazaga, C. (1991). Spontaneous openings of large and small conductance acetylcholine channels in *Xenopus* myocytes. *Neuroscience Letters* **124**, 195-199.

Rosenberg, R.L., Hess, P. & Tsien, R.W. (1988). Cardiac calcium channels in planar lipid bilayers. *Journal of General Physiology* **92**, 27-54.

Ryder-Cook, A.S., Sicinski, P., Thomas, K., Davies, K.E., Worton, R.G., Barnard, E.A., Darlison, M.G. & Barnard, P.J. (1988). Localization of the *mdx* mutation within the mouse dystrophin gene. *The EMBO Journal* **7**, 3017-3021.

Sachs, F. (1988). Mechanical transduction in biological systems *CRC Critical Reviews in Biomedical Engineering* **16**, 155-242.

Sachs, F. (1989). Ion channels as mechanical transducers. In *Cell Shape: Determinants, Regulation and Regulatory Role*, editors Stein, W.D. and Bronner, F., New York: Academic Press, Inc.

Salviati, G., Betto, R., Ceoldo, S., Biasia, E., Bonilla, E., Miranda, A.F., & Dimauro, S. (1989). Cell fractionation studies indicate that dystrophin is a protein of surface membranes of skeletal muscle. *Biochemical Journal* **258**, 837-841.

Sanchez, J.A. & Stefani, E. (1978). Inward calcium current in twitch muscle fibers of the frog. *Journal of Physiology* **283**,197-209.

Sandow, A. (1952). Excitation-contraction coupling in muscular response. *Yale Journal of Biological Medicine* **25**, 176-201.

Sanes, J.R. & Cheney, J.M. (1982). Laminin, fibronectin and collagen in synaptic and extrasynaptic portions of muscle fiber basement membrane. *The Journal of Cell Biology* **93**, 442-451.

Shainberg, A., Yagil, G. & Yaffe, D. (1969). Control of myogenesis in vitro by Ca^{2+} concentration in nutritional medium. *Experimental Cell Research* **58**, 163-169.

Shannon, R.D. (1976). Revised effective ionic radii and systematic studies of interatomic distances in halides and chalcogenides. *Acta Crystallographica* **A32**, 751-767.

Sicinski, P., Geng, Y., Ryder-Cook, A.S., Barnard, E.A., Darlison, M.G. & Barnard, PJ. (1989). The molecular basis of muscular dystrophy in the *mdx* mouse: A point mutation. *Science* **244**, 1578-1580.

Siegelbaum, S.A., Trautmann, A. & Koenig, J. (1984). Single acetylcholine-activated channel currents in developing muscle cells. *Developmental Biology* **104**, 366-379.

Slager, H.G., Good, M.J., Schaart, G., Groenewoud, J.S. & Mummery, C.L. (1992). Organization of non-muscle myosin during early murine embryonic differentiation. *Differentiation* **50**, 47-56.

Smith, J.S. (1988). Neuronal Cytomechanics: The actin-based motility of growth cones. *Science* **242**, 708-715.

Sokabe, M. & Sachs, F. (1990). The structure and dynamics of patch-clamped membrane: a study using differential interference contrast light microscopy. *Journal of Cell Biology* **111**, 599-606.

Sokabe, M., Sachs, F. & Jing, Z. (1991). Quantitative video microscopy of patch clamped membranes, stress, strain, capacitance, and stretch channel activation. *Biophysical Journal* **59**, 722-728.

Stauber, W.T., Fritz, V.K., Clarkson, P.M. & Riggs, J.E. (1991). An injury model myopathy mimicking dystrophy: Implications regarding the function of dystrophin. *Medical Hypotheses* **35**, 358-362.

Sumpio, B.E., Banes, A.J., Levin, L.G. & Johnson, G. (1987). Mechanical stress stimulates aortic endothelial cells to proliferate. *Journal of Vascular Surgery* **6**, 252-256.

Tinsley, J.M., Blake, D.J., Roche, A., Fairbrother, U., Riss, J., Byth, B.C., Knight, A.E., Kendrick-Jones, J., Suthers, G.K., Love, D.R., Edwards, Y.H. & Davies, K.E. (1992). Primary structure of dystrophin-related protein. *Nature* **360**, 591-593.

Trautmann, A., Delaporte, C. & Marty, A. (1986). Voltage-dependent channels of human muscle cultures.*Pflügers Archiv* **406**, 163-172.

Tsien, R.W. & Tsien, R.Y. (1990). Calcium channels, stores, and osscillations. *Annual Review of Cell Biology* **6**, 715-760.

Turner, P.R., Fong, P., Denetclaw, W.F. & Steinhardt, R.A. (1991). Increased calcium influx in dystrophic muscle. *The Journal of Cell Biology* **115**, 1701-1712.

Turner, P.R., Westwood, T., Regen, C.M. & Steinhardt, R.A. (1988). Increased protein degradation results from elevated free calcium levels found in muscle from *mdx* mice. *Nature* **335**, 735-738.

Wakelam, M.J.O. (1985). The fusion of myoblasts. *Biochemical Journal* **228**, 1-12.

Walton, J. & Gardner-Medwin, D. (1988).The muscular dystrophies. In *Disorders of voluntary muscle*, editor Walton, J., Edinburgh London and New York: Churchill Livingstone.

Watkins, S.C., Hoffman, E.P., Slayter, H.S. & Kunkel, L.M. (1988). Immunoelectron microscopic localization of dystrophin in myofibres. *Nature* **333**, 863-866.

Webster, C., Silberstein, L., Hays, A.P. & Blau, H.M. (1988). Fast muscle fibers are preferentially affected in Duchenne muscular dystrophy. *Cell* **52**, 503-513.

Weeds, A. (1982). Actin-binding proteins: regulators of cell architecture and motility. *Nature (London)* **296**, 811-816.

Weller, B., Karpati, G. & Carpenter, S. (1990). Dystrophin-deficient *mdx* fibers are preferentially vulnerable to necrosis induced by experimental lengthening contractions. *Journal of the Neurological Sciences* **100**, 9-13.

Williams, D.A., Head, S.I., Bakker, A.J. & Stephenson, D.G. (1990). Resting calcium concentrations in isolated skeletal muscle fibers of dystrophic mice. *Journal of Physiology* **428**, 243-256.

Winegar, B. & Lansman, J.B. (1990). Voltage-dependent block by zinc of single calcium channels in mouse myotubes. *Journal of Physiology* **425**, 563-578.

Yaffe, D. & Saxel, O. (1977). Serial passaging and differentiation of myogenic cells isolated from dystrophic mouse muscle. *Nature* **270**, 725-727.

Yang, X. & Sachs, F. (1989). Block of stretch-activated ion channels in *Xenopus* oocytes by gadolinium and calcium ions. *Science* **243**, 1068-1071.

Yellen, G. (1984). Ionic permeation and blockade in Ca^{2+}-activated K^+ channels of bovine chromaffin cells. *Journal of General Physiology* **84**, 157-186.

Yin, H.L. & Stossel, T.P. (1979). Control of cytoplasmic actin gel-sol transformation by gelsolin, a calcium-dependent regulatory protein. *Nature (London)* **281**, 583-586.

Yumura, S. (1991). Contraction of *Dictyostelium* ghost reconstituted with myosin II. *Cell Structure and Function* **16**, 481-488.

Zubrzycka-Gaarn, E.E., Bulman, D.E., Karpati, G., Burghes, A.H.M., Belfall, B., Klamut, H.J., Talbot, J., Hodges, R.S., Ray, P.N., & Worton, R.G. (1988). The Duchenne muscular dystrophy gene product is localized in sarcolemma of human skeletal muscle. *Nature* **333**, 466-469.